

AD-A137 641

LABORATORY EVALUATION OF NOVEL PARTICULATE CONTROL
CONCEPTS FOR JET ENGINE TEST CELLS(U) OREGON STATE UNIV
CORVALLIS R W BOUBEL DEC 83 AFESC/ESL-TR-83-02

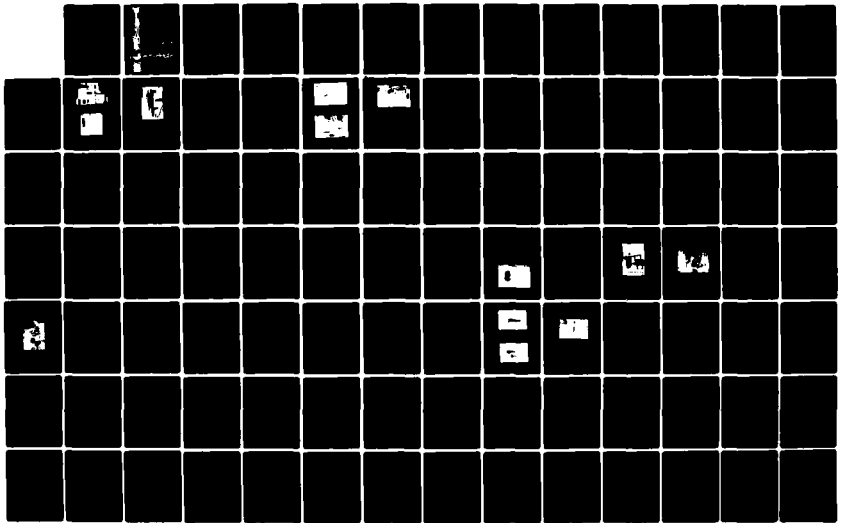
1/3

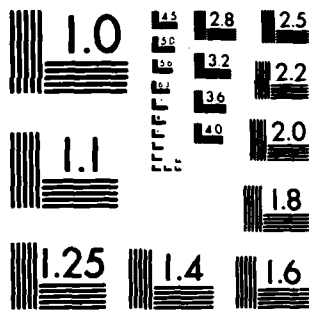
UNCLASSIFIED

F08635-81-K-0003

F/G 21/2

NL





MICROCOPY RESOLUTION TEST CHART
NATIONAL BUREAU OF STANDARDS-1963-A

ESL-TR-83-02

8

LABORATORY EVALUATION OF NOVEL PARTICULATE CONTROL CONCEPTS FOR JET ENGINE TEST CELLS

DR RICHARD W. BOUBEL
OREGON STATE UNIVERSITY
CORVALLIS, OREGON 97331

DECEMBER
JULY 1983

FINAL REPORT
7 JANUARY 1981 - 30 SEP 1982

DTIC
ELECTE
FEB 9 1984
S B

APPROVED FOR PUBLIC RELEASE: DISTRIBUTION UNLIMITED

AD A137641

DTIC FILE COPY



ENGINEERING & SERVICES LABORATORY
AIR FORCE ENGINEERING & SERVICES CENTER
TYNDALL AIR FORCE BASE, FLORIDA 32403

84 02 08 C19

NOTICE

PLEASE DO NOT REQUEST COPIES OF THIS REPORT FROM
HQ AFESC/RD (ENGINEERING AND SERVICES LABORATORY).
ADDITIONAL COPIES MAY BE PURCHASED FROM:

NATIONAL TECHNICAL INFORMATION SERVICE
5285 PORT ROYAL ROAD
SPRINGFIELD, VIRGINIA 22161

FEDERAL GOVERNMENT AGENCIES AND THEIR CONTRACTORS
REGISTERED WITH DEFENSE TECHNICAL INFORMATION CENTER
SHOULD DIRECT REQUESTS FOR COPIES OF THIS REPORT TO:

DEFENSE TECHNICAL INFORMATION CENTER
CAMERON STATION
ALEXANDRIA, VIRGINIA 22314

UNCLASSIFIED

SECURITY CLASSIFICATION OF THIS PAGE(When Data Entered)

emissions for each control device.

None of the three devices tested indicated enough reduction in plume opacity to justify construction of full-scale test cell control systems. Recommendations were made for future evaluation of modified wetted sand filter and ceramic fiber baghouse control devices.

UNCLASSIFIED

SECURITY CLASSIFICATION OF THIS PAGE(When Data Entered)

EXECUTIVE SUMMARY

For several years the U.S. Air Force has been concerned with visual emissions from jet engine test cells. These emissions are not only aesthetically undesirable but have also resulted in cases where the test cell emissions were in violation of local air pollution emission standards. Three different approaches have been suggested, and used, to reduce this problem:

1. Engine design and modification toward "smokeless" combustion.
2. Fuel additives, such as ferrocene, which reduce visible emissions by changing combustion, or postcombustion, reactions.
3. Installation of control equipment to remove, or modify, the emitted particulate matter causing the visual problem.

This study reports on the laboratory evaluation of three different control devices, tested on a small gas turbine engine exhaust, to predict their ability to reduce visual emissions from jet engine test cells. The three devices tested were:

1. A low-pressure drop wet scrubber typical of the type used at some test cell installations.
2. A wetted sand filter of the type used to control particulate matter emissions from similar, high opacity plumes.
3. A baghouse, using ceramic fabric bags, capable of withstanding the high temperature of the jet engine exhaust.

None of the three devices tested indicated enough reduction in plume opacity to justify construction of full-sized control equipment. The low-pressure drop scrubber did not significantly reduce the opacity of the plume. The high-temperature baghouse reduced the opacity only slightly. The wetted-sand filter accomplished the greatest opacity reduction of the three devices tested but still would not meet visual emission standards in the configuration used in this experiment.

Recommendations for future studies conclude this portion of the report.

The M.S. Thesis of a graduate student, Mr. William Faye, is Appendix C to the report. Mr. Faye reports on the NO_x emissions from the gas turbine as a function of both fuel-bound nitrogen and thermally generated NO_x . Appendix B is the Master's Project of a graduate student, Mr. George D. Ikonou. This report presents the results of an energy and material balance performed on the turbine and the results of an energy and material balance performed on the spray system.

PREFACE

This report covers research conducted during the period 7 January 1981 to 30 September 1982. The contractor was the Engineering Experiment Station, Oregon State University, Corvallis, Oregon. Richard W. Boubel, PhD, Professor of Mechanical Engineering at Oregon State University was the principal investigator. This work was funded by the Engineering and Services Laboratory, Air Force Engineering and Services Center (AFESC), Tyndall AFB, Florida, under Contract Number F08635-81-K-0003. The AFESC project officers were Capt James J. Tarquinio and 1st Lt Jeffery C. Jenkins.

This report has been reviewed by the Public Affairs Office (PA) and is releasable to the National Technical Information Services (NTIS). At NTIS it will be available to the general public, including foreign nationals.

This technical report has been reviewed and is approved for publication.

Jeffery C. Jenkins

JEFFERY C. JENKINS, 1Lt, USAF
Project Officer

John T. Slankas

JOHN T. SLANKAS, Maj, USAF
Chief, Environmental Sciences Branch

Jimmy N. Fulford

JIMMY N. FULFORD, Lt Col, USAF
Chief, Environics Division

Robert E. Boyer

ROBERT E. BOYER, Col, USAF
Director, Engineering and Services
Laboratory



Accession For	
NTIS GRA&I	<input checked="" type="checkbox"/>
DTIC TAB	<input type="checkbox"/>
Unannounced	<input type="checkbox"/>
Justification	
PER CALL JC	
By	
Distribution/	
Availability Codes	
Dist	Avail and/or Special
A-1	

TABLE OF CONTENTS

I. INTRODUCTION AND BACKGROUND 1

 A. PROBLEM STATEMENT 1

 B. COMPOSITION OF JET ENGINE "SMOKE" 1

 C. ALTERNATIVES AVAILABLE 2

II. OREGON STATE UNIVERSITY TURBINE LABORATORY 3

III. EVALUATION OF WET SCRUBBER 6

 A. SCRUBBER DESIGN 6

 B. EXPERIMENTAL DESIGN 6

 C. SCRUBBER TEST PROCEDURE 11

 D. RESULTS AND DISCUSSION-GAS CLEANING 11

 E. CONCLUSIONS-GAS CLEANING 20

 F. WATER QUALITY STUDY 20

 1. Chemical Characterization of Water Scrubber
 Samples 21

 2. Biotreatability of Scrubber Waters 25

 3. Physical-Chemical Treatability of Scrubber
 Waters 30

 4. Gas Chromatographic Study of Unburned Fuel and
 Polynuclear Aromatic Hydrocarbons 35

 5. Summary and Conclusions-Water Quality Study 36

 G. DATA ANALYSIS AND PERFORMANCE 37

 H. RECOMMENDATIONS 37

IV. EVALUATION OF WETTED-SAND FILTER 39

 A. EXPERIMENTAL DESIGN 40

 B. TEST PROCEDURE 46

 C. RESULTS AND DISCUSSION 47

 D. CONCLUSIONS 47

TABLE OF CONTENTS (Continued)

E. RECOMMENDATIONS 51

V. EVALUATION OF CERAMIC FABRIC BAGHOUSE 52

 A. EXPERIMENTAL DESIGN 52

 B. TEST PROCEDURE 57

 C. RESULTS AND DISCUSSION 57

 D. CONCLUSIONS 59

 E. RECOMMENDATIONS 59

VI. OVERALL OBSERVATIONS AND RECOMMENDATIONS 60

VII. NO_x EMISSIONS FROM TURBINE ENGINES 61

 REFERENCES 62

APPENDIX

A. SUPPORT DATA 63

B. DATA ANALYSIS AND PERFORMANCE EVALUATION OF A GAS
TURBINE EQUIPPED WITH A WET SCRUBBER 79

C. NO_x EMISSIONS FROM A GAS TURBINE AS A FUNCTION OF
FUEL-BOUND NITROGEN AND OTHER VARIABLES 119

LIST OF FIGURES

1. Gas Turbine and Support Systems	4
2. Gas Turbine Control Panel	4
3. SAE ARP 1179 A Smoke-Sampling System	5
4. Scrubbing System Components Prior to Final Assembly	8
5. Scrubbing Section Completed	8
6. Complete System	9
7. SAE Smoke Number as a Function of Fuel and Load	12
8. Cyclone Outlet Temperature as a Function of Water Pressure and Fuel Flow	14
9. Temperature Drop Across Wet Scrubber as a Function of Water Pressure and Load	16
10. SAE Smoke Number as a Function of Water Pressure and Fuel Flow	18
11. SandAir Filter System	39
12. Demister and Flow Control Valve	41
13. Test Facility	42
14. SandAir Filter Test System	43
15. SAE Smoke Number as a Function of Fuel and Load	44
16. Inlet Duct Velocity Traverse	45
17. Gas Flow Through SandAir Filter as a Function of Water Flow and Pressure Drop	48
18. SandAir Filter Outlet Smoke Number	49
19. Smoke Number Decrease Across SandAir Filter	50
20. Baghouse Frame and Housing	53
21. Ceramic Fabric Bag Used in Tests	53
22. Baghouse Test Facility	54
23. High-Temperature Baghouse Test	55
24. Bag Flow for Various Pressure Drops Over Time	58

LIST OF TABLES

1. Scrubber Test Variables	10
2. Mean Values of Turbine Outlet Temperature on CO ₂ Obtained in Preliminary Tests	13
3. Linear Regression Constants and Coefficients for Data Shown in Figure 8	15
4. Dependent Variables as a Function of Turbine Load	15
5. Linear Regression Constants and Coefficients for Data Shown in Figure 10	17
6. SAE Smoke Number as a Function of Fuel Mixture and Load	19
7. Linear Regression Constants and Coefficients for Data From Table 6	19
8. Linear Regression Constants and Coefficients for Data From Table 6 for Aromatic Fuels	20
9. Solids Analysis of Scrubber Waters	22
10. Chemical Characterization of Scrubber Waters	23
11. Biotreatability Results for Scrubber Water T-1	27
12. Biotreatability Results for Scrubber Water T-2	28
13. Biotreatability Results for Scrubber Water T-3	29
14. Alum Coagulation Treatability Test	32
15. Activated Carbon Adsorption Treatability Test	34
16. SandAir Filter Test Variables	46
17. Mean Values and Efficiency of SandAir Filter for Smoke Reduction	47
18. Smoke Number and Efficiency as a Function of Gas Flow (Design Gas Flow was 450 acfm)	51
19. Filter Test Variables	56

SECTION I

INTRODUCTION AND BACKGROUND

A stated goal of the U.S. Air Force (Reference 1) is to have an invisible exhaust plume from jet engine, or turbine-powered, aircraft. An invisible exhaust plume is obviously desirable in combat operations, but it is also desirable from an aesthetic standpoint. The U.S. Environmental Protection Agency (EPA) has proposed regulations governing emissions from aircraft engines (Reference 2) including regulations governing visual emissions, usually called "smoke." These regulations have only been proposed, not promulgated. Also, these proposed regulations do not apply to military aircraft.

A. PROBLEM STATEMENT

The exemption of military aircraft from the EPA regulations would appear to be a reason for the USAF, and other Department of Defense (DOD) agencies, to relax their concern about all engine emissions. This would be particularly true of the "smoke" since this is only an aesthetic consideration unless in combat. Such is not the case. Several local air pollution control agencies have ruled (and been upheld by court decisions) that an engine removed from an aircraft, and placed in a test cell, constitutes a stationary source of air pollution. The test cell is, therefore, subject to all rules and regulations of the local agency.

Some jet aircraft engines, when operated at full power in a test cell, do emit particulate matter dense enough to violate the plume opacity regulations of several local control agencies. The result is that the USAF, and other DOD facilities, have been issued notices of violation of air pollution regulations at several locations. Such violation notices usually require payment of a fine but the public relations aspect is usually of much greater concern to the DOD than the money involved.

B. COMPOSITION OF JET ENGINE "SMOKE"

The visible emissions from jet engines may be called by the simple generic term "smoke," but they are really a complex collection of aerosols, varying both qualitatively and quantitatively. A large percentage of the aerosol material is unburned carbon of submicron size. This carbon is black, nonreflective, nonpolar, and relatively stable, chemically and physically.

Another component of the exhaust particulate matter is aerosol hydrocarbons. This is a complex mixture of unburned, partially oxidized, and reformed hydrocarbons with varying vapor pressures, chemical reactivities, physical properties (such as size and shape), and optical properties (such as reflectance and transmittance).

The last aerosol component of the exhaust plume is ash which results from the trace amounts of uncombustible impurities contained in the fuel.

This component is negligible for jet engines operated on uncontaminated turbine fuels.

C. ALTERNATIVES AVAILABLE

Several alternatives have been proposed and/or used to reduce visual emissions from jet engine test cells to acceptable values. These include:

1. Diluting the exhaust plume with ambient air. This method is usually promoted by stating that the dilution air is used for cooling of the hot gases.

2. Using more highly refined, nonsmoking fuels. Kerosene is the optimum fuel in this regard as it is refined and blended to burn with a minimum of smoke.

3. Using an additive to promote or modify the combustion. The U.S. Navy has conducted considerable research using ferrocene as a fuel additive (Reference 3).

4. Designing and installing control equipment to collect the particulate matter before the hot gases are released to the atmosphere. The last alternative was investigated during this study.

SECTION II

OREGON STATE UNIVERSITY TURBINE LABORATORY

The Oregon State University Gas Turbine Laboratory Research Facility is located in Graf Hall and is one of the laboratories of the Department of Mechanical Engineering.

A gas turbine electric generator, Model 2CM 352 EI, manufactured by the General Electric Company was used to generate typical smoke. This smoke was composed of unburned carbon particles, unburned and partially oxidized hydrocarbons, and trace amounts of inorganic materials. The turbine generator was obtained as surplus equipment, originally manufactured for the U.S. Army Mobility Command. It was coupled to a resistance load system through an electrical switching/control panel. The generator output was a nominal 15 kw at full load with a maximum rating of 20 kw. The output was 240 volts, A.C., single phase. The turbine was governed at 48,000 rpm and consumed approximately 45 pounds of fuel per hour at full load.

Figure 1 shows the gas turbine used with the loading resistor and gas-measuring system in the background.

Figure 2 shows the turbine control panel.

The gas-sampling system consisted of a flow conditioner cabinet which cleaned the gas stream and pumped it to the CO₂ and NO_x analyzers. Both these analyzers had previously been calibrated at several points in their range by using certified calibration gases. During the test runs, the instruments were continually checked using "zero" and "span" gases alternately with the sample. The calibration curve for the CO₂ analyzer is shown in Appendix A.

The smoke sample was extracted and carried by a heated stainless steel line to the smoke measuring system. The Smoke Number was determined according to SAE, Aerospace Recommended Practice Specification ARP 1179 A. The smoke filters were analyzed on a B&L Spectronic 20 equipped with a reflectance attachment. Figure 3 shows the smoke sampling system with the sampling filter holder (square) and the bypass filter (round).

The smoke was generated by varying the type of fuel and load on the turbine. The cleanest effluent was obtained with 100 percent kerosene fuel at no output load on the turbine. The smokiest effluent was obtained with 100 percent toluene fuel at full load.

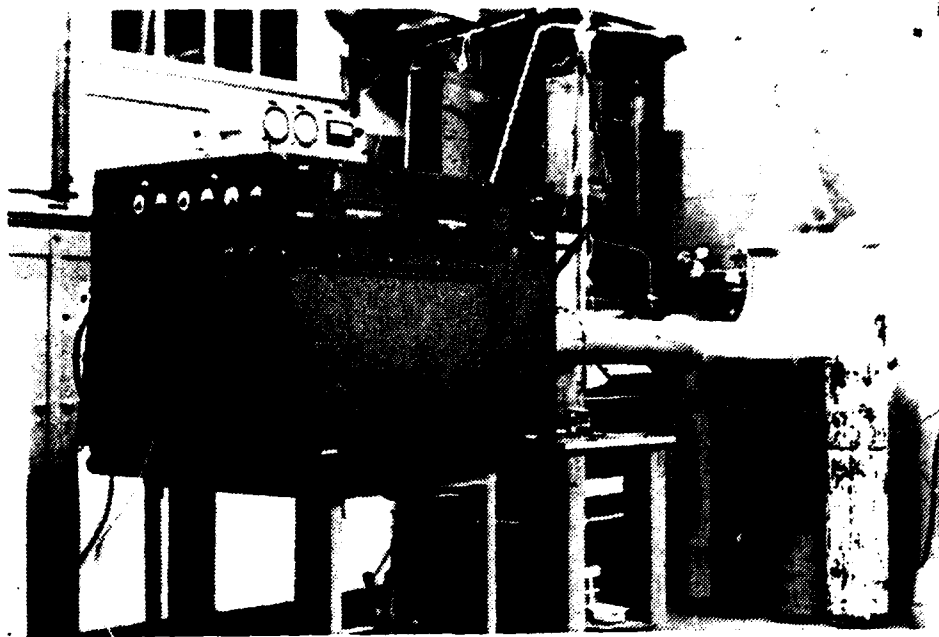


Fig. 1. Gas Turbine and Support Systems.



Fig. 2. Gas Turbine Control Panel.

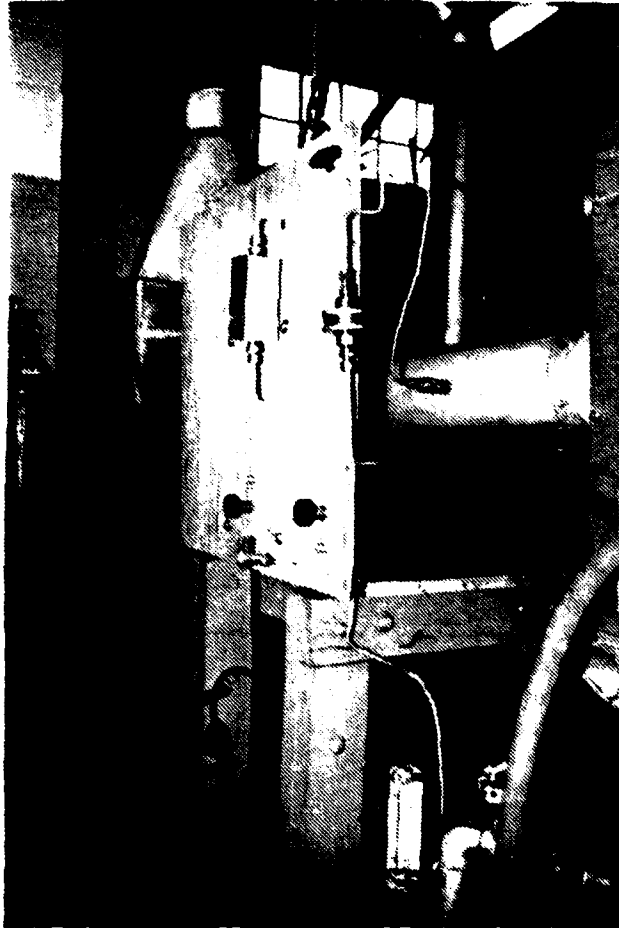


Fig. 3. SAE ARP 1179 A Smoke-Sampling System.

SECTION III

EVALUATION OF WET SCRUBBER

The first control device tested and reported in this study was a simple wet-scrubbing system, similar to many Department of Defense test cells which use water spray rings at the inlet end of the augmentor. Although the primary purpose of the water injection is to maintain structural integrity by cooling the augmentor tube walls, some particles are removed by the scrubbing action of the injected water (Reference 4).

A. SCRUBBER DESIGN

The wet scrubber tested was designed with four spray nozzles of varying capacity installed in a 5-inch diameter section of duct. Each spray nozzle was controlled by a shutoff/throttling valve with a pressure gage to determine the nozzle pressure. The nozzles were installed in the duct so that the spray was counterflow to the exhaust from the turbine. Figure 4 shows the partially assembled scrubber.

The nozzles were selected to give a complete range of water flow, from 1/2 gpm (which was all converted to the gas phase at full load) to 15 gpm at 60 psi with all nozzles open. Only the smallest nozzle (1/2 to 1.2 gpm) was eventually used, as explained later in this report. Figure 5 shows the completed scrubber.

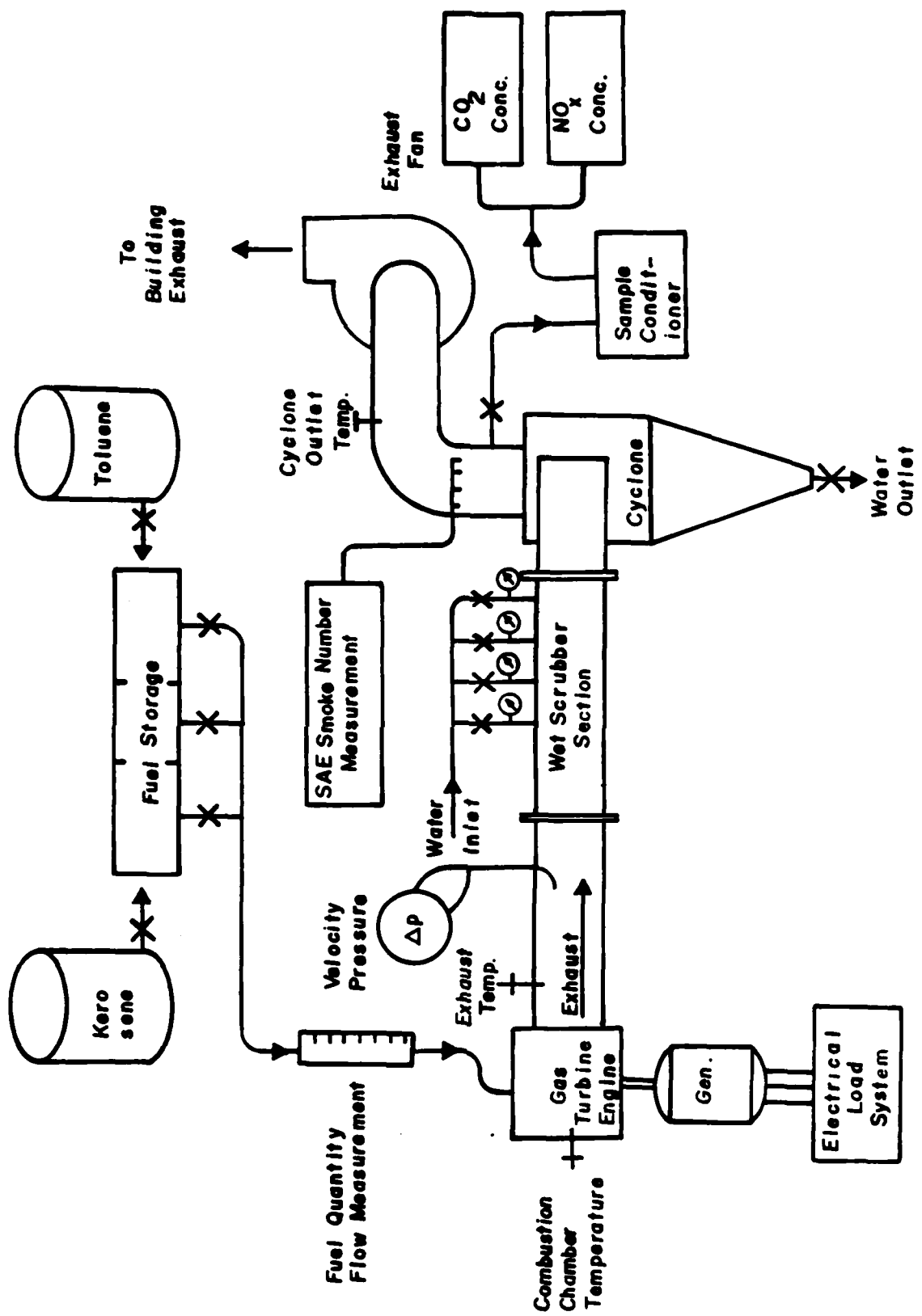
After the exhaust gas was passed through the scrubbing section it was ducted to a 2-foot diameter, 8-foot long cyclone which was used as a demister. The water removed from the exhaust was drained from the bottom of the cyclone and the exhaust gas, saturated with water, exited the top of the cyclone. The cyclone exhaust was the point at which the effluent was sampled for gaseous components (CO_2 , NO_x , and CO) and the smoke sample extracted. This would be the point at which an effluent sample would leave a similar control system on a full-sized test cell. In the laboratory system, the effluent from the cyclone was diluted with cooling air and ducted to an exhaust fan which blew the effluent into the building exhaust stack. Figure 6 shows the complete system.

A schematic flow diagram for the entire test facility is shown on the following page.

B. EXPERIMENTAL DESIGN

The variables measured during the test are shown in Table 1. Also measured were the wet and dry bulb ambient temperature and the barometric pressure.

Three fuel mixtures were used, 100 percent kerosene, 100 percent toluene and a 50/50 blend. Three turbine-output loads were available, "zero load" (which was at the governed 48,000 rpm but no electrical output), "1/2 load" (about 6 kw) and "full load" (about 15 kw).



Schematic of Test Facility for Wet Scrubber

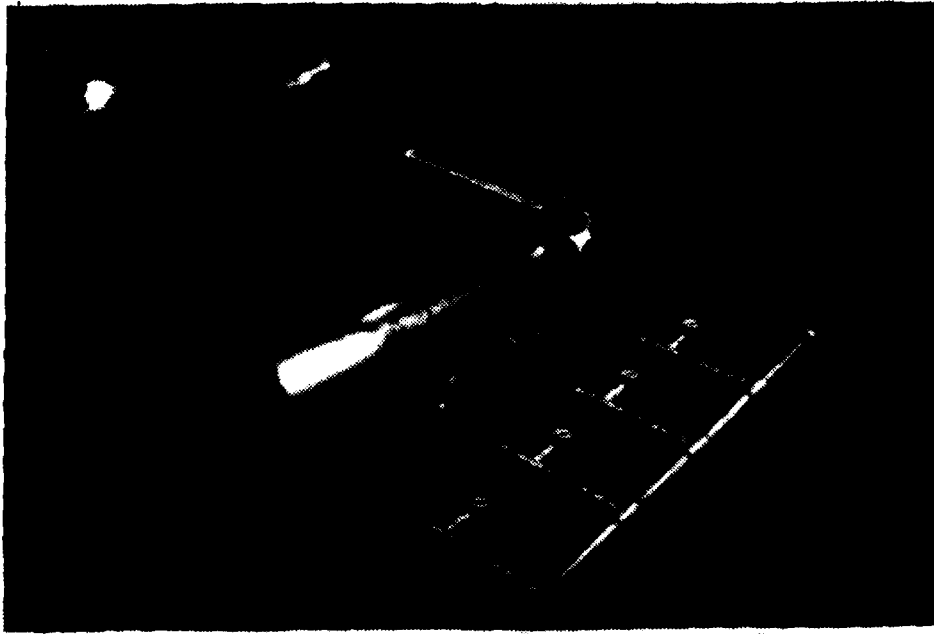


Fig. 4. Scrubbing System Components Prior to Final Assembly. Flow is From Top to Bottom Through the System. The Nozzles Are Rated at 1, 2, 4, and 6 Gallons Per Minute, Respectively at 40 psi.

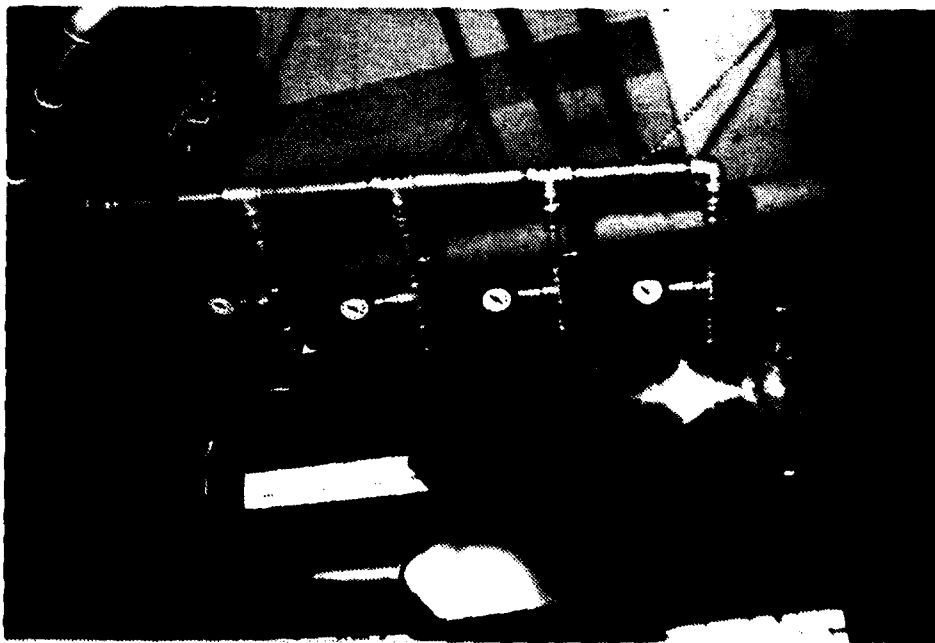


Fig. 5. Scrubbing Section Completed.

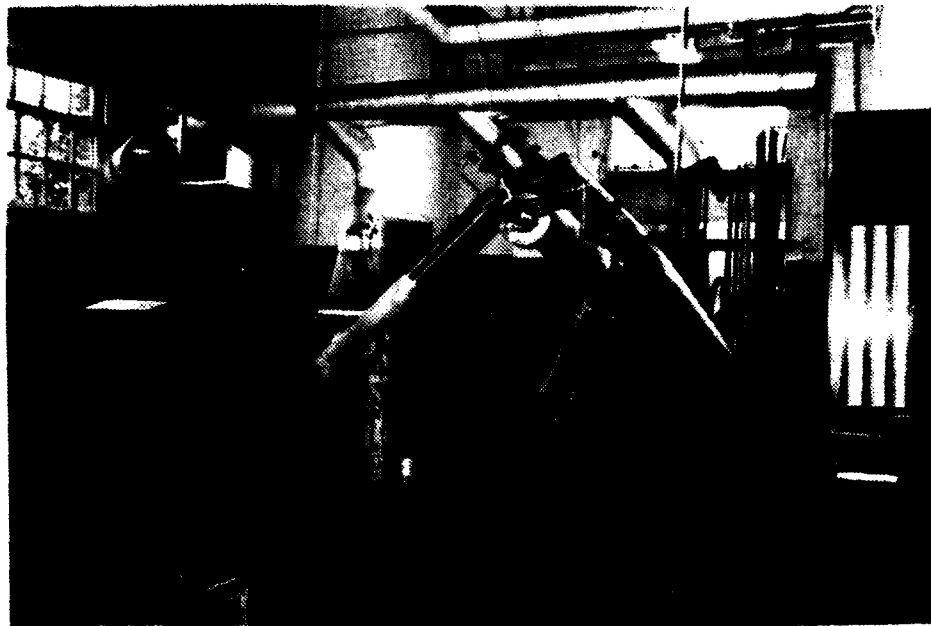


Fig. 6. Complete System. Turbine in Left Foreground, Duct from Turbine Outlet to Scrubbing Section, Scrubbing Section, Water-Disengagement Cyclone with Water Outlet at Lower End and Gas Outlet to Exhaust Fan. The Sample Lines Are Taken Off at the Cyclone Outlet. Fuel Control Panel is Partially Shown at the Right and the Gas Sample Conditioner is in the Center.

TABLE 1. SCRUBBER TEST VARIABLES

<u>FUEL VARIABLES</u>	<u>INDEPENDENT OR DEPENDENT</u>	<u>MEASUREMENT METHOD</u>
Kerosene/Toluene Ratio	I	Volume %
Hydrogen Content, %	I	Total Carbon Diff. Method
Flow Rate, lb/hr	D	Volumetric Burret & S.G.
 <u>ENGINE VARIABLES</u>		
Power Output, kw	I	Wattmeter
Frequency, % of 400 H	I	Panel Meter
Combustor Temp., °F	D	Thermocouple
Turbine Exhaust Temp., °F	D	Thermocouple
Turbine Exhaust Velocity, fpm	D	Pitot Tube
 <u>POLLUTION CONTROL SYSTEM VARIABLES</u>		
Water Flow, gpm	I	Pressure Gage & Curves
Cyclone Outlet Temp., °F	D	Thermocouple
CO ₂ Concentration	D	NDIR
NO _x Concentration	D	Chemiluminescence
CO Concentration	D	Reagent Tube
Smoke No.	D	SAE, ARP 1179 A

It was determined during trial runs that the smallest nozzle was the only one needed for the full range of tests. At 10 psi, 0.5 gpm, the water was all evaporated in the scrubber at full load. At 60 psi, 1.2 gpm, the nozzle put out enough water that the cyclone was at maximum equilibrium for water drainage. Any additional scrubbing water would have overloaded the cyclone demister and allowed an accumulation of water in the cyclone. Four water flows were set for the scrubbing system, 0 gpm (0 psi) which was taken as "no scrubbing system" and the exhaust gas was assumed to be untreated, 0.5 gpm (10 psi), 0.96 gpm (30 psi), and 1.2 gpm (60 psi).

A complete block experiment was selected, 3 fuels at 3 loads with 4 water flow rates. This resulted in $3 \times 3 \times 4 = 27$ runs for the complete test series. The runs were not randomized but were run for individual fuel mixes. This avoided continual purging and cleaning of the fuel system.

C. SCRUBBER TEST PROCEDURE

The tests required at least two persons to operate the turbine, sampling, and measuring systems. The SAE Smoke Number measurement requires four filters during each run. This required one person, full time.

Some data were obtained before the test run was started. These included initial filter reflectance, fuel H/C ratios, ambient temperatures and pressures, and background data such as date, time, and personnel.

Once the system was started it was operated at the set test conditions until temperatures and CO₂ concentration stabilized. The data were then collected and the required four filters obtained for Smoke Number. Water samples were collected at the cyclone outlet for future analysis by the Water Quality Study Team (see Section IIIF.). When the run was completed the system was shut down and the filters were measured to determine the reflectance of the smoke spot.

The operational checklist for the system and a blank data sheet are included in Appendix A.

D. RESULTS AND DISCUSSION - GAS CLEANING

Preliminary runs had been made on the system before the scrubber was installed. These were made to determine how the SAE Smoke Number, CO₂, and turbine outlet temperature varied with fuel mixture and load. A copy of the significant data and results is included in Appendix A. An analysis of variance was run on the data and the SAE Smoke Number was found to vary significantly (5 percent level) with the fuel mixture and load. Figure 7 on the following page shows this dependency. Turbine outlet temperature, and the CO₂ content of the exhaust were only a function of the load on the turbine and were not affected by variations in fuel compositions used in this study. Table 2 lists the mean values of the turbine outlet temperatures and CO₂ for the three turbine loads tested. The variations in the turbine outlet temperatures and CO₂ appeared to be random and could probably be attributed to the variation in ambient conditions of temperature, pressure, and humidity.

The test runs on the wet scrubber were made at only three fuel mixes because the preliminary tests indicated approximately a linear increase of SAE Smoke Number with increasing toluene percentage. The tests were run during the late summer and fall of 1981. A copy of significant data is included in Appendix A.

A size determination was made on the particulate emission using a cascade impactor (Pilat Mk III). The log-mean diameter was 0.092 microns and the standard geometric deviation was 10.3. These values agree with those reported by others for jet engine exhaust emissions (Reference 3). The size determination is shown in Appendix A.

An analysis of variance (ANOVA) was run on the data and the SAE Smoke Number was found to vary significantly (5 percent level) with the fuel mixture and the load on the turbine. The ANOVA did not show a

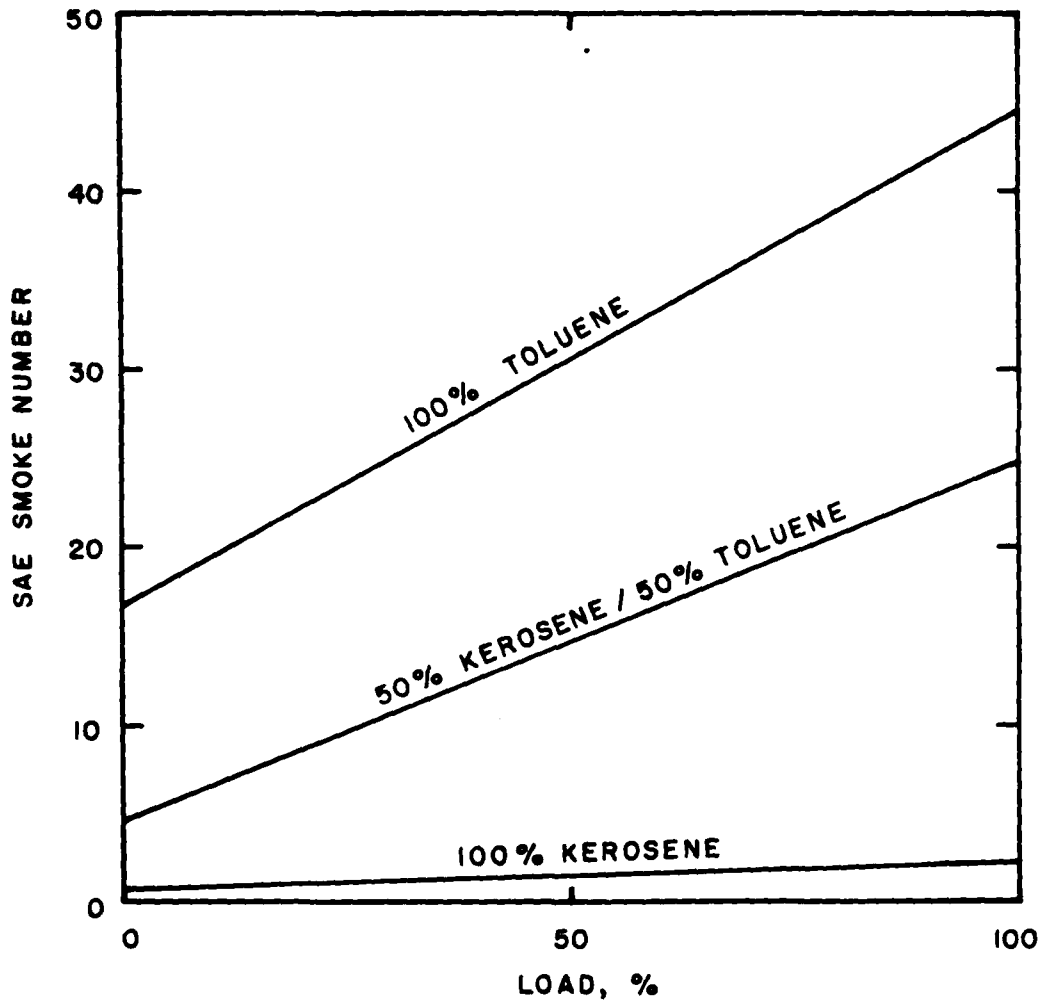


Fig. 7. SAE Smoke Number as a Function of Fuel and Load.
(Linear Regression of Data)

TABLE 2. MEAN VALUES OF TURBINE OUTLET TEMPERATURE AND CO₂ OBTAINED IN PRELIMINARY TESTS

TURBINE LOAD	TURBINE OUTLET TEMP., °F	CO ₂ , %
0	440	1.45
1/2	589	1.99
Full	815	2.91

significant variation (5 percent level) of the SAE Smoke Number with the amount of water used in the scrubber. The SAE Smoke Number remained essentially the same at all values of water flow. Even when no water was sprayed into the scrubber the SAE Smoke Number did not vary from those obtained with water added. This would appear to contradict previous studies (Reference 4) which indicated scrubbing efficiencies in jet engine test cells were significant ("at 95 percent rpm for a J75-P17 engine, the removal efficiencies ranged from 28 percent at a flow rate of 1900 L/min to 55 percent at a flow rate of 3700 L/min"). This same study states, "... water injected into test cells for structural cooling removes a substantial portion of engine-generated exhaust particles that cause test cells to violate opacity regulations."

There appears to be a contradiction within this study because the water collected at the cyclone drain did contain considerable material which discolored it. If the SAE Smoke Number did not change as the water flow was varied from zero to maximum, why did particulate removal occur in the scrubber-cyclone system? The answer was found in an article by A.J. Teller (Reference 5). He was measuring the particulate discharged from jet engine test cells, not the particulate collected in the cooling water. He states, "With cooling of the exhaust gas, (by quench water at the augmentor) the particulate loading is 10-100 percent greater than that measured at the engine because of condensation of hydrocarbons." The OSU tests, like those of Teller (Reference 5), measured the discharged particulate, which was composed of both carbon and unburned hydrocarbons. As the water flow rate was increased, it resulted in more hydrocarbons, because of condensation due to the lowered exhaust gas temperature. If the amount of condensed hydrocarbons approximated the amount of particulate removed by the water spray, the SAE Smoke Number would remain essentially the same. Therefore, both papers (References 4 and 5), and the results of this study can be assumed correct.

The cyclone outlet temperature was very dependent upon the amount of water added in the scrubber. Figure 8 shows this reduction in outlet temperature as a function of water pressure and fuel flow. The curve was plotted versus fuel flow, instead of percent load because ambient temperature variations caused fuel flow, and load, variations.

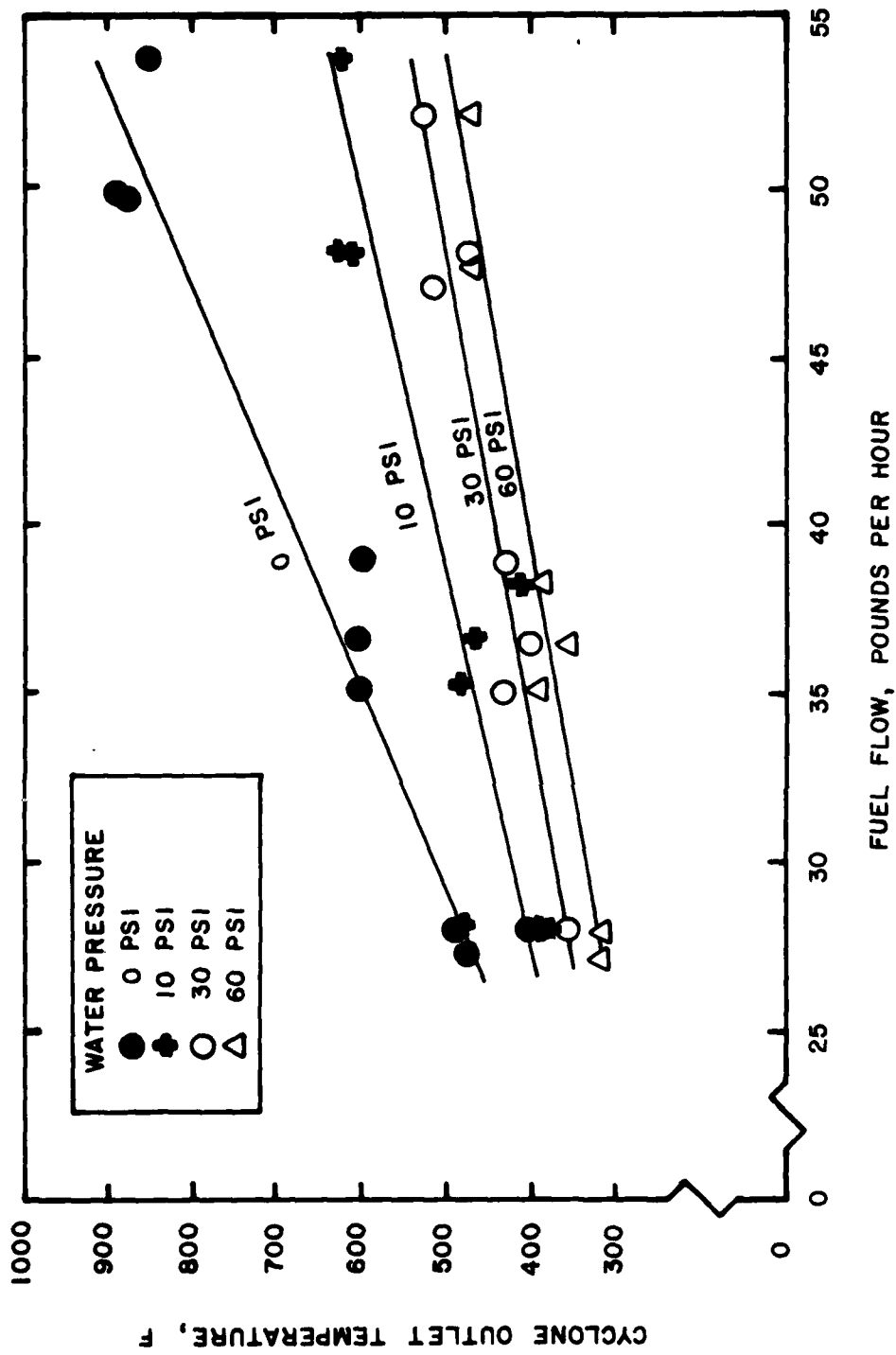


Fig. 8. Cyclone Outlet Temperature as a Function of Water Pressure and Fuel Flow.

The regression equations of the data shown in Figure 8 were of the form:

$$\text{Cyclone Outlet Temp., } ^\circ\text{F} = A + B (\text{fuel flow, lb/hr})$$

The values of the constants, and the regression coefficients, are shown in Table 3 for each water pressure.

TABLE 3. LINEAR REGRESSION CONSTANTS AND COEFFICIENTS FOR DATA SHOWN IN FIGURE 8.

WATER PRESSURE, psi	ZERO INTERCEPT "A"	SLOPE "B"	REGRESSION COEFFICIENT "r"
0	15.66	16.61	0.9815
10	149.46	0.05	0.8928
30	159.18	7.03	0.9688
60	128.66	6.88	0.9760

Figure 9 shows the average temperature drop across the scrubber for each load. Since the analysis of variance did not show a significant variation (5 percent level) in the temperature drop for different fuels, the data were averaged and the mean values used to plot the curves shown in Figure 9. With the exception of the 0 psi curve (no water through the scrubber) the data appear curvilinear.

Several dependent variables did not vary significantly (5 percent level) with variations in fuel composition (from 100 percent kerosene to 100 percent toluene). These are shown in Table 4, and are in excellent agreement with the preliminary run data shown in Table 2.

TABLE 4. DEPENDENT VARIABLES AS A FUNCTION OF TURBINE LOAD.

TURBINE LOAD	COMBUSTOR TEMP., $^\circ\text{F}$	TURBINE EXHAUST TEMP., $^\circ\text{F}$	EXHAUST GAS VOLUME, ACFM	CO ₂ , %	CO, ppm
0	860	461	1473	1.48	640
1/2	1145	595	1700	2.09	400
full	1565	848	1959	3.00	260

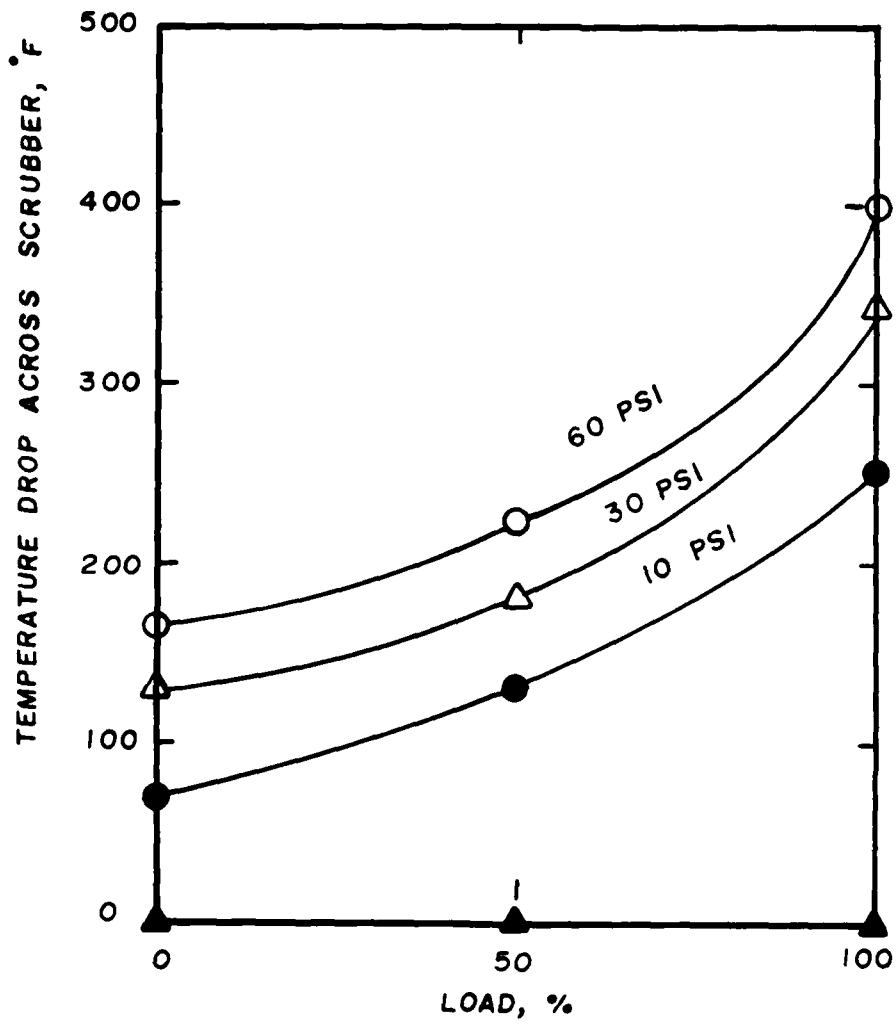


Fig. 9. Temperature Drop Across Wet Scrubber as a Function of Water Pressure and Load.

If the exhaust gas volumes, shown as actual cubic feet per minute in Table 3, are corrected to standard temperature (68°F), they indicate that an average of 829 standard cfm of exhaust gas was generated by the turbine.

The values of combustor temperature (taken just before the turbine) and carbon monoxide are in agreement with values reported by other authors for gas turbine engines (Reference 6). These values indicate that the CO decreases as combustor temperature increases, which is an expected result. Jet engines also show a decrease in CO with increasing load. Unburned hydrocarbons were not measured as a part of this study.

Since no significant variation (5 percent) level was determined for the analysis of variance performed on SAE Smoke Numbers for different water quantities, the only significant variables were fuel composition and load on the turbine. Figure 10 shows the dependency of SAE Smoke Number on load for the three fuel mixtures tested.

The regression equations of the data shown in Figure 10 were of the form:

$$\text{SAE Smoke Number} = A + B (\text{fuel flow, lb/hr})$$

The values of the constants and the regression coefficients are shown in Table 5 for each fuel mixture.

TABLE 5. LINEAR REGRESSION CONSTANTS AND COEFFICIENTS FOR DATA SHOWN IN FIGURE 10.

FUEL MIXTURE	ZERO INTERCEPT "A"	SLOPE "B"	REGRESSION COEFFICIENT "r"
100% Kerosene	- 0.969	0.0643	0.909
50/50	-22.735	0.9877	0.930
100% Toluene	-13.424	1.1045	0.985

Table 6 shows the mean values of SAE Smoke Number for the different fuels and loads.

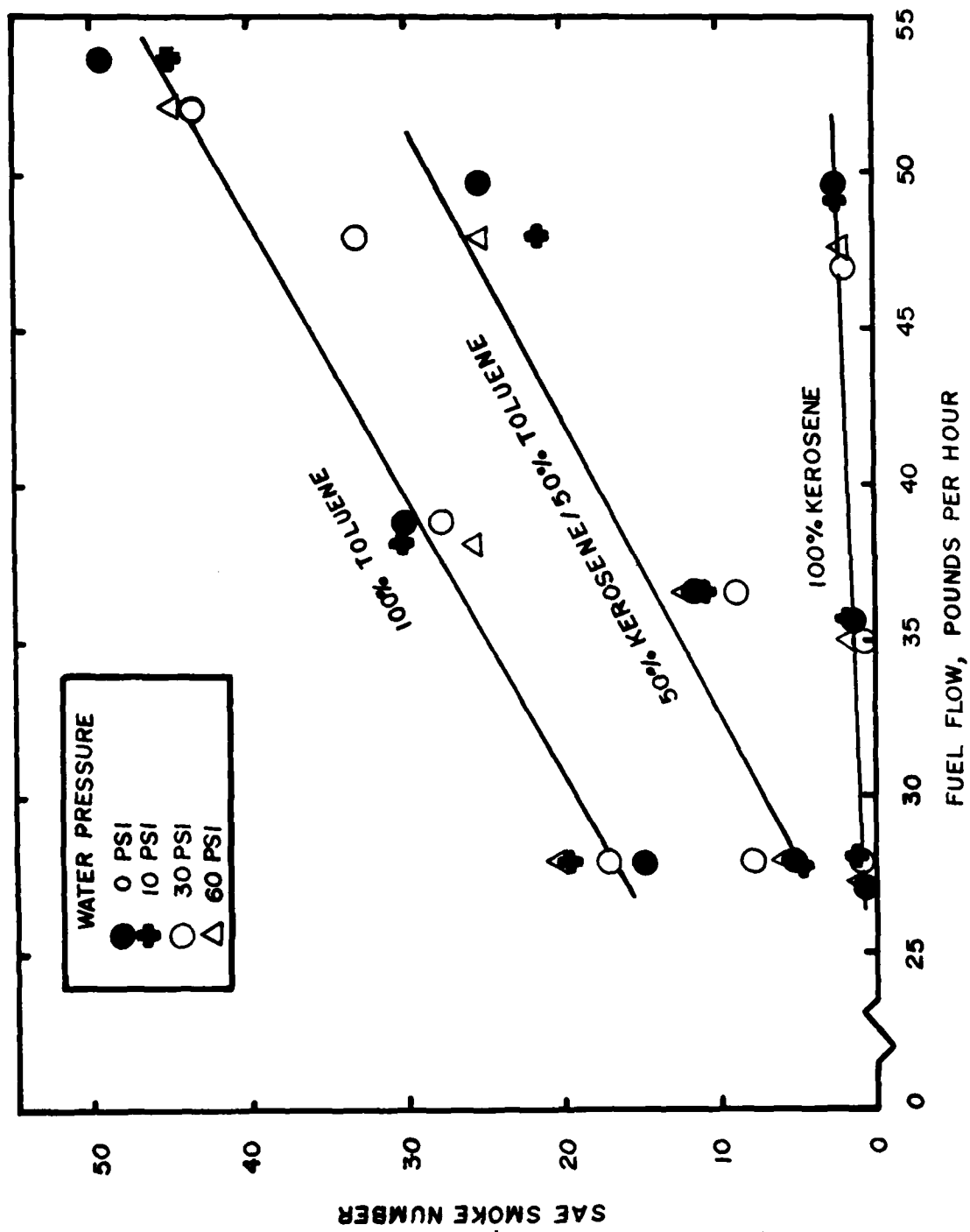


Fig. 10. SAE Smoke Number as a Function of Water Pressure and Fuel Flow.

TABLE 6. SAE SMOKE NUMBER AS A FUNCTION OF FUEL MIXTURE AND LOAD.

FUEL	LOAD	0	50	100
100% Kerosene		0.8	1.3	2.1
	50/50	6.3	10.9	26.2
100% Toluene		18.0	28.3	45.4

If the data in Table 6 are used as input to another series of linear regression equations of SAE Smoke Number on load (0, 0.5, 1.0) and fuel mixture, the values of the constants and the regression coefficients are as shown in Table 7.

TABLE 7. LINEAR REGRESSION CONSTANTS AND COEFFICIENTS FOR DATA FROM TABLE 6.

FUEL MIXTURE	ZERO INTERCEPT "A"	SLOPE "B"	REGRESSION COEFFICIENT "r"
100% Kerosene	0.75	0.013	0.991
50/50	4.52	0.199	0.955
100% Toluene	16.86	0.274	0.990

If a linear regression of the SAE Smoke Number is run on the aromatic content of the fuel, for the different turbine loads, an equation is generated in the form:

$$\text{SAE Smoke Number} = A + B (\text{aromatic content, \%})$$

The values of the constants and the regression coefficients are shown in Table 8 for the different loads.

TABLE 8. LINEAR REGRESSION CONSTANTS AND COEFFICIENTS FOR DATA FROM TABLE 6 FOR AROMATIC FUELS.

TURBINE LOAD, %	ZERO INTERCEPT "A"	SLOPE "B"	REGRESSION COEFFICIENT "r"
0	-0.233	0.172	0.9790
50	0	0.270	0.9864
100	2.917	0.433	0.9979

E. CONCLUSIONS - GAS CLEANING

The most important conclusion that can be made from this laboratory study is:

Scrubbing of gas turbine and jet engine exhaust with water spray systems may not decrease the loading of visible particulate in the exhaust. This is because the water spray removes a portion of the particulate and cools the exhaust, with resultant condensation of hydrocarbons, adding to the particulate loading. The overall net effect could vary from a decrease in particulate to an actual increase in particulate. The specific scrubber system used for this project showed neither a particulate increase nor decrease so it must be concluded that the particulate removal was offset by the formation of condensed hydrocarbon particulate.

Other conclusions that can be drawn from this study are:

1. The combustor temperature, and turbine exhaust temperature do not vary significantly as fuel aromatic content changes. They are only a function of load on the turbine.
2. The CO₂ and CO emissions do not vary significantly as fuel aromatic content changes. They are only a function of load on the turbine.
3. The SAE Smoke Number of the exhaust emissions varies directly with load and aromatic content of the fuel. The variation appears linear with both the load and the percent aromatics.

F. WATER QUALITY STUDY

The purpose of the water quality study were to first characterize the scrubber waters in terms of typical water quality parameters and to then evaluate the treatability of these waters for removal of significant pollutants. To evaluate both the initial water quality and that of the treated waters, comparison is made with typical values of water quality parameters for municipal wastewaters.

Treatability of the wastewater was evaluated in terms of both biological and physical-chemical treatment processes. In addition, a gas chromatographic study was made to determine the concentrations of unburned fuel and polynuclear aromatic hydrocarbons in the scrubber waters.

All scrubber waters tested are identified in terms of the type of fuel burned and the operating conditions of the combustion process.

1. Chemical Characterization of Water Scrubber Samples

Scrubber waters were analyzed for a full range of water quality parameters to characterize them chemically and to determine their extent of contamination. Parameters measured included pH, solids (total, dissolved, suspended, and their volatile fractions), chemical oxygen demand (COD), biochemical oxygen demand (BOD), total organic carbon (TOC), and alkalinity.

Scrubber waters analyzed included those from a full range of turbine operating (test) conditions and fuel ratios in terms of percent kerosene (K) and toluene (T). Table 9 summarizes solids analyses and Table 10 summarizes other water quality parameter values for the test scrubber waters. It is useful to discuss these results in the context of a typical municipal wastewater.

Solids data in Table 9 indicate that gross contamination of the scrubber waters did not occur. Total solids were typical of a weak municipal wastewater. The total solids were predominantly comprised of dissolved solids and the volatile fraction of dissolved solids was in the 25-40 percent range. The generally low values of suspended solids indicated little removal of particulate matter by the scrubber waters. Apparently, the major fraction of combustion residues removed by the scrubbers from the exhaust gases are volatile organic compounds in gaseous form that dissolve in the scrubber waters and form volatile dissolved solids (Corvallis tap water used for scrubber waters has a volatile dissolved solids content < 5 mg/l).

Chemical water quality parameters for the scrubber waters are summarized in Table 10. All parameters were not measured on each sample because of the duplication of test conditions for many samples.

pH values of samples were measured to determine whether acidic or basic components generated in the combustion process would alter the pH of scrubber waters. The results reported in Table 10, reveal that the pH values of the scrubber waters are not appreciably different from Corvallis tap water. This indicates that little or no acidic or basic inputs to the scrubber waters occurred.

As a further check on possible effects of exhaust gas inputs on the buffering capacity of the scrubber water, alkalinity measurements were made on a selected number of samples. In all cases, results indicated that scrubber waters remained unchanged from Corvallis, tap water, thus confirming the lack of significant acidic or basic components in the exhaust gases.

TABLE 9. SOLIDS ANALYSIS OF SCRUBBER WATERS¹

SAMPLE I. D.	TOTAL SOLIDS	TOTAL		VOLATILE		TOTAL		VOLATILE	
		VOLATILE SOLIDS	DISSOLVED SOLIDS	DISSOLVED SOLIDS	SUSPENDED SOLIDS	DISSOLVED SOLIDS	SUSPENDED SOLIDS	DISSOLVED SOLIDS	SUSPENDED SOLIDS
6	390	174	402	166	< 8	< 8	< 8	< 8	< 8
7	138	52	160	62	< 8	< 8	< 8	< 8	< 8
7	192	70	210	94	< 8	< 8	< 8	< 8	< 8
8	190	58	138	40	12	12	< 8	< 8	< 8
8	212	72	208	58	14	14	< 8	< 8	< 8
9	352	116	218	48	< 8	< 8	< 8	< 8	< 8
9	210	68	310	82	12	12	< 8	< 8	< 8
10	120	54	160	62	< 8	< 8	< 8	< 8	< 8
11	172	42	150	24	< 8	< 8	< 8	< 8	< 8
12	218	116	172	30	< 8	< 8	< 8	< 8	< 8
15	306	98	260	50	30	30	< 8	< 8	< 8
16	1094	216	548	230	200	200	24	24	24
23	362	118	356	106	16	16	< 8	< 8	< 8
25	214	56	176	42	< 8	< 8	< 8	< 8	< 8
26	238	130	252	58	56	56	22	22	22
27	226	88	222	76	24	24	18	18	18
28	214	62	206	56	50	50	46	46	46
T-1	920	772							
T-1	768	528							
T-2	410	348							
T-2	468	428							
T-3	542	392							

¹All results average of duplicate analyses, in mg/l.

TABLE 10. CHEMICAL CHARACTERIZATION OF SCRUBBER WATERS

SAMPLE I.D.	FUEL		TEST CONDITIONS			ALKALINITY mg/l as C _a CO ₃	pH	TOC mg/l	COD mg/l	BOD mg/l
	% K	% T	psi	LOAD	Pressure					
4	100	0	10	None		5.86	62			
7	100	0	30	None		6.57	40			
7	100	0	30	None		6.56	55			
8	100	0	30	Half		6.77	25			
8	100	0	30	Half		6.74	30			
9	100	0	30	Full		7.18	22			
11	100	0	60	Half		7.2				
15	50	50	10	Half		7.17				
17	50	50	30	Half		6.96				
23	0	100	10	Half	51.9	6.72	50			
25	0	100	30	Half		6.74	22			
26	0	100	10	Full		7.69	38			
28	0	100	60	Full		7.22	21			
1	50	50	30	Half		7.72			53	
2	50	50	30	Half		7.60			41	
-	0	100	30	Half					46	
-	0	100	30	Full					142	
-	0	100	60	Half					47	
-	0	100	60	None					167	
-	0	100	60	Full					172	
-	0	100	30	None					141	
-	0	100	10	None					55	
-	0	100	10	Half					45	
-	100	0	30	Half					20	
-	100	0	30	Full					33	
-	100	0	60	Full					80	
-	100	0	60	Half						
-	100	0	60	None						

(Continued)

TABLE 10. CHEMICAL CHARACTERIZATION OF SCRUBBER WATERS (Continued)

SAMPLE I.D.	FUEL		TEST CONDITIONS			ALKALINITY mg/l as C_aCO_3	pH	TOC mg/l	COD mg/l	BOD mg/l
	% K	% T	PRESSURE, psi	LOAD						
-	50	50	30	Half				270		
-	50	50	30	Half				90		
-	50	50	60	Half				50		
-	50	50	10	Full			59	130		
-	50	50	10	Half				100		
-	50	50	30	Full				60		
-	50	50	60	Full				40		
-	50	50	10	None				190		
-	50	50	30	None				155		
-	50	50	60	None				125		
5-1	-	-	-	-				195		
5-2	-	-	-	-		35.6	7.22	120		
5-3	-	-	-	-				120		
5-4	-	-	-	-			7.45	117		
T-1	-	-	-	-		53.4	7.56	19	55	< 5
T-1	-	-	-	-		45.2	7.58	20	40	< 5
T-2	-	-	-	-		49.5	7.54	16	27	< 5
T-2	-	-	-	-		50.0	7.52	14	24	< 5
T-3	-	-	-	-		38.5	7.59	18	31	< 5
Corvallis Tap Water						35-50	6.6-7.6	< 1	< 5	< 1

The remaining three parameters measured for the scrubber waters, TOC, COD, and BOD, were intended to quantify the organic carbon content of the scrubber waters. TOC is a measure of organic carbon, regardless of the oxidation state of the carbon, and hence its potential energy yield by biochemical oxidation reactions. COD provides a measure of the potential energy yield of carbon compounds present, but does not measure biodegradability. BOD provides an estimate of the biochemically available energy yield of the organic compounds present. The three parameters can be used comparatively to derive much useful information regarding the treatability of the scrubber waters by conventional biological treatment processes.

Results of the TOC, COD, and BOD analyses when compared to municipal wastewaters indicate that the scrubber waters are very dilute or low-strength organic wastes. For a weak municipal wastewater, typical values of TOC, COD, and BOD₅ would be 100 mg/l, 250 mg/l, and 100 mg/l, respectively. Values measured for TOC and COD for the scrubber waters range from about 15 to 60 percent of the weak municipal wastewater.

COD to TOC ratios are typically in the range of 2.5-3.0 for municipal wastewaters. Values of the ratio below this indicate an organic waste that is highly oxidized, relative to the proteins and carbohydrates of municipal wastewaters, while higher values of the ratio indicate a less oxidized organic waste. The average ratio for the scrubber waters, based on six representative samples, was 2.0. Thus, the organic carbon in the scrubber waters is in a relatively oxidized state and would have a lower energy yield in biochemical oxidation reactions than an equivalent amount of carbon in a municipal wastewater.

BOD₅ results for the scrubber waters are very questionable but appear to indicate that the organic carbon in the scrubber waters was largely nonbiodegradable. The BOD test was very difficult to run effectively for the scrubber waters because it was necessary to acclimatize the bacterial culture first before inoculating the test bottles. Acclimatization was achieved by operating a fill-and-draw aerated reactor for 10 days using increasing ratios of scrubber water/primary effluent (Corvallis municipal system) as the feed. The biological solids concentration decreased sharply toward the end of the acclimatization period which could be attributed to the dilute strength of the water but perhaps was aggravated by the organic carbon being nonbiodegradable. The biotreatability study reported in a later section tends to confirm the nonbiodegradable nature of the scrubber water organics.

2. Biotreatability of Scrubber Waters

Chemical characterization of the scrubber waters determined that they would generally be classified as very dilute wastewaters, based on carbon content. The waters were also low in suspended solids, indicating that most of the scrubber water constituents were in dissolved forms. BOD test results demonstrated a low biochemically available fraction for the organic carbon, but acclimating the bacterial culture to scrubber waters was difficult because of their dilute nature. Based on the above, it was decided to determine the biotreatability of the scrubber waters in

a fill-and-draw reactor system taking care to allow adequate acclimation time for the bacterial culture.

The biotreatability study consisted of laboratory-scale reactors operated in a completely mixed mode by diffused aeration. An activated sludge bacterial culture was obtained from the aeration channel at the Corvallis, Oregon, Wastewater Reclamation Plant. The bacterial culture was placed under aeration in the reactor and operated on a fill-and-draw feeding and wasting schedule which typically consisted of: 23 hours aeration; 1-hour settling; decanting of supernatant; addition of feed solution with nutrients and buffering; resume aeration. The reactor operating volume was 1 liter. Nutrients consisted of a 1N NH_4Cl stock solution added to achieve 30 mg/l $\text{NH}_3\text{-N}$ in the reactor and a 1N $\text{KH}_2\text{PO}_4\text{-K}_2\text{HPO}_4$ stock solution (pH = 7.2) added to achieve 10 mg/l $\text{PO}_4\text{-P}$ in the reactor and also to provide buffering.

The feed solution consisted of filtered primary effluent from the Corvallis Wastewater Reclamation Plant and scrubber waters such that the ratio of primary effluent/scrubber water was decreased by a schedule over the duration of the test.

Bacterial solids wasting occurred immediately prior to the 1-hour settling period. One-third of the completely mixed volume of the reactor was wasted to achieve a nominal solids retention time (sludge age) of 3 days. However, after 5 days operation, when the scrubber water fraction of the reactor feed solutions reached 50 percent, wasting of bacterial solids was discontinued due to the decreasing solids content in the reactors. The initial solids content in all reactors was 840 mg/l but this value decreased to an average of 130 mg/l after the 11-day test period.

The three scrubber waters selected for bioavailability testing were considered representative of the range of test conditions used for the gas turbine. The chemical characterization results and the turbine test conditions for the three scrubber waters were previously summarized in Tables 9 and 10 and identified as samples T-1, T-2, and T-3.

Results of the 11-day biotreatability study for the three scrubber waters are reported in Tables 11, 12, and 13 for test water samples T-1, T-2, and T-3, respectively. Results are summarized in terms of percent COD reduction, since the influent COD values to the reactors necessarily changed as the ratio of scrubber water to primary sewage effluent changed. COD removal percentages for all three scrubber waters followed a similar pattern of decreasing removal over the duration of the test. Initially, high COD removal was achieved when the influent (feed) to the reactors was predominantly primary sewage effluent. As the percentage of primary sewage in the influent to the reactors decreased, so did percent COD of removal. The bacterial culture appeared to be unable to adapt to the scrubber waters; thus, COD removal of the scrubber water fraction of the influent feed solution was minimal. The rapid decrease in bacterial solids content of the reactors is further evidence of the nonbiodegradability of the scrubber water organics. The biotreatability studies thus support the results of the BOD tests and strongly suggest that the organic

TABLE 11. BIOTREATABILITY RESULTS FOR SCRUBBER WATER T-1¹

DAYS OF OPERATION	% PRIMARY EFFLUENT	INFLUENT COD ² , mg/ℓ	EFFLUENT COD ² , mg/ℓ	% COD REMOVAL
1	90	88	16	82
2	90	88	17	81
3	70	75	18	80
4	70	75	16	79
5	50	58	16	72
6	50	58	17	71
7	50	58	16	72
8	30	45	16	64
9	30	45	28	38
10	10	34	25	26
11	10	34	26	24

¹Test Conditions: Fuel 100% Toluene
 Pressure 30 psi
 Full Load

²COD of filtered (Whatman GF-C) samples.

TABLE 12. BIOTREATABILITY RESULTS FOR SCRUBBER WATER T-2¹

DAYS OF OPERATION	% PRIMARY EFFLUENT	INFLUENT COD ² , mg/l	EFFLUENT COD ² , mg/l	% COD REMOVAL
1	90	87	25	71
2	90	87	23	74
3	70	73	20	73
4	70	73	22	70
5	50	53	17	68
6	50	53	16	70
7	50	53	16	70
8	30	39	17	56
9	30	39	18	54
10	10	31	28	10
11	10	31	29	6

¹Test Conditions: Fuel 50% Toluene, 50% Kerosene
 Pressure 30 psi
 Full Load

²COD of filtered (Whatman GF-C) samples.

TABLE 13. BIOTREATABILITY RESULTS FOR SCRUBBER WATER T-3¹

DAYS OF OPERATION	% PRIMARY EFFLUENT	INFLUENT COD ² , mg/ℓ	EFFLUENT COD ² , mg/ℓ	% COD REMOVAL
1	90	87	20	77
2	90	87	19	78
3	70	74	18	76
4	70	74	16	78
5	50	56	16	68
6	50	56	17	66
7	50	56	16	68
8	30	43	25	47
9	30	43	30	30
10	10	32	29	9
11	10	32	29	9

¹Test Conditions: Fuel 100% Kerosene
 Pressure 30 psi
 Full Load

²COD of filtered (Whatman GF-C) samples.

compounds in the scrubber waters are refractory to biological treatment.

3. Physical-Chemical Treatability of Scrubber Waters

Two physical-chemical treatment processes were investigated for COD removal from the scrubber waters. The processes, evaluated separately, were coagulation with alum and adsorption with activated carbon. The scrubber waters were the same three as those tested for biotreatability.

Coagulation tests were conducted, using a standard, six-place jar test apparatus. The apparatus consists of a stirring paddle mechanism with variable speed drive and six separate reactors of 1-liter volume that are simultaneously mixed at the same speed. Conditions similar to those of full-scale coagulation processes can be simulated, including rapid mixing of chemical, slow mixing to promote flocculation, and quiescent conditions to simulate sedimentation basins.

The specific procedure used in the coagulation jar tests was as follows:

1. Place 1-liter sample in 1.5-liter beaker reactor.
2. Begin rapid mix at 100 rpm.
3. Add alum from stock solution (1000 mg/l as $\text{Al}(\text{OH})_3(\text{s})$) to achieve desired dose.
4. Add base (1N NaOH) as required to raise pH to 6.0.
5. Decrease stirring speed to 15-30 rpm for 30-60 minutes. Observe flocculation.
6. Stop stirring and remove stir bars. Settle for 1-2 hours.

Alum was selected as the coagulant of choice because of its common application in water and wastewater treatment. Use of a clay (kaolin) coagulant aid was also investigated. Alum forms a polymeric structure of aluminum hydroxide complexes when dissolved in water. At a pH value below about 5.0, the aluminum polymers are negatively charged, while above this pH value they are positively charged. At a pH value of 6.0, the point of zero charge, the net charge is neutral. The organic materials removed from the turbine combustion gases, predominantly highly oxidized structures containing oxygen, are expected to be neutral in charge when removed in the scrubber waters. Thus, the pH of alum coagulation was maintained at 5.0 to maximize the affinity of the neutral organic compounds for a neutrally charged coagulant suspension. The organic materials in the scrubber waters were mostly dissolved in form. Coagulation would be expected to be effective in removing the suspended solids and the high molecular weight dissolved forms. Lower molecular weight dissolved organic compounds, especially those in an oxidized form containing oxygen, would not be expected to be effectively removed by alum coagulation.

Results of the alum coagulation tests are summarized in Table 14. The three test scrubber waters were first coagulated with alum at two different dosages and then with alum at the lower dosage and adding a clay (kaolin) coagulant aid. Results are presented in terms of effectiveness in reducing the COD of the test waters.

From the results, it is apparent that alum coagulation alone is ineffective in removing COD from the scrubber waters. Thus, according to the expected results based on theory, the COD is comprised predominantly of dissolved, low molecular weight, oxidized chemical forms or high molecular weight, nonadsorbable forms of organic compounds.

Addition of a coagulant aid improved COD removal to between 30-70 percent. This would tend to support the evidence that approximately one-half of the organic compounds are high in molecular weight and colloidal in nature. Unless high-alum doses are applied alone, these organic materials are very difficult to coagulate. However, with use of a coagulant aid to improve floc formation, these materials are more effectively removed.

Adsorption using activated carbon is commonly employed to remove dissolved organic materials. It is effective for dissolved organic compounds with high molecular weights that tend to be hydrophilic in nature. As the molecular weight of dissolved organic compounds decreases, particularly if they contain polar functional groups such as oxygen-containing moieties, activated carbon becomes less effective at removal.

Two forms of activated carbon are commonly used in water and wastewater treatment practice and were tested for their effectiveness with the scrubber waters. Granular activated carbon is typically used in a packed or fluidized column. The columns may be arranged in parallel or series, and in the fluidized mode may be designed for continuous operation with new carbon addition and spent carbon removal occurring without removing the column from operation. Powdered activated carbon is usually added to a completely mixed basin for contact with the water to be treated either on a batch or continuous basis.

For this evaluation, it was only desired to determine whether granular and/or powdered carbon could effectively remove the scrubber water organics over a realistic contact time for wastewater treatment. For this reason, both carbons were tested in completely mixed reactors with an excess of carbon relative to the concentration of organic compounds to be removed so as to avoid approaching saturation of the activated carbon surface. No attempt was made to derive adsorption isotherms or kinetic data.

The specific procedure used in the activated carbon adsorption tests was as follows:

1. Dry carbon at 103°C for 12 hours. Cool and desiccate.
2. Weigh desired carbon dosage and add to Erlenmeyer flask reactor.

TABLE 14. ALUM COAGULATION TREATABILITY TEST¹

SAMPLE I.D. ²	INITIAL COD ³ , mg/ℓ	ALUM DOSE ⁴ , mg/ℓ	CLAY ⁵ DOSE, mg/ℓ	FINAL COD ³ , mg/ℓ	FINAL pH	% COD REDUCTION
T-1	31	20	0	32	6.0	0
T-1	31	40	0	31	6.0	0
T-1	31	20	20	9	6.0	71
T-2	23	20	0	19	6.0	17.4
T-2	23	40	0	23	6.0	0
T-2	23	20	20	15	6.0	35
T-3	28	20	0	28	6.0	0
T-3	28	40	0	30	6.0	0
T-3	28	20	20	19	6.0	32

¹All results are averages of duplicate tests.

²See Table 10 for turbine test conditions.

³COD of filtered (Whatman GF-C) samples.

⁴Alum dose as alum flocc, Al(OH)₃(s).

⁵Kaolin clay used as coagulant aid.

3. Add 250 ml sample and mix on wrist shaker for 4 hours at 25°C.
4. Filter sample (Whatman GF-C) to remove carbon and measure soluble COD.

Results of the activated carbon adsorption tests are summarized in Table 15. The same three scrubber waters were used as for the coagulation and biotreatability studies. Granular activated carbon was added at 1.0 g/l while powdered activated carbon was tested at two concentrations, 0.4 g/l and 5.0 g/l. Results are reported in terms of COD removal effectiveness.

The results of the carbon adsorption tests show a range of 30-83 percent COD reduction in the test scrubber waters for all carbon types and dosages. Powdered activated carbon appeared to be somewhat more effective under the test conditions employed. However, for a 4-hour reaction time, the granular activated carbon systems were unlikely to have achieved an equilibrium distribution between adsorbate and adsorbent, whereas the powdered carbons probably had reached equilibrium.

Based on an average of approximately 50-percent COD removal, it can be surmised that about this same fraction of the organic compounds in the scrubber waters are sufficiently hydrophobic (high in molecular weight and/or nonpolar) to have a greater affinity for the activated carbon surface than for the aqueous solution. Conversely, about one-half of the organics are low molecular weight and polar, thus not being adsorbed and remaining in solution. This supports the results of the coagulation test with coagulant aid added in which a similar range of COD was removed and attributed to the high molecular weight fraction of organic compounds in the scrubber waters.

4. Gas Chromatography Study of Unburned Fuel and Polynuclear Aromatic Hydrocarbons

Scrubber waters were found to be relatively dilute in chemical composition and to be largely nonbiodegradable in BOD and biotreatability studies. This implies that effects on receiving streams, at least from an oxygen budget standpoint, will be minimal. However, the nature of the organic compounds in the scrubber waters may be such that toxic effects are exhibited. Because of the great expense and difficulty of running bioassay tests and the often ambiguous results, it was decided that an analytical approach would be more productive. Therefore, a gas chromatographic study was undertaken to measure concentrations of the toxic constituents most likely to be present from the combustion process.

The organic constituents selected for gas chromatographic analysis were unburned fuel components (kerosene and toluene) and a family of polynuclear aromatic hydrocarbons (PAHs). Unburned fuel was considered a likely fraction of the scrubber water organic compounds as incomplete combustion of fuel is often associated with nonuniform temperature distributions and other nonideal conditions of a combustion engine. PAHs are well-known byproducts of fossil fuel combustion. They are of concern because of their toxic and carcinogenic properties and would require

TABLE 15. ACTIVATED CARBON ADSORPTION TREATABILITY TEST¹

SAMPLE I.D. ²	INITIAL COD ³ , mg/l	GRANULAR CARBON		POWDERED CARBON		FINAL COD ³ , mg/l	% COD REDUCTION
		DOSE, mg/l	DOSE, mg/l	DOSE, mg/l	DOSE, mg/l		
T-1	31	1.0	0	17	45		
T-1	31	0	0.4	13	58		
T-1	31	0	5.0	17	47		
T-2	23	1.0	0	16	30		
T-2	23	0	0.4	15	35		
T-2	23	0	5.0	20	56		
T-3	28	1.0	0	17	39		
T-3	28	0	0.4	13	54		
T-3	28	0	5.0	8	83		

¹All results are averages of duplicate tests.

²See Table 10 for turbine test conditions.

³COD of filtered (Whatman GF-C) samples.

removal by treatment processes prior to disposal should concentrations exceed water quality criteria.

Scrubber waters selected for gas chromatographic analysis were again the same as those used in the treatability studies. Each was analyzed for unburned fuel by one extraction and chromatographic procedure and for PAHs by a separate extraction procedure and two separate chromatographic procedures.

The extraction and chromatographic procedure for unburned fuel is detailed in the following:

900 ml scrubber water was mixed with 25 g Na_2SO_4 . After the salt was dissolved, the mixture was extracted with 9 ml hexane. The hexane extract was dried by passing through $\text{MgSO}_4 \cdot \text{H}_2\text{O}$, then analyzed directly by GC. (Hexane extract was not concentrated to avoid loss of kerosene and toluene.) In control runs, a single hexane extraction recovered 86 percent of the toluene and 98 percent of the kerosene.

Gas chromatograph parameters were as follows:

Column: 10 feet x 1/8 inch stainless steel
Packing: 10 percent SP2100 on 100/120 mesh Sulpoport® (Supelco)
Operation: N_2 carrier, 20 ml/min; 45°C
Flame-ionization detector; Air 200 Kpa,
 H_2 300 Kpa

The extraction and chromatographic procedures for PAHs were as follows:

One thousand ml scrubber water were mixed with 25 g Na_2SO_4 and then extracted three times with 50 ml dichloromethane (DCM). The combined DCM extracts were filtered through MgSO_4 to dry and concentrated to 1-3 ml in a Kuderna-Danish apparatus. Then 3-4 ml cyclohexane was added, the solution concentrated again to 1 ml in the K-D apparatus, and analyzed by GC. The procedure was checked by a sample containing pyrene and the recovery was 60 percent. Compounds determined were fluorene, phenanthrene, anthracene, fluoranthrene, pyrene, benz [a] anthracene, and chrysene.

Gas chromatograph parameters were as follows:

Column: 6 feet x 2 mm I.D. glass
Packing: 3 percent SP2250DB on 100/120 mesh Sulpoport® (Supelco)
Operation: N_2 carrier; 40 ml/min.
Initial temp. 100°C, 8°C/min. to 260°C, then hold.
Flame-ionization detector; Air 200 Kpa,
 H_2 125 Kpa

For the higher molecular weight PAHs an alternative gas chromatographic procedure was used, as follows:

The extraction and concentration procedure is identical with that of the lower molecular weight PAHs. Compounds determined were benzo [a] pyrene, perylene, benzo [a] pyrene, benzo [g,h,i] perylene, and dibenzo [a,h] anthracene. A standard test mixture (PAH-2, Alltech Chemical Co.) containing 10 ppm of the above compounds was used for quantification.

Gas chromatograph parameters were as follows:

Column: 10 feet x 1/8 inch stainless steel
Packing: 10 percent SP2100 on 100/120 mesh Sulpoport®
(Supelco)
Operation: N₂ carrier, 20 ml/min; temp. 330°C
Flame ionization detector; Air 200 Kpa,
H₂ 300 Kpa

Chromatographic scans for unburned fuel components showed no measurable peaks at the retention times of kerosene and toluene in any of the scrubber waters. The lower limit of detection for kerosene was 0.7 mg/l and for toluene, 0.03 mg/l. These negative analyses for unburned fuels indicate either that scrubbers did not effectively remove unburned fuel from the exhaust gases or, more likely, that the combustion processes were highly efficient in burning the fuels.

For the lower molecular weight PAH analyses, chromatographic scans found no detectable amounts at a lower limit of detection of 1 ug/l. Higher molecular weight PAHs, analyzed separately, were also undetectable at a lower detection limit of 1 ug/l. For all chromatographic scans, peaks were detected at retention times other than those for compounds being analyzed. These could simply represent oxidized fuel combustion products with no environmental significance or possibly more exotic organic compounds of environmental concern. A more complete analysis would be required involving gas chromatography-mass spectrometry to identify these unknown organic compounds.

5. Summary and Conclusions - Water Quality Study

Chemical characterization of scrubber waters from a wide range of turbine operating conditions and two different fuels (kerosene and toluene) has revealed that wastewaters equivalent in strength to very dilute municipal wastewater are generated. Solid analyses generally showed very low levels of suspended particulates in the scrubber waters representing predominantly mineral residues. Dissolved solids, incorporating most of the material removed from the turbine exhaust gases, ranged from 15-40 percent volatile matter. The volatile dissolved solids were analyzed as COD and TOC, the ratio of which indicated a more highly oxidized state than typical municipal wastewater organics. No detectable BOD was exerted by the scrubber water organics, indicating that the organic compounds were refractory to the bacterial organisms. pH and alkalinity values of the scrubber waters were unaffected by the scrubbing process.

Biotreatability studies confirmed the refractory nature of the organic compounds in the scrubber waters. Activated sludge bacteria slowly acclimated to the scrubber waters were unable to metabolize the organics for growth or energy requirements.

Both coagulation with alum plus a coagulant aid (kaolin clay) and activated carbon adsorption removed an average of about 50 percent of the scrubber water COD. These physical-chemical processes showed the greatest promise for treating the scrubber waters. More detailed studies employing one or both of these processes are required to optimize COD removal. Chemical oxidation processes were not investigated but may also be feasible because of the dilute strength of the scrubber waters.

Chromatographic analyses for unburned fuel components, kerosene and toluene, and for polynuclear aromatic hydrocarbon compounds in the scrubber waters were below detection limits. No further attempt was made to specifically identify the organic compounds present.

In conclusion, based on oxygen demand and (BOD) only for the scrubber waters tested in this study, no wastewater treatment would be required to meet typical effluent guidelines of 10-30 mg/l BOD. Effluent standards based on COD may dictate some level of treatment is required, particularly if the higher range of COD values was present in a test facility scrubber water. In this case, carbon adsorption treatment, possibly in conjunction with chemical coagulation, should be employed.

G. DATA ANALYSIS AND PERFORMANCE

Concurrently with the evaluation of the wet-scrubbing system as a smoke-removal device an evaluation was made to determine the heat loss through the system, the turbine efficiency, and the extent of evaporation of the scrubber water. All were found to be dependent on the turbine load while the water spray section was found to be adiabatic. This work resulted in an M.S. project for a graduate student, Mr. George D. Ikonou. The full report of this project is published separately as Appendix B.

H. RECOMMENDATIONS

Based upon this study, and work of others, it does not appear that a simple wet-scrubbing system alone can reduce particulate matter in gas turbine or jet engine exhaust enough to result in compliance with opacity or particulate loading regulations. Because additional hydrocarbons are formed by condensation, the simple scrubber should be followed by another device capable of removing submicron particles. This will be reported in the next tests conducted on the wetted sand filter used after a simple scrubber.

It is possible that installation of wet scrubbers on jet engine test cells, or flooding the augmentor section with large quantities of water, has reduced opacity complaints. It is suspected that this is because the wet plume masks the particulate matter, allowing it to disperse sufficiently to be nearly invisible by the time the wet plume evaporates. The observations made at NAS Alameda tend to confirm this suspicion. The wet

plume causes extensive soiling of the area surrounding the test cell, indicating that it still contains a large quantity of particulate as it leaves the test cell exhaust.

The cost of the simple wet scrubber is very low compared to other control devices which could be applied to a test cell. However, if it cannot satisfactorily clean the exhaust, the cost/benefit ratio becomes high because of the small benefit. To operate properly, the simple wet scrubber should be followed by another device in series. This would increase both the "cost" and the "benefit" but could result in a lower cost/benefit ratio.

Teller (Reference 5) estimates that a satisfactory "nucleator system" to collect the fine particulate to meet opacity and loading regulations would cost about \$600,000 (1976 dollars) for a single jet engine test cell capable of handling a 17,000-pound thrust engine. This value appears to be realistic.

SECTION IV

EVALUATION OF WETTED-SAND FILTER

The control device tested and reported in this section was the "SandAir" filter, manufactured by Rader Companies, Inc. of Portland, Oregon. It is a wetted-sand filtration system in which water is sprayed on top of a bed of graded sand. The turbine effluent gas flowed concurrent with the water through the sand bed and the cleaned gas and dirty water were exhausted at the bottom of the system.

The SandAir filter tested was a pilot model-sized cell with a baffled demisting section in the gas stream after the cell. Four spray nozzles were located in the top of the cell, spraying concurrently with the incoming turbine exhaust. A valve and pressure gage in the water line to the spray nozzles allowed the water flow to be varied from zero flow to the maximum (9-1/2 gpm @ 40 psi). The water sprayed into the cell impinged upon the top of the sand, located about midway up the cell. The sand was 2 inches in depth, supported on a stainless steel screen. The water was drained from the cell, after passing through the sand, and the cleaned gas was ducted to a demisting section, where the remaining water was removed. The cleaned gaseous effluent was then exhausted, through a roots blower, to the building exhaust fan. Figure 11 shows the SandAir filter cell with the spray nozzles at the top, the top gas inlet, the demister section, air bypass flow control valve, and roots blower.

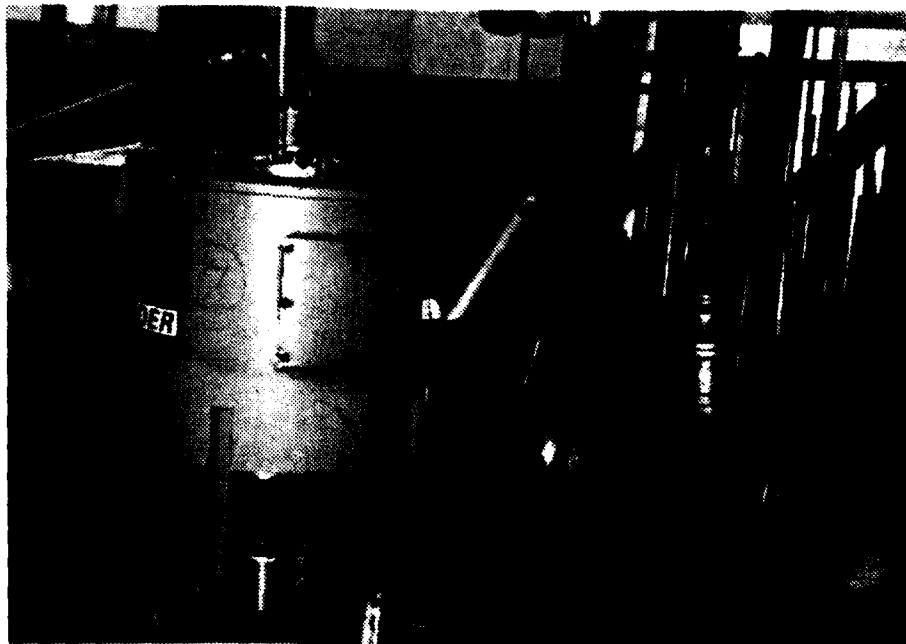


Fig. 11. SandAir Filter System.

Figure 12 shows the demister on the left, the pressure gage which indicated the pressure drop across the SandAir unit, and the bypass flow control valve.

Figure 13 shows the entire system with the turbine at the left, the ductwork from the turbine to the filter, the filter, flow control valve, roots blower, exhaust to the building system, and the heated sampling lines at the gas inlet to the SandAir filter.

The configuration shown in Figure 13 was used to determine the Smoke Number of the inlet sample. For outlet smoke samples, the heated sampling line was connected between the demister and the dilution air bypass valve.

The smoke sample was carried by the heated stainless steel line to the smoke-measuring system. The Smoke Number was determined according to SAE, Aerospace Recommended Practice Specification ARP 1179 A. The smoke filters were analyzed on a B&L Spectronic 20 equipped with a reflectance attachment.

A schematic flow diagram for the test facility is shown in Figure 14.

A. EXPERIMENTAL DESIGN

The variables measured during the test are shown in Table 16. Also measured were the wet and dry bulb ambient temperature and the barometric pressure.

Preliminary runs indicated that 100 percent kerosene fuel resulted in such a low Smoke Number at both zero load and full load that it would not be useful to test with such a clean effluent. Figure 15 indicates the SAE Smoke Numbers for the three fuel mixes.

The gas flow through the SandAir filter was determined by a pitot traverse in the duct leading to the filter. The filter unit was operated at its design point of 100 feet per minute face velocity at 3 different water flow rates. Figure 16 shows the velocity traverse being conducted.

Two separate experiments were designed, based on the preliminary runs. The first design varied turbine load (zero and full loads), the fuel mix (50/50 and 100 percent toluene), and the water flow rate through the spray nozzles (2.9, 4.5, and 5.7 gpm). The gas flow to the SandAir filter was maintained at 450 actual cfm for all runs. This was accomplished by setting the pressure drop across the SandAir filter at 18 inches of water for zero load and 10 inches of water for full load. A complete block experiment was selected. This resulted in $2 \times 2 \times 3 = 12$ runs for the test series.

The second experiment was run to determine if the change in pressure drop across the SandAir filter, which changed the gas volume through the filter, changed the efficiency of the filter for smoke removal. The water flow was held constant at 2.9 gpm and the fuel was 100 percent toluene for four tests. Two were made at zero load (300 acfm and 475

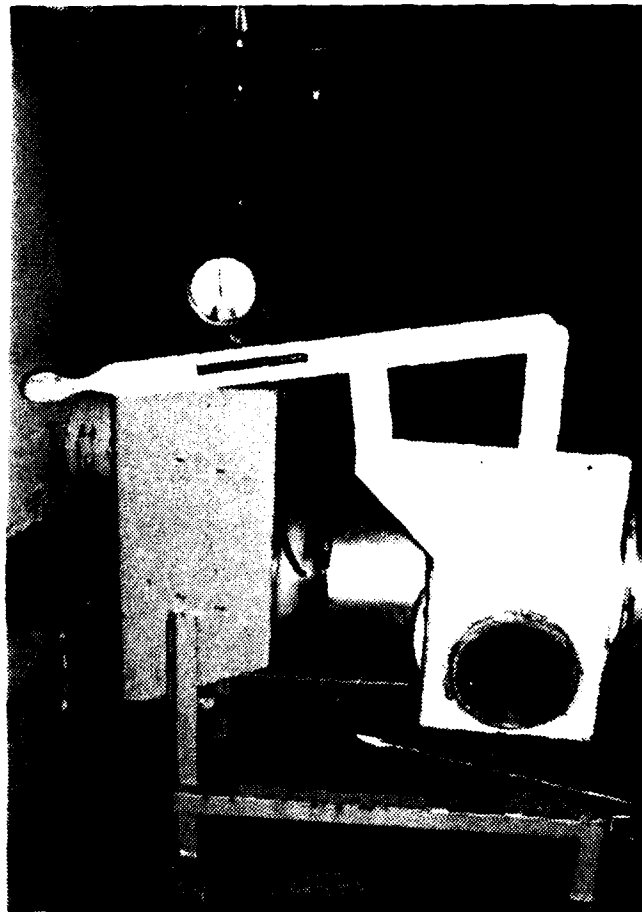


Fig. 12. Demister and Flow Control Valve.

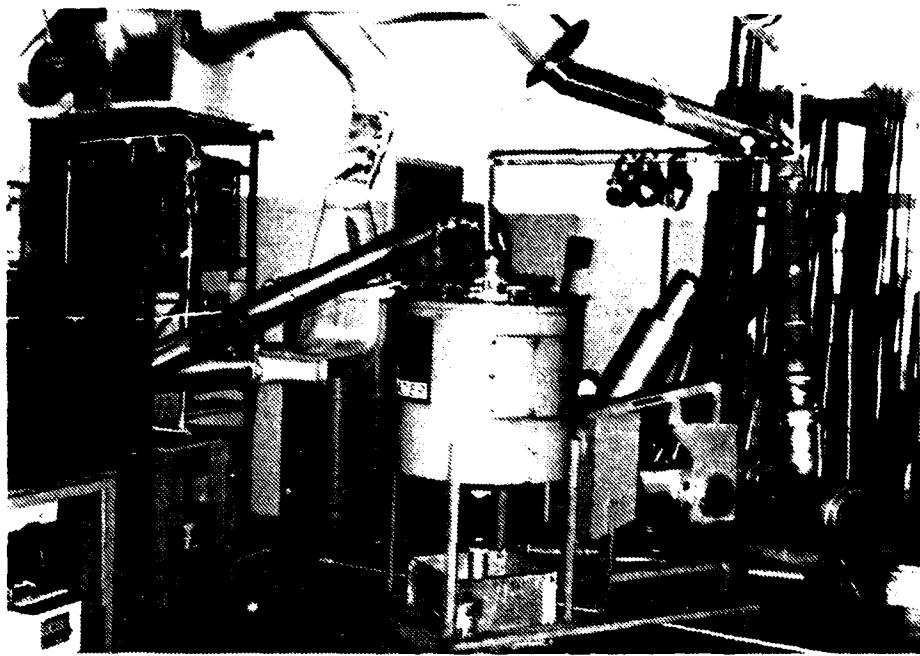
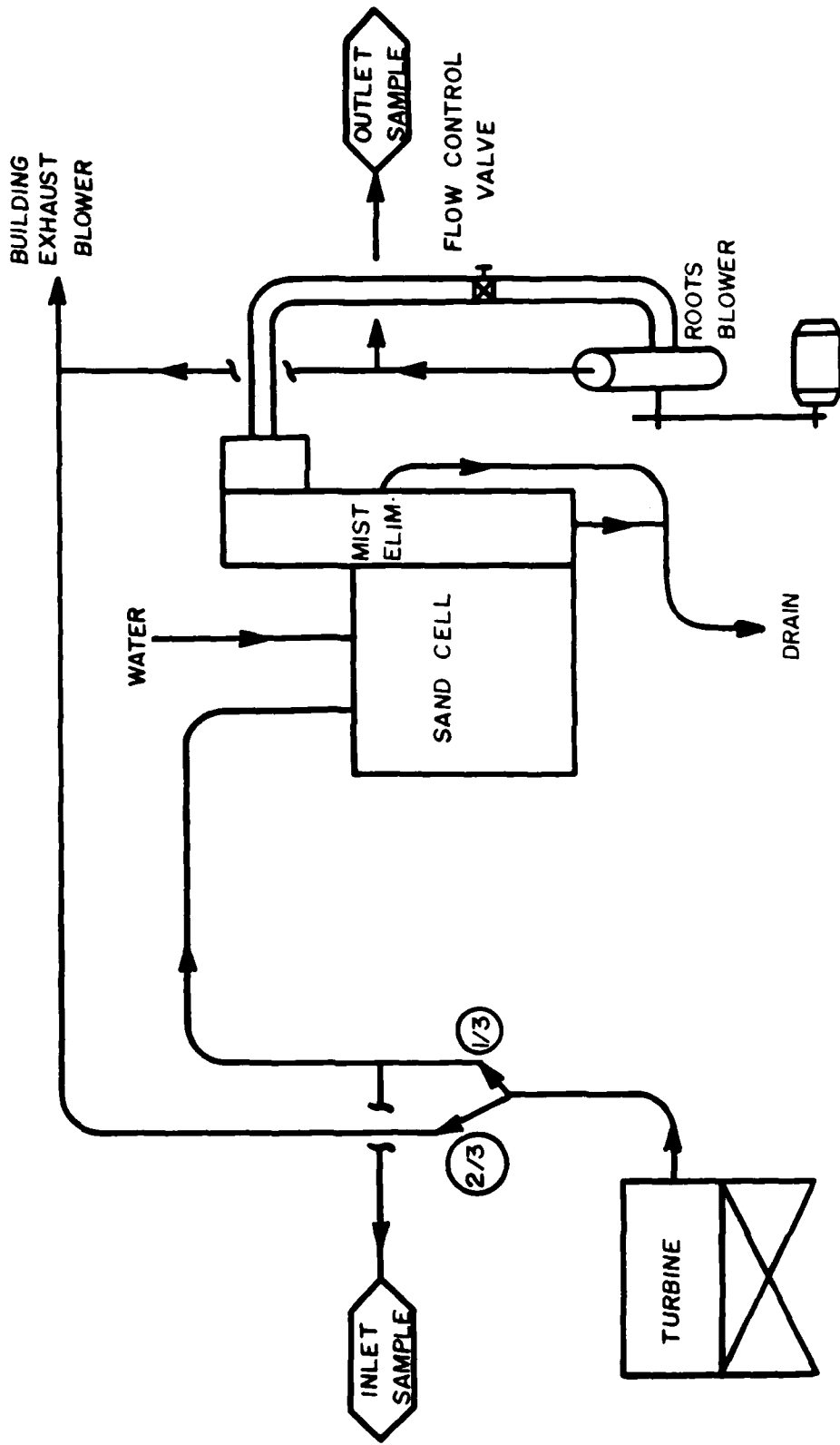


Fig. 13. Test Facility.



SANDAIR FILTER VERSION "B"

(NOT TO SCALE)

Fig. 14. SandAir Filter Test System.

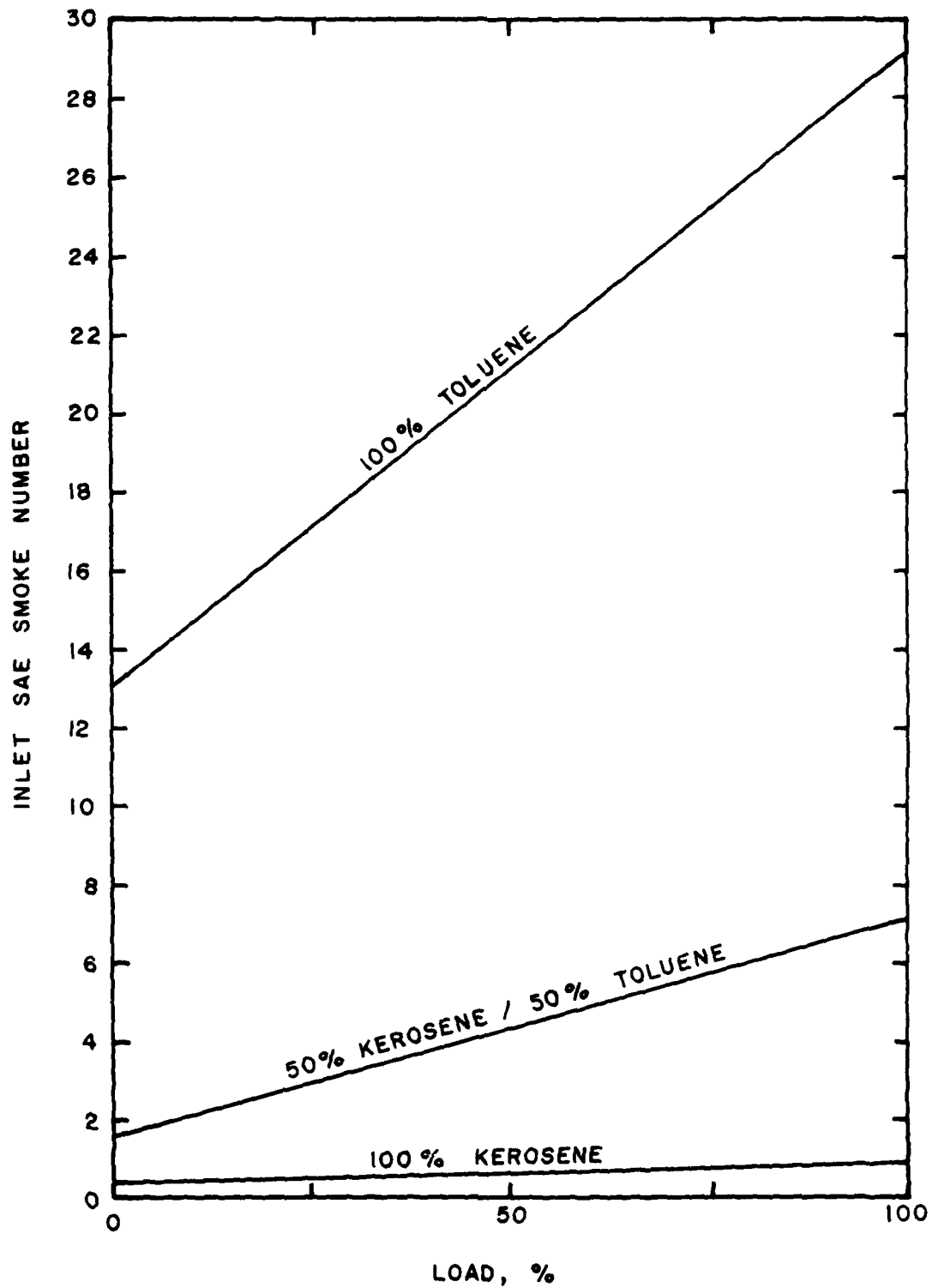


Fig. 15. SAE Smoke Number as a Function of Fuel and Load.
(Linear Regression of Data)

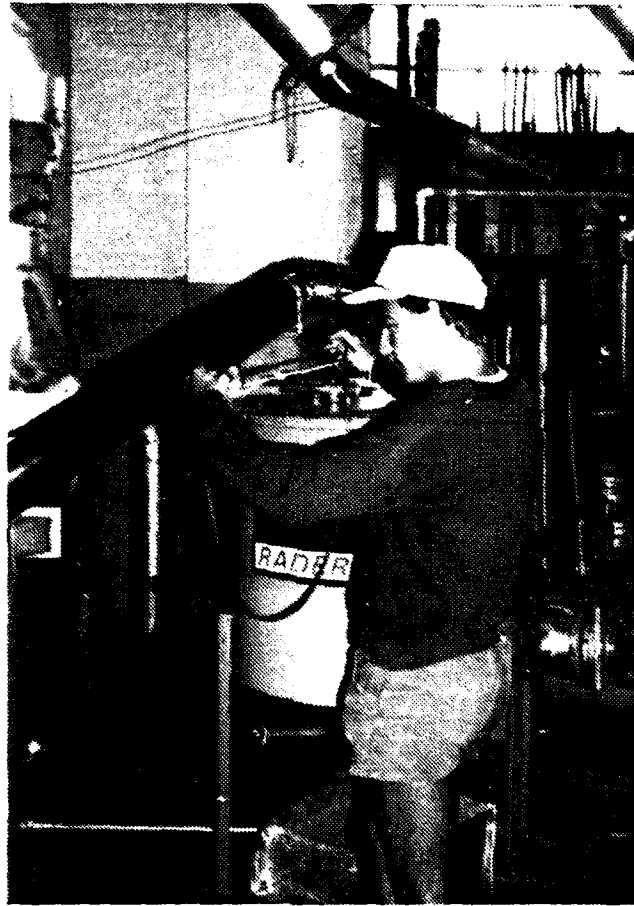


Fig. 16. Inlet Duct Velocity Traverse.

TABLE 16. SANDAIR FILTER TEST VARIABLES

<u>FUEL VARIABLES</u>	<u>INDEPENDENT OR DEPENDENT</u>	<u>MEASUREMENT METHOD</u>
Kerosene/Toluene Ratio	I	Volume %
Hydrogen Content, %	I	Total Carbon Diff. Method
Flow Rate, lb/hr	D	Volumetric Burret & S.G.
 <u>ENGINE VARIABLES</u>		
Power Output, kw	I	Wattmeter
Frequency, % of 400 H	I	Panel Meter
Combustor Temp., °F	D	Thermocouple
Turbine Exhaust Temp., °F	D	Thermocouple
Turbine Exhaust Velocity, fpm	D	Pitot Tube
 <u>POLLUTION CONTROL SYSTEM VARIABLES</u>		
SandAir ΔP , in. H ₂ O	D	Pressure Gage
Water Flow, gpm	I	Pressure Gage & Curves
Filter Gas Outlet Temp., °F	D	Thermocouple
CO ₂ Concentration	D	NDIR
CO Concentration	D	Reagent Tube
Smoke Number	D	SAE, ARP 1179 A

acfm) and two at full load (475 acfm and 625 acfm). The design value for this unit was 100 cfm per square foot, which was equal to 450 cfm.

B. TEST PROCEDURE

The tests required at least two persons to operate the turbine, sampling, and measuring systems. The SAE Smoke Number measurement requires four filters during each run. This required one person, full-time.

Some data were obtained before the test run was started. These included initial filter reflectance, fuel H/C ratios, ambient temperatures and pressures, and background data such as date, time, and personnel.

Once the system was started it was operated at the set test conditions until temperatures, and CO₂ concentration, stabilized. The data were then collected and the required four filters were obtained for Smoke Number. When the run was completed the system was shut down and the filters were measured to determine the reflectance of the smoke spot.

A blank data sheet and an operational check list for the SandAir system are included in Appendix A.

C. RESULTS AND DISCUSSION

The test and calculated data for the SandAir experiment are included in Appendix A.

The flow of gas through the filter was determined to be a function of both the water flow to the sand bed and the pressure drop across the filter unit. Figure 17 shows this dependency.

Figure 18 shows the SAE Smoke Number at the filter outlet for the first experiment. The water flow through the SandAir filter was not a significant variable, so only the turbine load and fuel mix affected the outlet Smoke Number. Figure 19 shows the numerical reduction of the Smoke Number across the SandAir filter. A significant Smoke Number reduction was obtained by using the SandAir filter as a control device. The results of the first experiment are indicated in Table 17.

TABLE 17. MEAN VALUES AND EFFICIENCY OF SANDAIR FILTER FOR SMOKE REDUCTION.

TURBINE LOAD, %	FUEL MIX. % TOLUENE	SAE SMOKE NUMBER			SANDAIR FILTER EFFICIENCY, %
		INLET	OUTLET	DECREASE	
0	50	1.6	0.1	1.5	94
0	100	13.1	9.8	3.3	25
100	50	7.1	4.6	2.5	35
100	100	29.1	17.0	12.1	41

The second experiment indicates that when the flow through the filter exceeded the design value of 450 acfm, the Smoke Number increased significantly. Table 18 shows these results.

D. CONCLUSIONS

The Radar SandAir filter did significantly reduce the SAE Smoke Number of the turbine exhaust. In the area of concern (opacity over 20 percent) the device was 25 percent to 40 percent efficient. It does not appear that this device, as tested, would clean the effluent enough to meet a 20 percent opacity standard. The SandAir filter should not be operated at a flow greater than its design capacity of 100 cfm per square foot of sand surface.

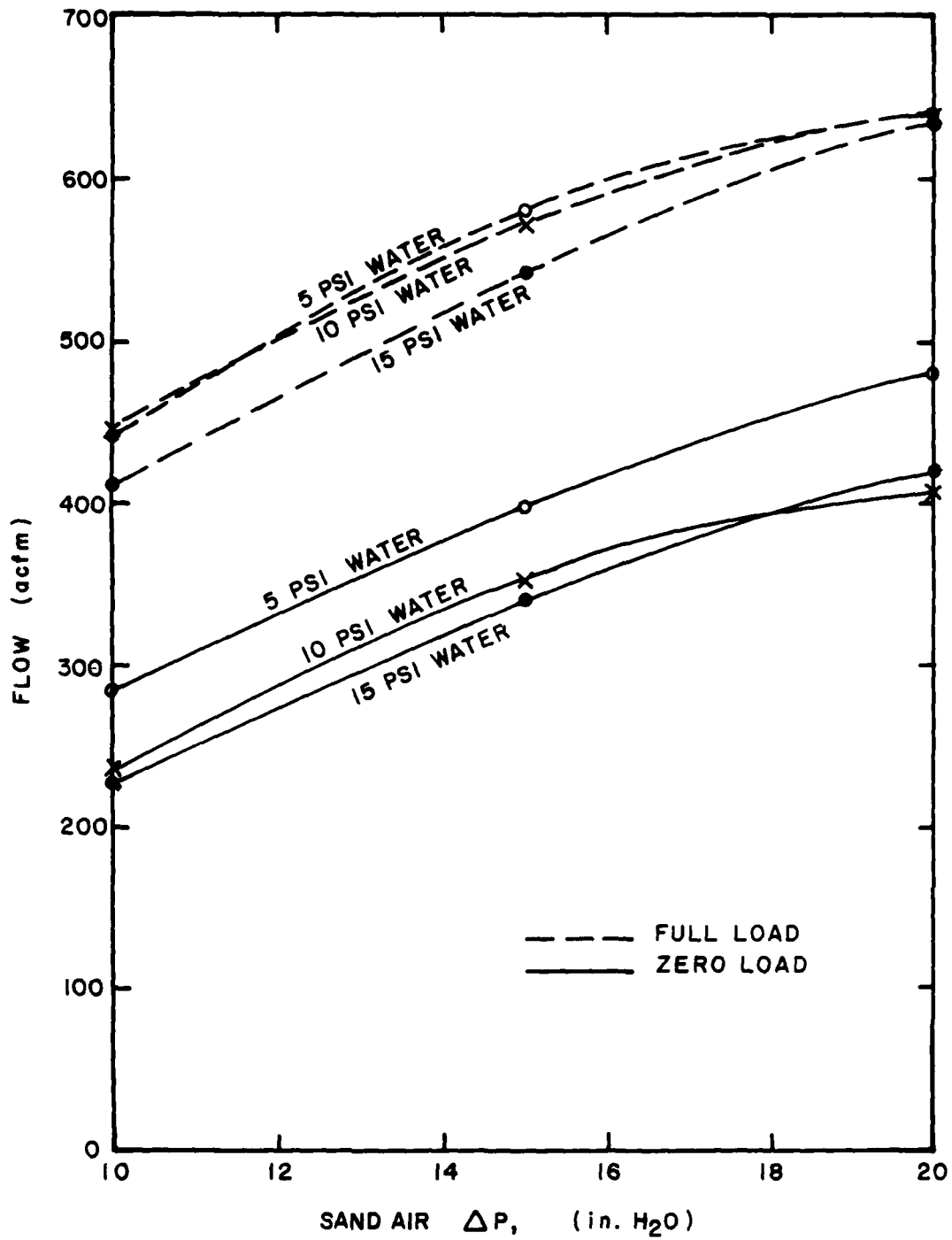


Fig. 17. Gas Flow Through SandAir Filter as a Function of Water Flow and Pressure Drop.

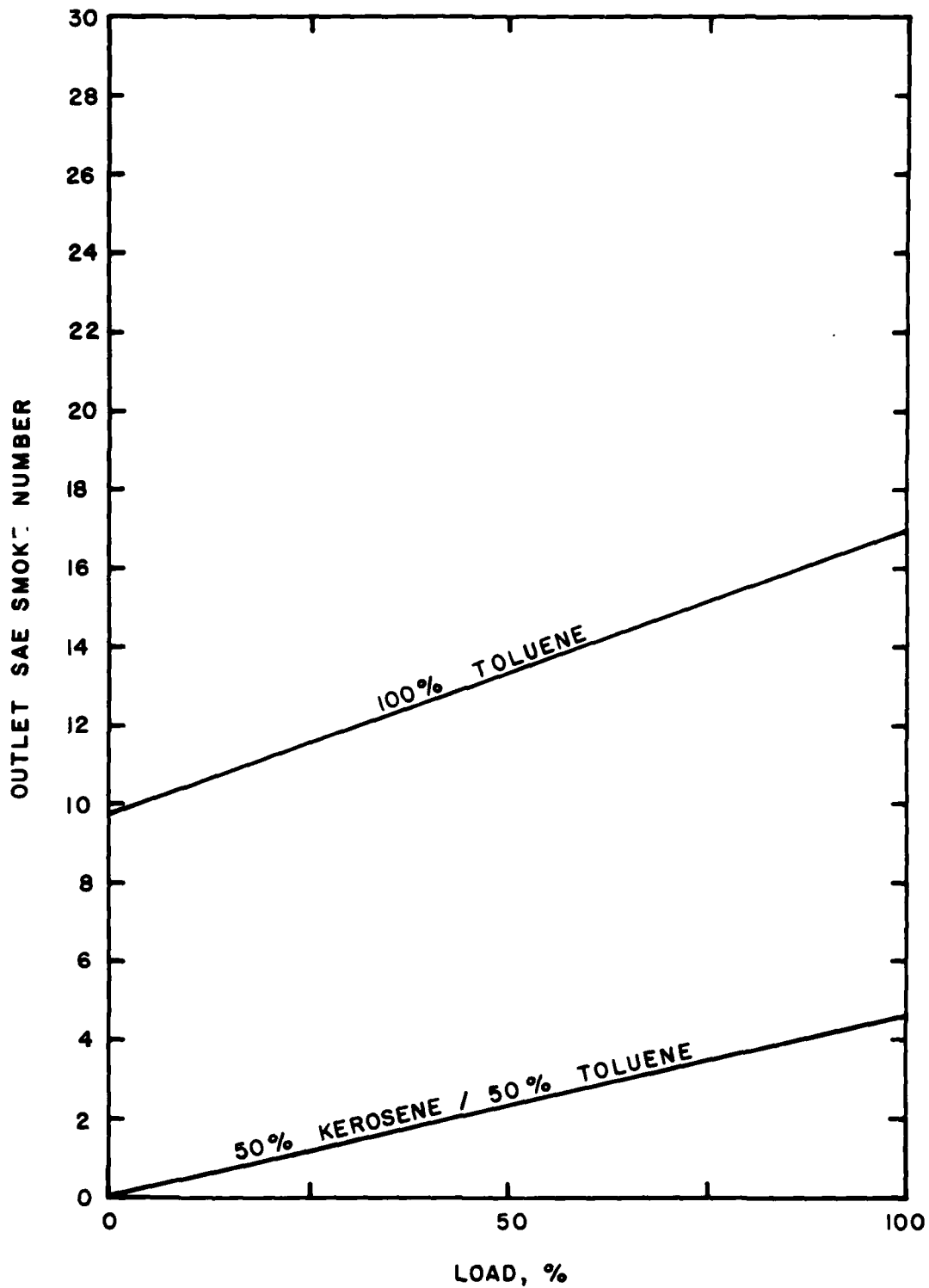


Fig. 18. SandAir Filter Outlet Smoke Number.

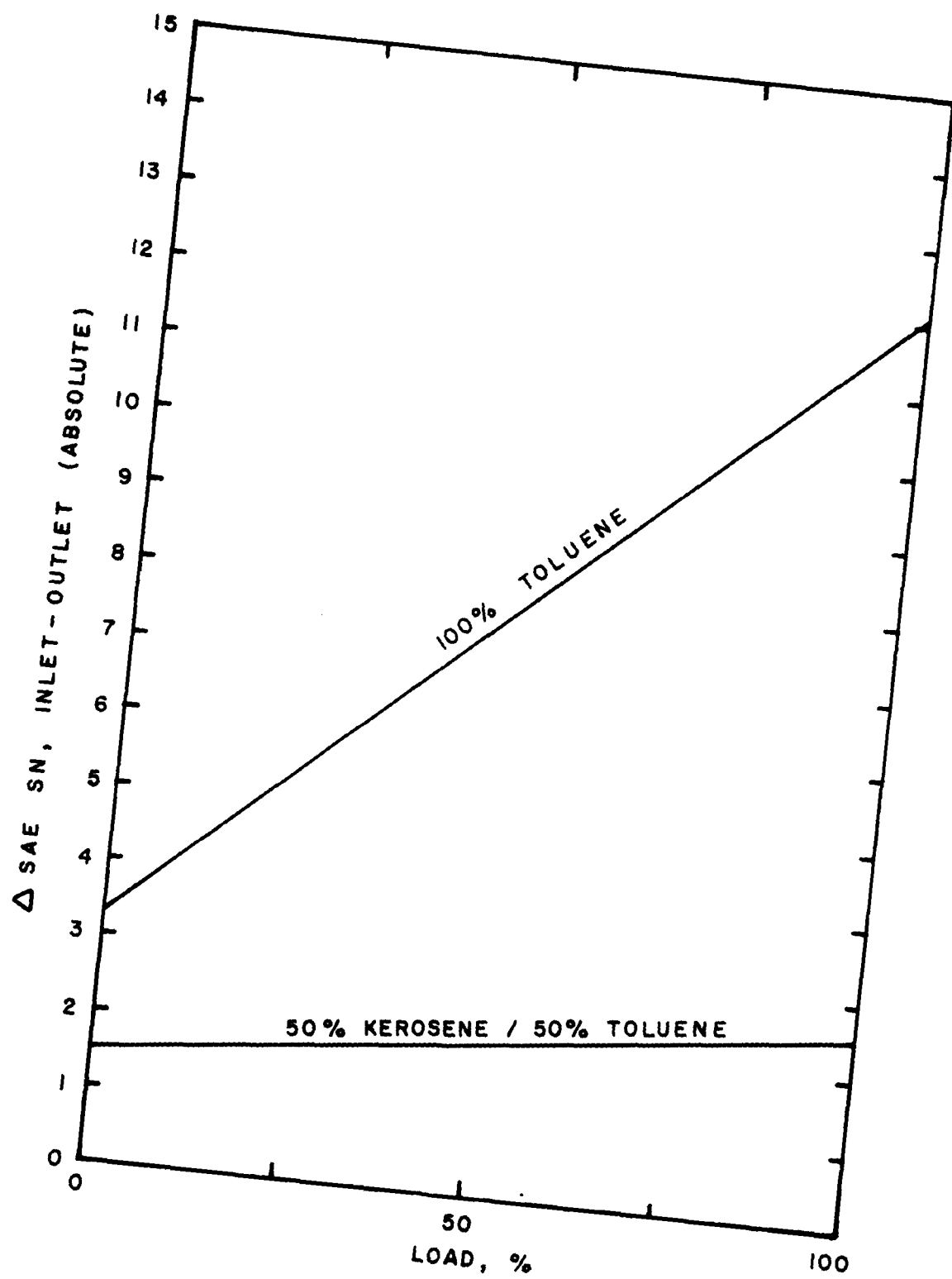


Fig. 19. Smoke Number Decrease Across SandAir Filter.

TABLE 18. SMOKE NUMBER AND EFFICIENCY AS A FUNCTION OF GAS FLOW
(DESIGN GAS FLOW WAS 450 ACFM).

TURBINE LOAD, %	PRESSURE DROP ACROSS FILTER, IN. H ₂ O	GAS FLOW, ACFM	SAE SMOKE NUMBER	EFFICIENCY, %
0	10.8	300	11.8	10
0	18.0	450	9.8	25
0	19.0	475	11.4	13
100	10.0	450	17.0	41
100	11.0	475	19.8	32
100	18.5	625	23.0	21

E. RECOMMENDATIONS

The SandAir filter could possibly be used advantageously with two changes. First, a finer sand could be used which would increase the efficiency but also the horsepower requirement. As the unit was tested the flow was 100 cfm per square foot of sand surface for a total flow of 450 cfm. The air horsepower was 1-1/4 so the fan input horsepower was approximately 2-1/2 horsepower. If the unit were scaled up to USAF needs, the gas flow would be 450,000 cfm requiring 2,000+ horsepower for the fan. A rough cost estimate would be in the \$2 million to \$4 million range.

The unit tested used a once through water system. The water was obtained from the city main, sprayed into the SandAir unit, and dumped down the city storm sewer. In an actual system the water is recirculated from a sump. This does allow some possibility for water treatment which could increase the efficiency of the unit. A larger scale unit would have to be tested, with water treatment and recirculation to determine if a satisfactory efficiency could be obtained.

It does not appear that the SandAir filter can be recommended as a control system for jet engine test cell smoke at this time. It does show some promise but more extensive tests are required before a full-scale application should be considered.

SECTION V

EVALUATION OF CERAMIC FABRIC BAGHOUSE

The control device tested and reported in this section was a baghouse utilizing Nextel® ceramic fabric bags as the filtration media. Nextel® is manufactured by the 3M Company, St. Paul, Minnesota. It appears similar to fiberglass cloth but is usable at a much higher temperature (extended-use temperature 1427°C, 2600°F and short-term use temperature 1650°C, 3000°F). The material is woven from Alumina-Borica-Silica and is nonoxidizing. It has been used extensively on experimental, high-temperature filters (Reference 7,8).

The ceramic fabric baghouse tested was a pilot model-sized unit with a single bag 12 inches in diameter x 40 inches long for one test and 12 inches in diameter x 32 inches long for the other test. The bag was clamped to a frame and was not sewn. Figure 20 shows the filter frame standing alongside the housing.

Figure 21 shows the bag after it was wrapped around the frame. In this photo the bag consists of three layers of Nextel® 8H24 fabric.

Figure 22 shows the entire baghouse in place and ready for testing. The exhaust from the turbine is split and a portion (about 1/3) is ducted to the baghouse. Inlet smoke samples are taken at the top of the unit while outlet smoke samples were taken at the bottom, just ahead of the air dilution valve. Figure 23 is a schematic drawing of the baghouse test system.

Smoke samples were carried by a heated stainless steel line to the smoke-measuring system. The Smoke Number was determined according to SAE Aerospace Recommended Practice Specification ARP 1179 A. The smoke filters were analyzed on a B&L Spectronic 20 equipped with a reflectance attachment.

A. EXPERIMENTAL DESIGN

The variables measured during the test are shown in Table 19. Also measured were the wet and dry bulb ambient temperature and the barometric pressure.

The preliminary analysis of the system indicated that a maximum gas flow of about 50 to 100 acfm should be passed through the bag. This was chosen because the literature reports typical filter face velocities of 5 to 10 feet per minute for a 2-inch to 4-inch pressure drop. When the initial velocity traverses were made it was found that at zero load, 4 inches of water pressure drop gave 658 acfm, about 10 times the amount expected. It was concluded that the ceramic material had a very loose weave and, therefore, offered little flow resistance. Even 1 inch of water pressure drop gave a flow rate of 302 acfm, about five times that expected.

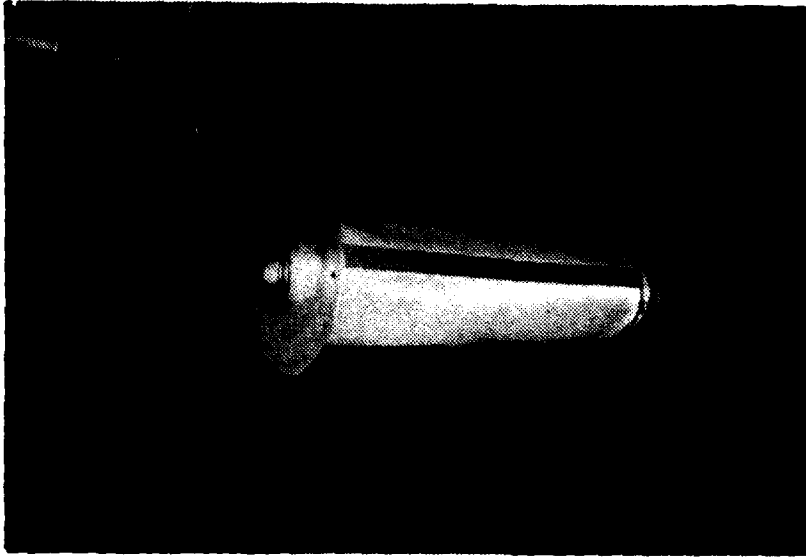


Fig. 21. Ceramic Fabric Bag Used in Tests.

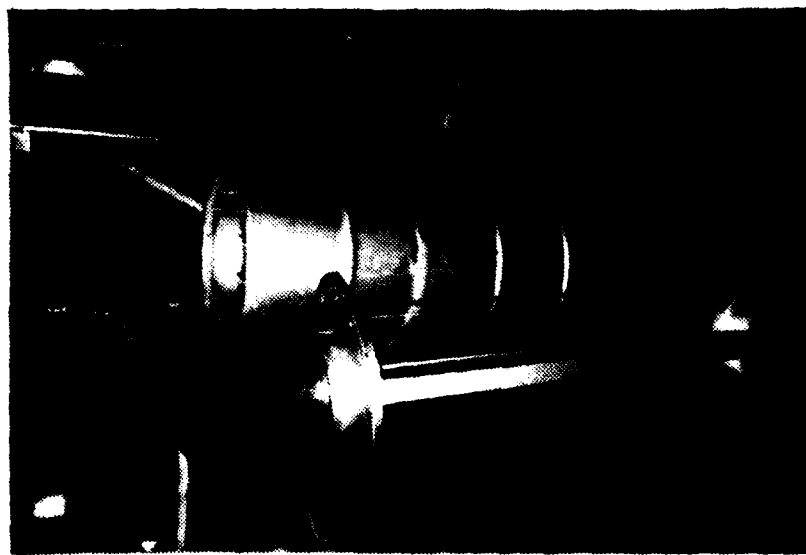


Fig. 20. Baghouse Frame and Housing. Gas Inlet at the Top of the Frame Unit and Outlet at Lower End of Housing.



Fig. 22. Baghouse Test Facility.

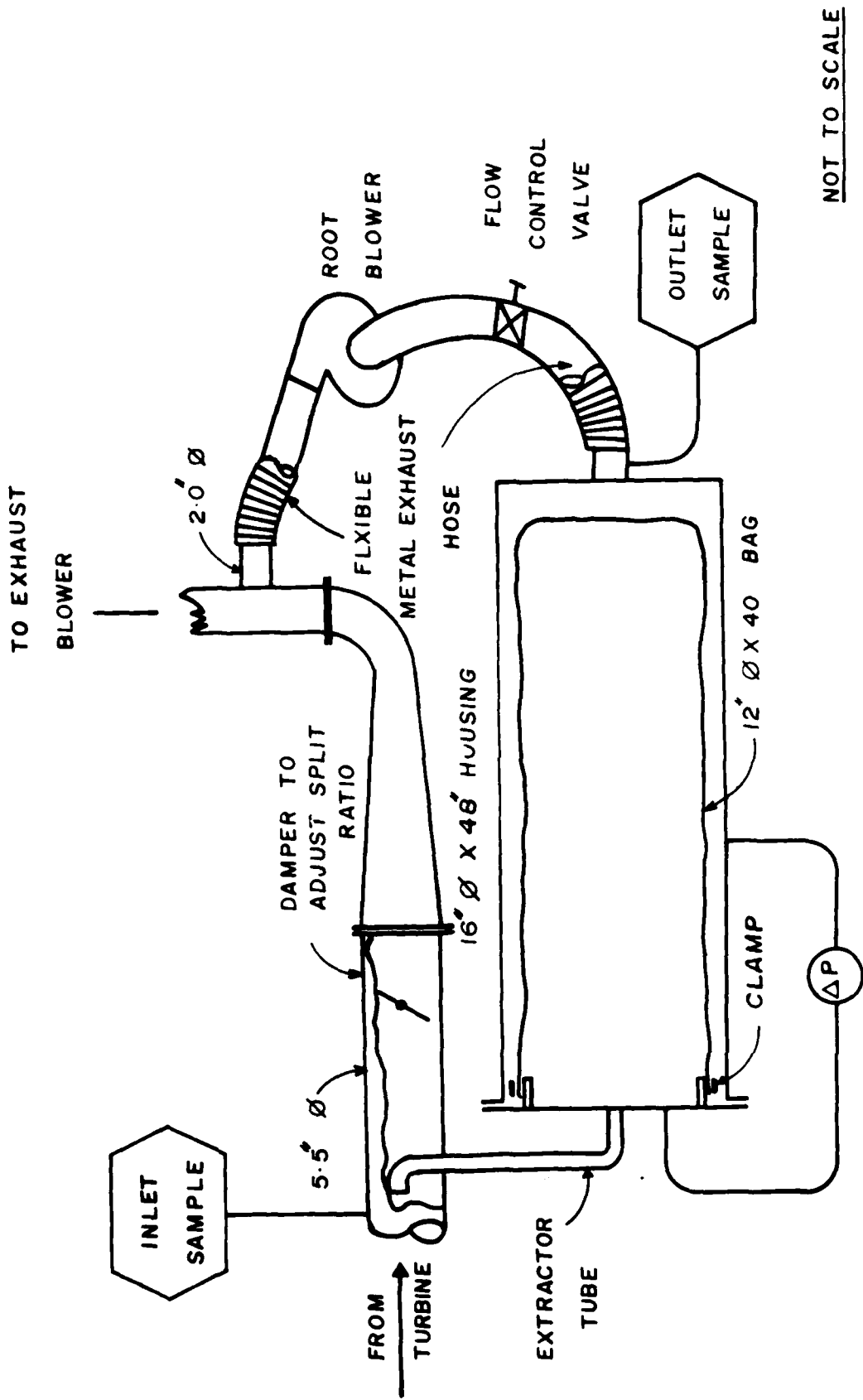


Fig. 23. High-temperature baghouse test.

TABLE 19. FILTER TEST VARIABLES.

<u>FUEL VARIABLES</u>	<u>INDEPENDENT OR DEPENDENT</u>	<u>MEASUREMENT METHOD</u>
Kerosene/Toluene Ratio	I	Volume %
Hydrogen Content, %	I	Total Carbon Diff. Method
Flow Rate, lb/hr	D	Volumetric Burret & S.G.
 <u>ENGINE VARIABLES</u>		
Power Output, kw	I	Wattmeter
Frequency, % of 400 H	I	Panel Meter
Combustor Temp., °F	D	Thermocouple
Turbine Exhaust Temp., °F	D	Thermocouple
Turbine Exhaust Velocity, fpm	D	Pitot Tube
 <u>POLLUTION CONTROL SYSTEM VARIABLES</u>		
Filter Pressure Drop, in. H ₂ O	I	Pressure Gage
Filter Outlet Temp., °F	D	Thermocouple
CO ₂ Concentration	D	NDIR
CO Concentration	D	Reagent Tube
Smoke Number	D	SAE, ARP 1179 A

It was decided that the pure kerosene fuel gave very little smoke and that more conclusive results could be obtained with the smokier effluent. Pure toluene was used for all runs.

Three separate experiments were run:

1. A factorial experiment using two loads (0 and 100 percent) and three filter pressure drops (1 inch, 2 inches, and 4 inches of water). This gave six runs with both inlet and outlet smoke samples taken. Three layers of 8H24 fabric were used for the filter. The filter was originally put through a slow-heating process where it was taken from room temperature to 500°F in a 3-hour period. The manufacturer suggested going to 700°F to 1000°F for a 20-hour period but this was not done for the first series of runs so the Teflon® coating remained on the bag.

2. The filter bag was annealed by burning off the Teflon® with a propane torch. A second experiment was then run using 1 wrap of the 8H24 fabric at zero load and 1 inch and 4 inches of water pressure drops. Inlet and outlet smoke samples were taken.

3. The final experiment consisted of changing the fabric to one wrap of 5H40 Nextel®, unannealed and running at zero and full load, 1

inch and 4 inches of water pressure drops. Only outlet Smoke Numbers were measured. This gave four runs which could be compared among themselves or compared to the previous tests.

B. TEST PROCEDURE

The tests required at least two persons to operate the turbine, sampling, and measuring systems. The SAE Smoke Number measurement requires four filters during each run. This required one person, full time.

Some data were obtained before the test run was started. These included initial filter reflectance, fuel H/C ratios, ambient temperatures and pressures, and background data such as date, time, and personnel.

Once the system was started it was operated at the set test conditions until temperatures, and CO₂ concentration, stabilized. The data were then collected and the required four filters obtained for Smoke Number. When the run was completed the system was shut down and the filters measured to determine the reflectance of the smoke spot.

The operational checklist for the system and a blank data sheet are included in Appendix A.

C. RESULTS AND DISCUSSION

The flow through the bag, for the same pressure drop, decreased with time. This was because the bag slowly was plugging with the particulate from the exhaust gases. Figure 24 shows the time history of the bag used in Experiment No. 1.

The Smoke Numbers at the outlet of the baghouse did not change significantly as the pressure drop across the unit changed. This was true for both the zero-load and full-load runs.

The Smoke Numbers for the annealed, one-wrap bag were not significantly different than the Smoke Numbers for the unannealed, three-wrap bag. This was true for both the zero-load and full-load runs.

The Smoke Numbers from the 5H40 material bag outlet were not significantly different than those from the 8H24 material bag outlet. This was true for both zero-load and full-load runs.

The efficiency of the baghouse at zero load (18.2 percent) was significantly higher than the efficiency of the baghouse at full load (14.8 percent).

Test and calculated data are shown in Appendix A.

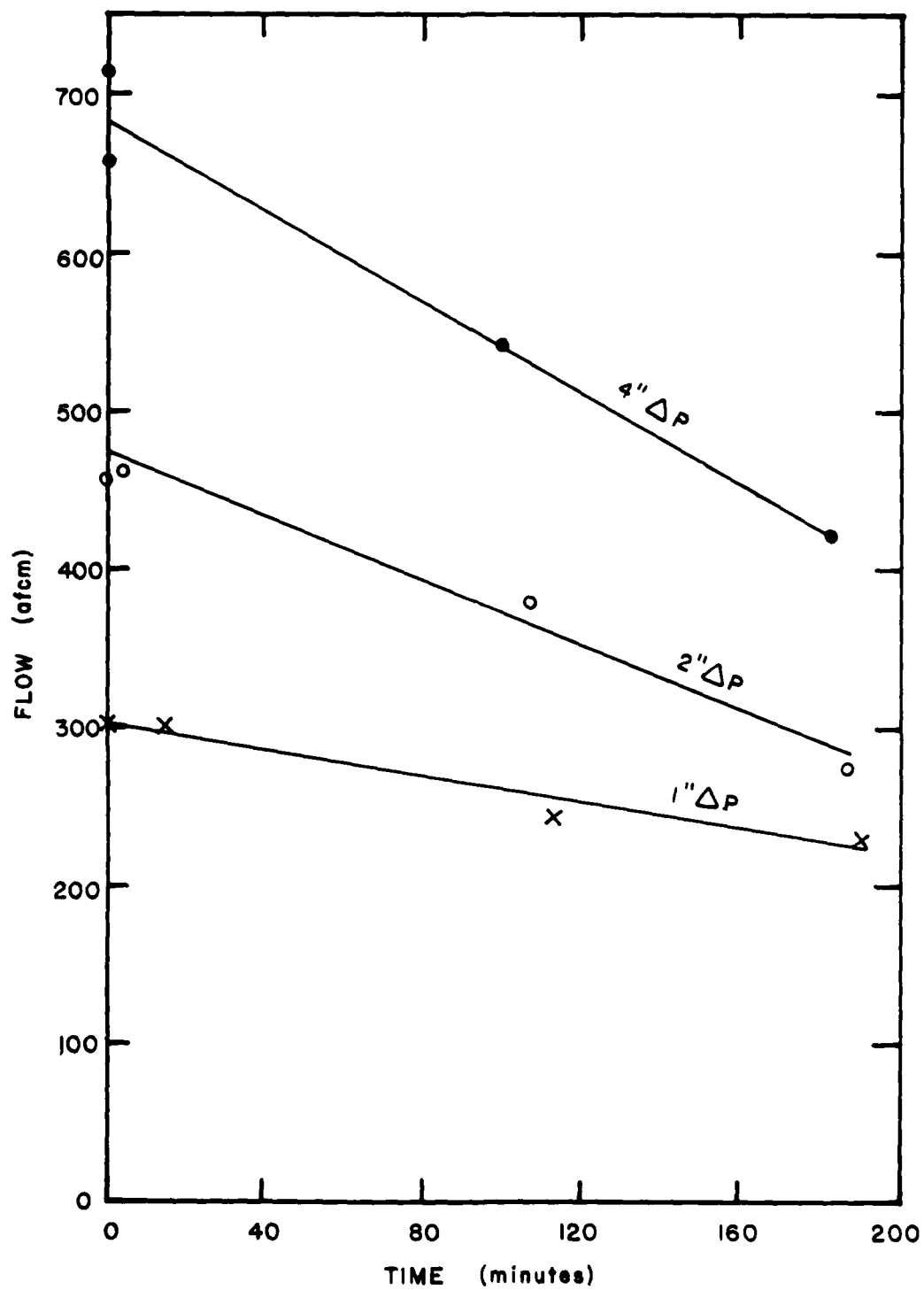


Fig. 24. Bag Flow for Various Pressure Drops Over Time.

D. CONCLUSION

The Nextel® ceramic fabric baghouse did significantly reduce the SAE Smoke Number of the turbine exhaust. The reduction was in the range of 14 to 18 percent, which does not appear to be enough to clean the effluent from a test cell to a required opacity standard of 20 percent. This low efficiency is due to the loose weave of the fabric which does not effectively filter the 1/2 micron particles. Buildup of a filter cake, to increase filtration efficiency, was occurring as shown by the flow decrease with time at the same pressure drop. It would be impractical to operate the baghouse long enough to get a sufficient filter cake to meet opacity standards as the unit would be in violation from original startup time until sufficient cake was deposited. This could be 5 to 10 hours.

E. RECOMMENDATIONS

The Acurex Corporation has developed a modification of the standard Nextel® fabric which may have possibilities (Reference 8). This material is made of fine ceramic fibers (Nextel® 3/2 Blown Ceramic Microfiber) sandwiched between two layers of the standard Nextel® fabric. They report high efficiency (for 5-micron and larger mass means for the particulate) with quite rapid filter cake buildup (cleaning cycle times were about 5-minute intervals). This material may have the properties to meet opacity standards. Acurex was not willing to sell us the material but instead wanted to subcontract with us on a demonstration project.

Even if the Acurex material cleaned the exhaust to meet opacity standards it might not be acceptable from a practical standpoint. If an engine exhaust of 450,000 acfm were cleaned, at a high air to cloth ratio of 10 cfm per square foot, the baghouse would have 45,000 square feet of material. At \$100 per square yard this would cost \$500,000 just for the first set of bags. If the bags were 6 inches in diameter by 8 feet long, the baghouse would contain 3580 bags just for cleaning. If 420 extra bags were installed so that about 12 percent of the bags could be on cleaning cycles at one time, and a "square" baghouse with 6-inch spacing between the tubes was constructed, it would have an outside dimension (plan view) of about 125 feet x 125 feet. This would be quite a massive structure, costing approximately \$1.5 million. With fans, ductwork, etc., the initial cost of such a baghouse would be approximately \$3 million. Fan horsepower would be about 1000 horsepower.

The 3M Company has offered to supply sample fabrics, of the required size, to Oregon State University at no cost if we wish to continue testing.

SECTION VI

OVERALL OBSERVATIONS AND RECOMMENDATIONS

It appears that none of the three devices tested should be considered as practical for reducing visual emissions from jet engine test cells. The wetted-sand filter and ceramic baghouse may be possible candidates, but they would both have to be tested with the modifications suggested in this report.

Low-pressure drop wet scrubbers, such as added water in the augmentor section, do not result in a reduction of visual particulate emissions. Instead they mask the emission and deposit it downwind from the test cell as a dirty, black mist.

SECTION VII

NO_x EMISSIONS FROM TURBINE ENGINES

An additional experimental study was conducted on the gas turbine engine between the tests on the wet scrubber and those on the wetted-sand filter. Mr. William Faye, a graduate student, operated the turbine at different loads and with fuels doped with different quantities of pyridine (a nitrogen bearing compound). His thesis, which is published separately as Appendix C, contributes to the understanding of NO_x formation in gas turbine and jet engines.

SECTION VIII

REFERENCES

1. R.W. Boubel and J.A. Martone, USAF Aircraft Engine Emission Goals: An Analysis and Critical Review, ESC-TR-79-30, AFESC, Tyndall AFB, FL, March 1980.
2. _____, "EPA Proposed Revisions to Gaseous Emissions Rules for Aircraft and Aircraft Engines," U.S. Federal Register, Volume 43, 12615, March 24, 1978.
3. _____, Volume I - Particulate Emissions Test Program - Jet Engine Test Cell 19, Building 337, AE50 Report No. 110-D1-81, Naval Air Systems Command, North Island, California, October 1981.
4. J.D. Stockham, M.D. Lannis, M.G. MacNaughton, and J.J. Tarquinio, "Control of Particulate Emissions from Turbine Engine Test Cells by Cooling Water Injection," JAPCA, Volume 31, No. 6, June 1981.
5. A.J. Teller, "Gas Turbine Emission Control: A Systems Approach," JAPCA, Volume 27, No. 2, February 1977.
6. R.A. Farrell and M.E. Thomas, "Effects of Inlet Conditions and Water Injection on Emissions from a Dual-Fuel Industrial Gas Turbine," Paper presented at Gas Turbine Division, ASME, Conference, Houston, Texas, March 1981.
7. D.A. Furlong, and T.S. Shevlin, "Fabric Filtration at High Temperature," Chemical Engineering Progress, pp. 89-91, January 1981.
8. M. Shackleton, R. Chang, J. Sawyer, E. Turner, and W. Kuby, "High-Temperature Ceramic Filters for Advanced Fossil Fuel Conversion Systems," AIChE Annual Meeting, Los Angeles, CA June 1982.

APPENDIX A
SUPPORT DATA

	<u>Page</u>
FIGURE A-1 - BECKMAN NDIR CO ₂ CALIBRATION	64
GAS TURBINE DATA SHEET (SCRUBBER)	65
GAS TURBINE OPERATING PROCEDURE (MODIFIED 6/26/81)	66
TABLE A-1 - PRELIMINARY DATA FOR GAS TURBINE SYSTEM WITH NO CONTROL SYSTEM	68
TABLE A-2 - GAS TURBINE WITH WET SCRUBBER CONTROL SYSTEM	69
FIGURE A-2 - TURBINE PARTICULATE EMISSION SIZE ANALYSIS	70
GAS TURBINE DATA SHEET (SANDAIR)	71
GAS TURBINE-SANDAIR STARTUP PROCEDURE	72
TABLE A-3 - GAS TURBINE WITH RADAR SANDAIR FILTER SYSTEM	74
GAS TURBINE-BAGHOUSE STARTUP PROCEDURE	75
GAS TURBINE DATA SHEET (BAGHOUSE)	77
TABLE A-4 - GAS TURBINE WITH CERAMIC (3M) FABRIC BAGHOUSE	78

BECKMAN NDIR CO₂
CALIBRATION 2-27-81

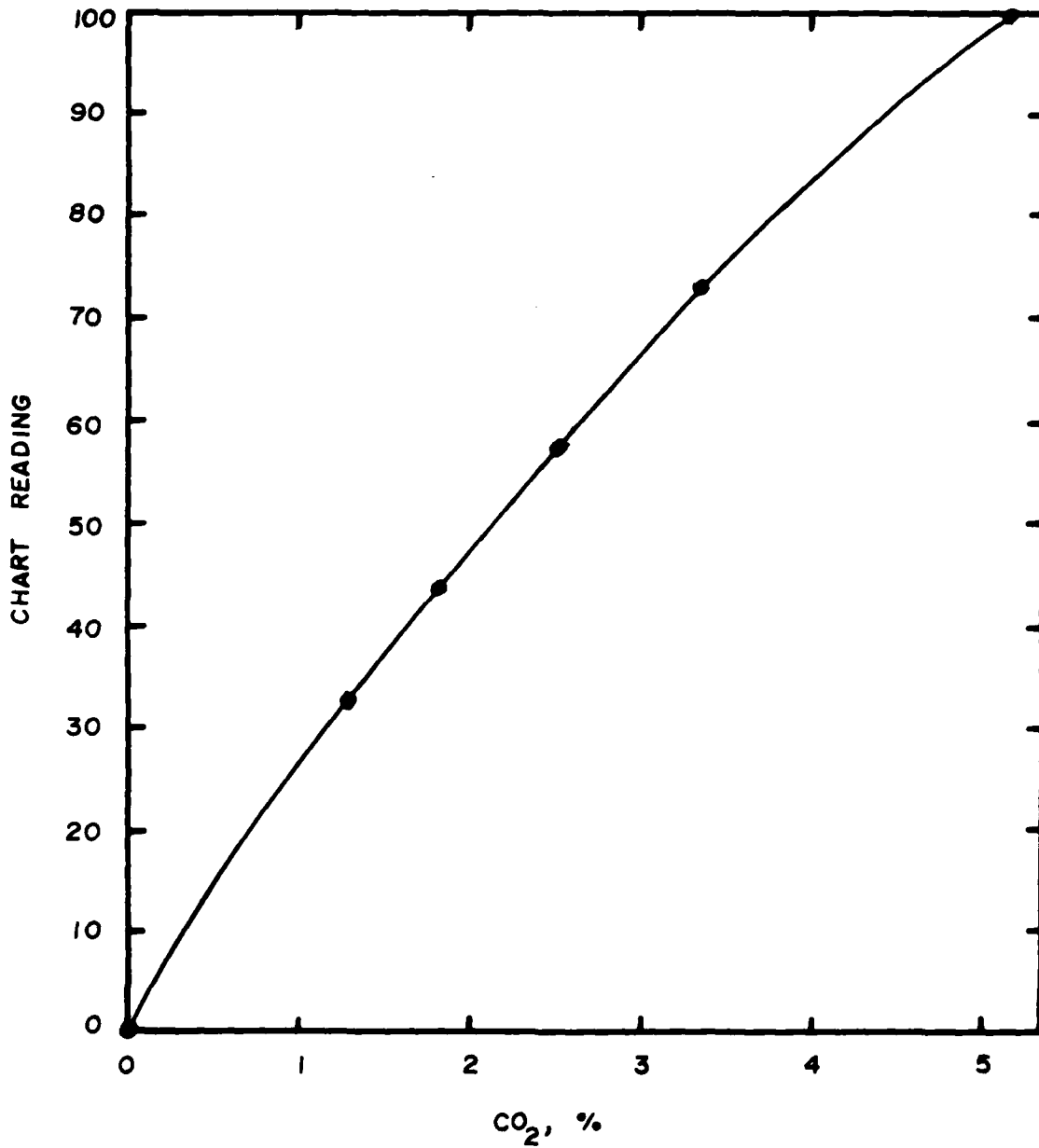


Figure A-1. Beckman NDIR CO₂ Calibration.

GAS TURBINE DATA SHEET

USAF Project - Laboratory Evaluation of Novel Particulate Control Concepts for Jet Engine Test Cells

Principal Investigator Prof. R. W. Boubel
Oregon State University

Date _____ Time _____

Test Crew _____

Type of Control Device _____

Fuel: % Kerosene _____, % Toluene _____

Ambient Temperature, °F _____ Barometric Pressure, in. Hg _____

Fuel Flow: Seconds per 2000 cc _____, Pounds per hour _____

Fuel Pressure, psi _____ Compressor Outlet Pressure, psi _____

Turbine Load (0, 1/2, Full), Kw _____

Exhaust: CO₂, Reading _____, % _____ Opacity, % _____

Turbine Outlet Temperature, °F _____

NO_x, Reading _____, % _____

Velocity Pressure (1 in. from top), in. H₂O _____ Vel., fpm _____

Smoke Sample: Orifice Δp, in. H₂O _____ Time, Sec. _____

Flow, cfh _____ Gas Volume, cubic feet _____

Sample Temperature, °F _____

Rw (Reflectance of clean filter) _____

Rs (Reflectance of Sample Spot) _____

Smoke Number _____

Maximum Duct Temperature, °F _____

Remarks _____

GAS TURBINE OPERATING PROCEDURE (modified 6/26/81)

A. 2 hours before test

- 1) Place NOx Exhaust and Bypass out window
- 2) Turn on N₂ Cylinder and adjust to 10 psi
- 3) Turn on Power to CO₂ analyzer and turn switch to TUNE
- 4) Turn on Power to NOx analyzer and push the ZERO and CONV buttons on NOx system
- 5) Turn ~~three-way~~ valve on CO₂ system to N₂ and adjust flow through CO₂ system to 800 cc/min
- 6) Adjust NOx analyzer to 5½ psi (sample valve) and 1½ SCFH flow rate

B. Test procedure

- 1) Open test turbine exhaust duct damper
- 2) Ensure fuel supply in proper tanks (measuring burette filled)
- 3) Turn on fuel supply valves to turbine (four valves in all)
- 4) Connect battery (red to positive)
- 5) Turn on panel lights (if lights come on battery's are o.k.)
- 6) Turn on opacity monitor blower (plug in)
- 7) Turn on opacity monitor and recorder (adjust zero and span on both)
- 8) Turn on exhaust duct blower (switch is on column next to fuel tank)
- 9) Turn on electrical load-cooling blower
- 10) Turn on Relative Humidity-measuring device
- 11) Turn on CO₂, NOx span and Air Tanks
- 12) Adjust CO₂ pressure to 5-6 psi and the NOx and Air Tanks to 10-15 psi
- 13) Turn on all Line Valves (following regulators)
- 14) With ~~three-way~~ valve in N₂ position adjust the CO₂ analyzer until the meter reads zero.
- 15) Adjust the CO₂ recorder to zero
- 16) Turn ~~three-way~~ valve to CO₂ and adjust the instrument gain to get 100% on recorder
- 17) Recheck N₂+CO₂ until consistent values are obtained.
- 18) Turn on compressed air to sample delivery system (on wall hear boiler)
- 19) Plug in sample delivery system (electrical)
- 20) Turn on Ambient and pump switches on sample delivery system panel
- 21) Turn ~~three-way~~ valve to sample and adjust CO₂ instrument flow to 800 cc/min
- 22) Press samp switch on NOx instrument (light should glow)
- 23) Adjust sample pressure to 5.5 psi
- 24) Adjust sample flow to 1.5 SCFH
- 25) Turn on OXY button and adjust air pressure to 5.5 psi
- 26) Turn on O₃ and NOx buttons
- 27) Zero adjust for NOx
 - a) Press Zero button; press 100 range switch
 - b) Zero instrument to slightly positive
 - c) Check recorder and adjust zero with span (screw driver) if needed
- 28) Span adjustment for NOx
 - a) Press Span button and 100 range scale
 - b) Adjust cylinder until sample pressure reads 5.5
 - c) Adjust gain to proper value on instrument
 - d) Check recorder for same value and adjust with the zero if necessary

- 29) Recheck zero and span and adjust as needed to obtain consistent values
- 30) Make notation on chart of pot settings, date and run number
- 31) Press the Samp switch on the NOx instrument
- 32) Press the sample switch on the sample delivery system panel
- 33) Record, Tdbulb, Twb
- 34) Check turbine panel switches all off or open
- 35) Start turbine (RPM-100%, Volts-240, amps &KW-0)
- 36) Set load switch to position L₁ L₃ PH 3
- 37) Select 0, ½, or Full Load
- 38) Take all Data (see accompanying sheet)
- 39) Rerecord Tdbulb, Twb
- 40) Shut down turbine
- 41) Purge NOx and CO₂ instruments with N₂ or ambient Air
- 42) Recheck all calabrations and note changes on strip shcrt
- 43) Purge sample line and cooling system by pushing the Shop Air and Trap drain buttons on sample transport system panel
- 44) Shut down all machinery and equipment in the reverse order of startup

TABLE A-1
 PRELIMINARY DATA FOR GAS TURBINE
 SYSTEM WITH NO CONTROL SYSTEM

FUEL MIX, %		LOAD	TURBINE OUTLET TEMP., °F	CO ₂ , %	SAE SMOKE NO.
KEROSENE	TOLUENE				
100	0	0	430	1.4	0.9
100	0	1/2	550	2.0	1.8
100	0	full	800	2.8	3.3
95	5	0	425	1.5	1.7
95	5	1/2	550	1.8	1.8
95	5	full	805	2.8	3.3
90	10	0	420	1.4	1.5
90	10	1/2	600	2.0	2.0
90	10	full	850	2.8	3.9
80	20	0	475	1.5	2.0
80	20	1/2	625	2.0	3.5
80	20	full	800	2.8	4.0
65	35	0	450	1.5	2.6
65	35	1/2	600	2.0	4.1
65	35	full	800	3.0	4.2
50	50	0	430	1.6	2.7
50	50	1/2	600	2.1	7.1
50	50	full	800	3.0	12.8
0	100	0	450	1.5	9.3
0	100	1/2	600	2.0	30.0
0	100	full	850	3.2	44.1

TABLE A-2

GAS TURBINE WITH WET SCRUBBER CONTROL SYSTEM

Tested Summer & Fall 1981 @ Oregon State University

TEST NO.	LOAD, %	FUEL COMPOSITION KEROSENE/TOLUENE	WATER PRESSURE, PSI	WATER FLOW, GPM	AMBIENT TEMP., °F	BAROM. PRESSURE IN. HG	COMPRESSOR OUTLET PRESS., PSI	FUEL PRESSURE, PSI	FUEL FLOW, LB/HR	CO ₂ %	EXH. VOLUME ACFM	GAS TURBINE OUTLET TEMP., °F	CYCLONE OUTLET TEMP., °F	SAE SHOCK NO.
1	0	100/0	0	0	70	29.85	16.5	90	27.17	1.3	1500	450	475	0.6
2	50	"	"	"	65	29.85	18.0	100	35.06	1.65	1664	600	600	1.3
3	100	"	"	"	70	29.85	18.0	105	49.60	3.0	1882	900	875	2.3
4	0	"	10	.50	70	29.82	17.0	92	28.13	1.5	1500	475	476	1.0
5	50	"	"	"	70	29.82	17.0	95	35.35	1.7	1664	600	480	1.6
6	100	"	"	"	70	29.85	17.5	106	48.29	2.8	1882	850	626	2.2
7	0	"	30	.86	70	29.80	16.5	90	28.00	1.5	1500	490	356	0.8
8	50	"	"	"	70	29.80	17.0	96	34.97	2.0	1664	600	430	0.6
9	100	"	"	"	70	29.80	17.0	105	47.05	2.75	1882	820	516	1.9
10	0	"	60	1.20	78	30.00	17.0	94	27.23	1.45	1500	470	320	0.9
11	50	"	"	"	75	29.95	17.0	99	35.16	1.95	1664	600	390	1.6
12	100	"	"	"	70	29.95	17.5	108	47.58	2.55	1882	805	470	2.1
13	50	50/50	0	0	64	30.00	18.0	96	36.58	2.15	1732	600	607	11.6
14	100	"	"	"	74	30.00	18.0	110	49.73	3.0	2045	875	880	25.1
15	50	"	10	.50	70	30.00	17.0	97	36.58	2.15	1732	600	467	11.0
16	100	"	"	"	80	30.00	18.0	110	47.94	3.0	2045	850	609	21.5
17	50	"	30	.86	62	29.47	18.5	97	36.58	2.15	1732	580	403	8.9
18	100	"	"	"	64	29.47	18.8	113	47.94	3.0	2045	800	470	33.0
19	50	"	60	1.20	76	29.47	18.4	98	36.58	2.15	1732	600	355	12.2
20	100	"	"	"	76	29.47	18.7	110	47.94	3.0	2045	825	470	25.0
21	50	0/100	0	0	70	29.92	17.0	100	38.87	2.4	1704	590	598	30.0
22	100	"	"	"	70	29.90	18.0	110	53.75	3.35	1950	850	850	48.6
23	50	"	10	.50	65	29.96	18.0	100	38.22	2.30	1704	590	410	30.1
24	100	"	"	"	70	29.90	18.0	110	53.75	3.35	1950	900	620	45.0
25	50	"	30	.86	70	29.92	17.0	100	38.87	2.25	1704	580	430	27.2
26	100	"	"	"	70	29.95	18.0	120	52.12	3.1	1950	900	525	43.2
27	50	"	60	1.20	70	29.96	18.0	100	38.22	2.25	1704	600	390	25.8
28	100	"	"	"	70	29.95	18.0	120	52.12	3.1	1950	800	470	44.8
29	0	50/50	0	0	53	30.10	18.6	92	28.00	1.5	1459	475	483	5.5
30	0	"	10	.50	60	30.10	18.5	93	28.00	1.5	1459	500	392	4.9
31	0	"	30	.86	64	30.10	18.5	93	28.00	1.5	1459	450	355	8.8
32	0	"	60	1.20	63	30.10	18.5	93	28.00	1.5	1459	450	320	6.0
33	0	0/100	0	0	70	29.33	18.5	91	28.00	1.5	1459	450	490	14.8
34	0	"	10	.50	72	29.33	18.3	91	28.00	1.5	1459	405	381	19.8
35	0	"	30	.86	72	29.33	18.3	91	28.00	1.5	1459	500	348	17.1
36	0	"	60	1.20	70	29.33	18.4	92	28.00	1.5	1459	420	317	20.4

For 1 Hydrogen/Carbon Ratios: Kerosene 9.09/90.98 Toluene 8.56/91.07

Carbon Monoxide Emulsions: Zero Load 640 ppm 1/2 Load 400 ppm Full Load 260 ppm

Compressor Outlet Temperature: Zero Load 860°F 1/2 Load 1145°F Full Load 1565°F

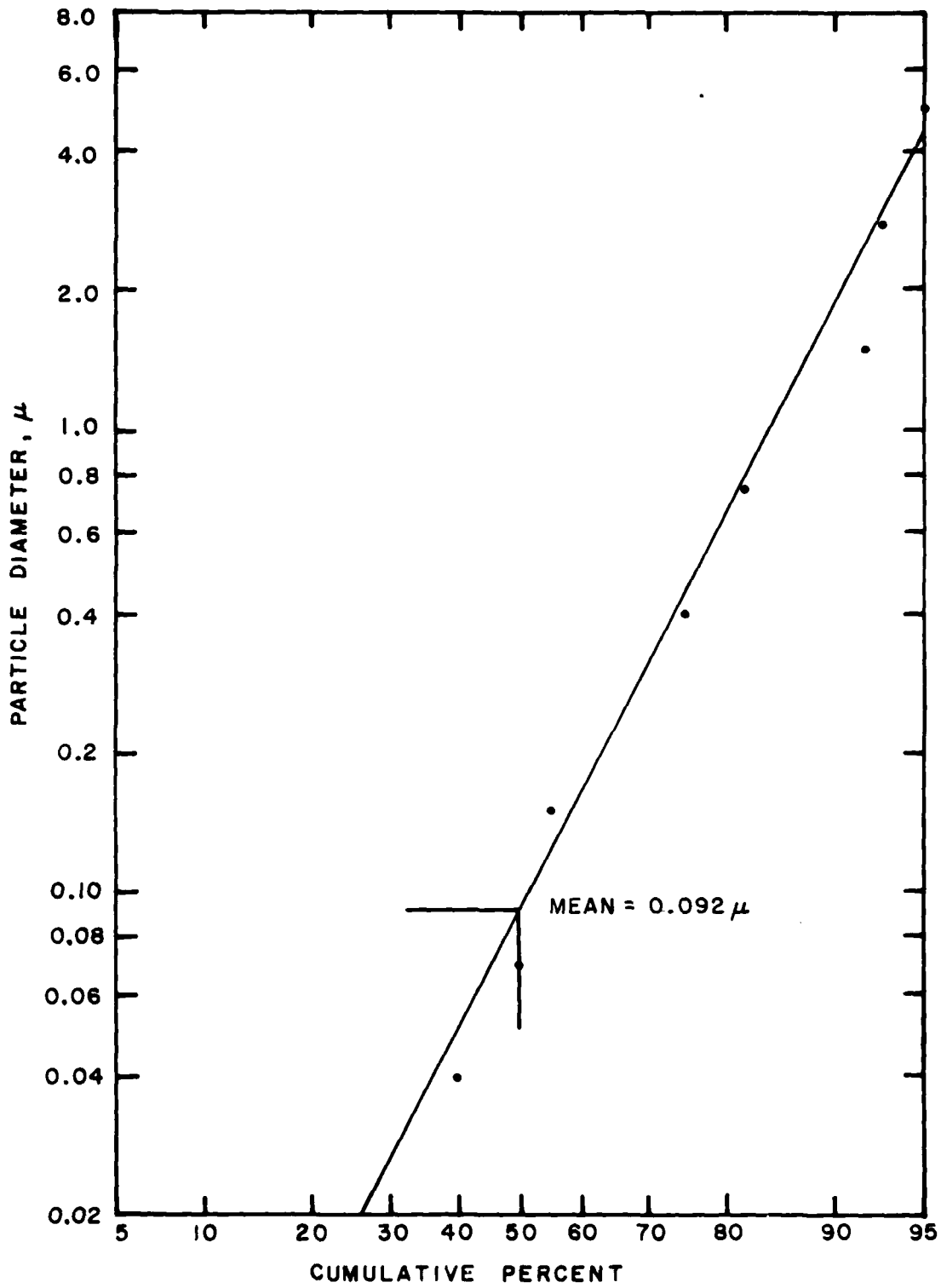


Figure A-2. Turbine Particulate Emission Size Analysis.

GAS TURBINE DATA SHEET

USAF Project - Laboratory Evaluation of Novel Particulate Control Concepts for Jet Engine Test Cells

Principal Investigator Prof. R. W. Boubel
Oregon State University

Date _____ Time _____

Test Crew _____

Type of Control Device _____

Fuel: % Kerosene _____, % Toluene _____

Ambient Temperature, T_6 _____ °F Barometric Pressure, in. Hg _____

Fuel Flow: Seconds per 500 cc _____, Pounds per hour _____

Fuel Pressure, psi _____ Compressor Outlet Pressure, psi _____

Turbine Load (0, 1/2, Full), Kw _____, Comb. Chamber Temp, T_2 _____ °F

Exhaust: CO_2 , Reading _____, % _____ Opacity, % _____

Turbine Outlet Temperature, T_3 _____ °F

Sandair Outlet Temperature, T_5 _____ °F

Velocity Pressure Upstream, in. H_2O _____ Vel., fpm _____

Velocity Pressure (Down Stream), in H_2O _____ Vel., fpm _____

Smoke Sample: Orifice Δp , in. H_2O _____ Time, Sec. _____

Flow, cfh _____ Gas Volume, cubic feet _____

Sample Temperature, T_4 _____ °F

Rw (Reflectance of clean filter) _____

Rs (Reflectance of Sample Spot) _____

Smoke Number _____ W/A _____

Maximum Overhead Duct Temperature, _____ °F

Remarks: Twb1- Tdb1- Twb2- Tdb2- _____

Sandair Sump Water Temperature, T_7 _____ °F

GAS TURBINE - SANDAIR STARTUP PROCEDURE

1. Open test turbine exhaust duct damper.
2. Close boiler damper.
3. Turn on CO₂ and N₂ tanks at tank values (set pressure regulators at 5 psi).
4. Turn on CO₂ and N₂ line valves.
5. Turn on sample pump (4 way valve in sample position, line valve open).
6. Turn selector valve to N₂ and adjust flow rate to 800 cc/min.
7. Turn on CO₂ instrument and recorder and temperature indicator.
8. Check fuel drain line valves - closed positions.
9. Check fuel supply in tank (measuring burette extension tube filled).
10. Check battery charger for less than 10 amps charge rate, if battery is low, charge in parallel and shut down equipment.
11. Connect batteries in series red to positive.
12. Check water level in tanks for legs (should be filled to drain hole).
13. With sample valve in N₂ position, adjust instrument zero to achieve 0% on recorder, (20 minutes after turning on).
14. Turn sample valve to CO₂ and adjust instrument gain to achieve 100% on recorder.
15. Recheck N₂ and CO₂ until consistent 0% and 100% are obtained.
16. Turn on electrical load-cooling blower.
17. Turn on exhaust duct blower (starter in column next to fuel stand).
18. Open knife valve.
19. Turn on water to sandair (10 psi).
20. Turn on roots.
21. Check turbine panel switches - all off (or open).
22. Start turbine (note RPM @100%, volts @240 amps, and KW @0)
23. Set load switch to position L₁ L₃ PH₃.
24. Select 1/2 or full load on electrical breaker.
25. Adjust knife valve to ΔP desired. (or ΔP₁ for flow rate).
26. Adjust water inlet pressure to obtain desired flow rate.

27. Take all appropriate data.
28. For shutdown, stop turbine then proceed from No. 20 to No. 3 turning off equipment and valves.
29. Reconnect batteries in parallel and connect battery charger.

TABLE A-3

GAS TURBINE WITH RADER SANDAIR FILTER SYSTEM
Tested Summer 1982 at Oregon State University

Filter Nos.	Fuel Composition Kerosene/Toluene	Sample Location	Load, %	Ambient Temp., °F	Barometric Pressure, in. HG	Scrubber Water Press, psi	Scrubber Water Flow, GPM	SandAir ΔP, in. H ₂ O	Turbine Outlet Temp., °F	SandAir Gas Flow ACPM	SandAir Gas Outlet Temp., °F	SandAir Gas Flow SCFM	SandAir Water Out Temp., °F	SAE Smoke Number
2-5	100/0	INLET	0	71	29.90	5	2.9	19.6	452	475	89	271	86	0.2
6-9	100/0	INLET	Full	77	29.90	5	2.9	11	798	475	85	196	82	0.9
10-13	0/100	INLET	0	72	29.90	5	2.9	19.6	464	475	93	267	90	13.1
14-18	0/100	INLET	Full	77	29.90	5	2.9	11	826	475	88	192	87	29.1
19-22	50/50	INLET	0	74	29.90	5	2.9	19.6	464	475	90	267	87	1.6
23-26	50/50	INLET	Full	75	29.90	5	2.9	11	802	475	90	196	88	7.1
27-30	50/50	OUTLET	0	71	29.97	5	2.9	18	451	450	94	257	93	0.1
31-34	50/50	OUTLET	0	71	29.97	10	4.5	18	462	450	85	254	79	0.1
35-38	50/50	OUTLET	0	73	29.95	15	5.7	18	463	450	81	254	77	0.1
39-42	50/50	OUTLET	Full	75	29.95	5	2.9	10	808	450	92	185	85	4.1
43-46	50/50	OUTLET	Full	77	29.90	10	4.5	10	794	450	88	187	81	3.8
47-50	50/50	OUTLET	Full	79	29.90	15	5.7	10	798	450	74	186	69	5.8
51-54	0/100	OUTLET	0	70	29.90	5	2.9	18	468	450	86	252	86	9.3
55-58	0/100	OUTLET	0	72	29.90	10	4.5	18	467	450	86	252	81	10.5
59-62	0/100	OUTLET	0	72	29.90	15	5.7	18	468	450	80	252	76	9.7
63-66	0/100	OUTLET	Full	76	29.90	5	2.9	10	811	450	86	184	78	17.4
67-70	0/100	OUTLET	Full	77	29.90	10	4.5	10	806	450	78	185	72	16.3
71-74	0/100	OUTLET	Full	78	29.90	15	5.7	10	814	450	74	184	68	17.4
75-78	0/100	OUTLET	Full	78	29.90	5	2.9	11	816	475	89	194	79	19.8
79-82	0/100	OUTLET	Full	79	29.90	5	2.9	18.5	813	625	111	255	98	23.0
83-86	0/100	OUTLET	0	76	29.90	5	2.9	19.0	485	475	95	261	88	11.4
87-90	0/100	OUTLET	0	75	29.90	5	2.9	10.8	492	300	83	164	76	11.8

FUEL HYDROGEN/CARBON RATIO: KEROSENE 9.09/90.38, Toluene 8.56/91.07

VARIABLE ZERO LOAD FULL LOAD

Fuel Press., psi	90	105
Fuel Flow, lb/hr	27.7	49.5
Compt. Out Press, psi	16.5	17.0
Combustion Chamber Temp, °F	868	1467
CO ₂ %	1.6	3.0
CO ₂ ppm	640	260

GAS TURBINE - BAGHOUSE STARTUP PROCEDURE

1. Open test turbine exhaust duct damper.
2. Close boiler damper.
3. Turn on CO₂ and N₂ tanks at tank valves (set pressure regulators at 5 psi).
4. Turn on CO₂ and N₂ line valves.
5. Turn on sample pump (4 way valve in sample position, line valve open).
6. Turn selector valve to N₂ and adjust flow rate to 800 cc/min.
7. Turn on CO₂ instrument and recorder and temperature indicator.
8. Check fuel drain line valves - closed positions.
9. Check fuel supply in tank (measuring burette extension tube filled).
10. Check battery charger for less than 10 amps charge rate, if battery is low, charge in parallel and shut down equipment.
11. Connect batteries in series red to positive.
12. Drain fuel from turbine plenum chamber.
13. With sample valve in N₂ position, adjust instrument zero to achieve 0% on recorder, (20 minutes after turning on).
14. Turn sample valve to CO₂ and adjust instrument gain to achieve 100% on recorder.
15. Recheck N₂ and CO₂ until consistent 0% and 100% are obtained.
16. Turn on electrical load-cooling blower.
17. Turn on exhaust duct blower (starter in column next to fuel stand).
18. Open knife valve.
19. Close doors (unlocked) and open windows.
20. Turn on roots.
21. Check turbine panel switches - all off (or open).
22. Start turbine (note RPM @100%, volts @240 amps, and KW @0).
23. Set load switch to position L₁ L₃ PH₃.
24. Select 1/2 or full load on electrical breaker.
25. Adjust knife valve to ΔP desired, (or ΔP_v for flow rate).

26. Take all appropriate data.
27. For shutdown, stop turbine then proceed from No. 20 to No. 3 turning off equipment and valves.
28. Reconnect batteries in parallel and connect battery charger.
29. If run was made on fuel containing toluene, drain system, fill with kerosene, and run for 15 minutes to flush. Leave fuel system full of kerosene.

GAS TURBINE DATA SHEET

USAF Project - Laboratory Evaluation of Novel Particulate Control Concepts for Jet Engine Test Cells

Principal Investigator Prof. R. W. Boubel
Oregon State University

Date _____ Time _____

Test Crew _____

Flow Rate, ACFM _____ Baghouse ΔP , in. H_2O _____

Fuel: % Kerosene _____, % Toluene _____

Ambient Temperature, T_6 _____ $^{\circ}F$ Barometric Pressure, in. Hg _____

Fuel Flow: Seconds per 500 cc _____, Pounds per hour _____

Fuel Pressure, psi _____ Compressor Outlet Pressure, psi _____

Turbine Load (0, 1/2, Full), Kw _____, Comb. Chamber Temp, T_2 _____ $^{\circ}F$

Exhaust: CO_2 , Reading _____, % _____ Opacity, % _____

Turbine Outlet Temperature, T_3 _____ $^{\circ}F$

Baghouse Inlet Temperature, T_2 _____ $^{\circ}F$

Velocity Pressure Upstream, in. H_2O _____ Vel., fpm _____

Baghouse Outlet Temperature, T_5 _____ $^{\circ}F$

Smoke Sample: Orifice Δp , in. H_2O _____ Time, Sec. _____

Flow, cfh _____ Gas Volume, cubic feet _____

Sample Temperature, T_4 _____ $^{\circ}F$

R_w (Reflectance of clean filter) _____

R_s (Reflectance of Sample Spot) _____

Smoke Number _____ W/A _____

Maximum Overhead Duct Temperature, _____ $^{\circ}F$

Remarks: _____

No. of Wraps of Fabric: _____

TABLE A-4
 GAS TURBINE WITH CERAMIC (3M) FABRIC BAGHOUSE
 Tested Summer 1982 at Oregon State University

Filter Nos.	Fuel Composition Kerosene/Toluene	Sample Location	Load %	Ambient Temp, °F	Barometric Press., in. HG	Filter Material	Number of Filter Wraps	Baghouse ΔP, in. H ₂ O	Baghouse Gas Flow, ACFM	Turbine Outlet Temp, °F	Baghouse Inlet Temp, °F	Baghouse Outlet Temp, °F	Bag Completely Annealed	SAE Smoke Number
1-4	0/100	INLET	100	91	29.75	8H24	3	1.0	295	852	537	346	No	31.8
5-8	0/100	INLET	100	91	29.75	8H24	3	2.0	440	853	657	445	No	35.8
9-12	0/100	INLET	100	91	29.70	8H24	3	4.0	645	847	754	583	No	31.8
13-16	0/100	OUTLET	100	84	29.80	8H24	3	1.0	285	889	520	270	No	27.2
17-20	0/100	OUTLET	100	87	29.80	8H24	3	2.0	4.5	863	634	405	No	29.0
21-24	0/100	OUTLET	100	87	29.80	8H24	3	4.0	595	862	734	569	No	27.7
25-28	0/100	OUTLET	0	75	28.50	8H24	3	1.0	260	484	374	286	No	9.3
29-32	0/100	OUTLET	0	75	28.50	8H24	3	2.0	325	485	402	300	No	8.6
33-36	0/100	OUTLET	0	75	28.50	8H24	3	4.0	475	469	425	362	No	8.8
37-40	0/100	INLET	0	68	28.50	8H24	3	1.0	245	479	343	223	No	10.0
41-44	0/100	INLET	0	69	28.50	8H24	3	2.0	300	476	386	270	No	11.6
45-48	0/100	INLET	0	69	28.50	8H24	3	4.0	435	460	414	334	No	12.6
51-54	0/100	INLET	0	69	29.85	8H24	1	1.0	300	469	368	256	Yes	9.9
55-58	0/100	INLET	0	69	29.85	8H24	1	4.0	661	456	454	407	Yes	11.0
59-62	0/100	OUTLET	0	71	29.85	8H24	1	1.0	309	469	371	250	Yes	8.8
63-66	0/100	OUTLET	0	71	29.85	8H24	1	4.0	655	458	452	397	Yes	9.0
67-70	0/100	OUTLET	0	76	29.86	5H40	1	1.0	253	469	357	277	No	9.0
71-74	0/100	OUTLET	0	76	29.86	5H40	1	4.0	563	471	447	409	No	8.1
75-78	0/100	OUTLET	100	80	29.86	5H40	1	4.0	500	864	677	585	No	28.8
79-82	0/100	OUTLET	100	83	29.86	5H40	1	1.0	224	841	467	358	No	28.3

APPENDIX B

MASTERS PROJECT

DATA ANALYSIS AND PERFORMANCE EVALUATION OF A GAS TURBINE
EQUIPPED WITH A WET SCRUBBER

Prepared by: George D. Ikonou
Graduate Research Assistant
Oregon State University
Corvallis, Oregon

Supervisor: Richard W. Boubel, Ph.D.
Professor of Mechanical Engineering
Oregon State University
Corvallis, Oregon

April 1, 1982

NOTE: This Thesis was reproduced exactly as written, including
numbering of tables, figures and equations.

SECTION I

INTRODUCTION

A smoking stationary jet engine test cell has been simulated in a research project conducted by R. W. Boubel at Oregon State University for the U.S. Air Force (reference 1). In an effort to control particulate emissions, a wet scrubber system was used. It consisted of a spray nozzle downstream of the engine exhaust followed by a cyclone (demister); schematic diagrams of the system are shown in Figures B-1 and B-2. In order to determine the effectiveness of the particulate removal system, SAE Smoke Number measurements were taken at different spray water pressures using three fuel mixtures. The Smoke Number results, as well as the temperature drops across the spray system, were analyzed and it was concluded that visible particulate loadings did not decrease during water spray use (see reference 1).

In the present work, complete material and energy balances were performed on the system using the data collected by R. W. Boubel (reference 1). The calculations are divided into two parts: a) material and energy balances around the turbine and b) material and energy balances around the spray system. What follows is a presentation of the equations used, the results, and a discussion of their meaning.

SECTION II

NOMENCLATURE

- A_{cs} = Cross sectional area, ft^2
 C_p = Heat capacity, $btu/lb\ ^\circ F$.
 E = Energy flow rate, btu/hr .
 F = Molar flow rate, $lbmoles/hr$.
 h = Enthalpy, btu/lb .
 HHV = Fuel higher heating value, btu/lb .
 ΔH = Heat of reaction, btu/lb .
 KE = Kinetic energy, btu/hr .
 LHV = Lower heating value, btu/lb .
 M = Mass flow rate, lb/hr .
 M_H = Fuel hydrogen content, $lb\ H/lb$.
 M_C = Fuel carbon content, $lb\ C/lb$.
 MH = Molecular weight.
 P = Ambient pressure, $in\ Hg$.
 \dot{Q} = Heat loss, btu/hr .
 R = Universal gas constant.
 T = Temperature, $^\circ F$.
 V = Volumetric flow rate, ft^3/min .
 v = Velocity, ft/s .
 \dot{W} = Work, btu/hr .

Y = Moisture content, lb water/lb dry air.
y = Molar or % volume compositions.
 λ = Latent heat of vaporization, btu/lb.
 ρ = Density, lb/ft³.

Subscripts

a = Air

CO = Carbon monoxide

CO₂ = Carbon dioxide

e = Exhaust

f = Fuel

H₂ = Hydrogen

l = Liquid

N₂ = Nitrogen

O₂ = Oxygen

s = Spray section

t = Turbine

v = Vapor

W = Water

WL = Liquid water

WV = Vapor water

1,2,3,4,5 = stream numbers of Figure 4.

1D,3D = streams 1 or 3 on a dry (water free) basis.

Double subscripts on flow or composition quantities, $X_{i,j}$, indicate

i = species and j = stream number as shown in Figure 1.

For example, $M_{w,3}$ = Mass flow of water in stream 3.

Double subscripts on enthalpies, $h_{i,j}$, indicate i = species,
 j = temperature.

For example, $h_{a,5}$ = enthalpy of air at temperature T_5 .

SECTION III

EXPERIMENTAL

Even though data acquisition is not a part of this work, it is important to describe the experiment so that the reader is familiar with the experimental procedure and the data source. Referring to Figures 1 through 4, the various parts of the system may be identified.

The variables which were controlled by the experimenter were fuel composition (kerosene, toluene, and 50/50 mixture of kerosene and toluene), spray water pressure (0, 10, 30, 60 psi), and percent load (0, 40, and 100). During each run, the fuel and load were fixed and the four water pressures were varied, each allowing enough time for all of the measurements to be made. The measured quantities were: T_1 , % RH, spray water flow (gpm), P , M_2 , $y_{CO,3}$, $y_{CO_2,3}$, V_3 (ACFM), T_3 , T_5 , and SAE Smoke Number. The remaining data were taken later in the following manner: API gravity of the three fuels and exhaust diameter were measured while HHV, water data, ambient air compositions and enthalpy values were obtained from references 5, 6, 6, and 4, respectively. A more detailed description of the system and data acquisition may be found in Reference 1.

SECTION IV

METHOD OF ANALYSIS

A diagram pertaining to the analysis is shown on Figure 1. All symbols are defined in Section III. Appendix 1 in Section VII contains the data used for the analysis. For the first analysis only, the engine is analyzed, while in the second analysis only the spray system is the subject of analysis. First, the assumptions are listed and the equations follow. Detailed derivations can be found in Appendix 2.

For the material balances, the following assumptions are made:

- 1) All gaseous streams behave as ideal gases;
- 2) Unburned fuel at the exhaust (carbon and unburned hydrocarbons) are in negligible amounts;
- 3) Oxides of nitrogen are neglected;
- 4) Engine exhaust pressure is taken as ambient;
- 5) Because of the large amounts of excess air, the fraction of O_2 used in the turbine combustor is very small.

Therefore, exhaust stream properties (molecular weight, density, enthalpy, etc.) are taken as those of air.

This assumption is widely used throughout the literature (see reference 2).

For the energy balances, the following assumptions are made:

- 1) Intake kinetic energy, friction losses and elevation effects are negligible;
- 2) Reference states are the intake or ambient conditions;
- 3) Fuel enters the system at ambient temperature;
- 4) Heat into and work done by the system are taken as positive.

Part A. Analysis of the Turbine

To determine the compositions of all streams, material balances can be performed.

An overall mass balance gives:

$$F_1 = 2.746 \frac{V_3 P}{459.7 + T_3} - \frac{M_2}{28.96} \quad (1)$$

where F_1 is in lb moles/hr, V_3 in ACFM, P in in. Hg, T_3 in °F and M_2 in lb/hr. Note that V_3 , P , T_3 and M_2 are all given as data. Next the intake compositions are calculated.

$$y_{O_2} = y_{O_2,1D} / [1 + 1.609 Y_1] \quad (2)$$

$$y_{N_2,1} = y_{N_2,1D} / [1 + 1.609 Y_1] \quad (3)$$

$$y_{CO_2,1} = y_{CO_2,1D} / [1 + 1.609 Y_1] \quad (4)$$

$$y_{W,1} = 1.609 Y_1 / [1 + 1.609 Y_1] \quad (5)$$

An elemental balance on hydrogen yields:

$$y_{W,3} = \left[\frac{y_{W,1} F_1 + m_H M_2 / 2.02}{2.746 V_3 P} \right] (T_3 + 459.7)$$

AD-A137 641

LABORATORY EVALUATION OF NOVEL PARTICULATE CONTROL
CONCEPTS FOR JET ENGINE TEST CELLS(U) OREGON STATE UNIV
CORVALLIS R W BOUBEL DEC 83 AFESC/ESL-TR-83-02

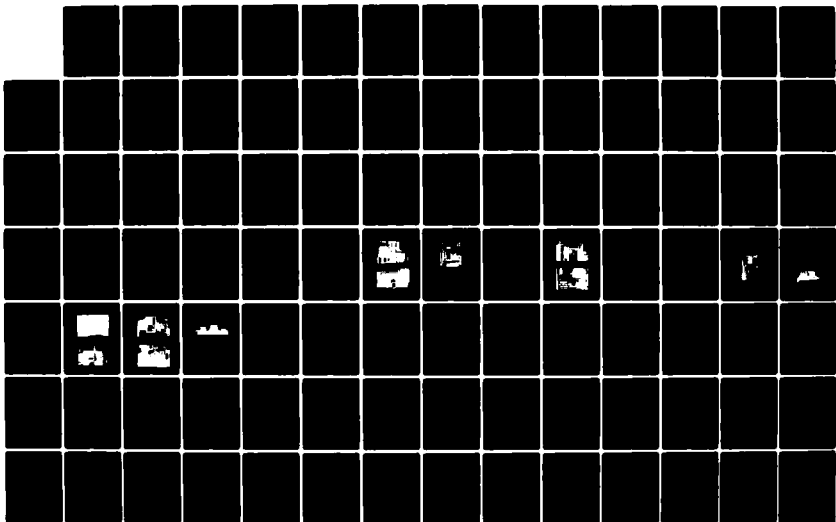
2/3

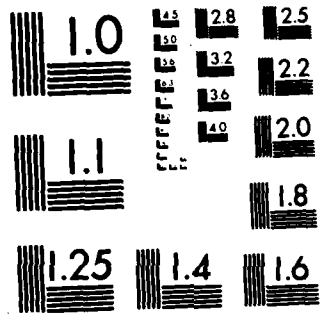
UNCLASSIFIED

F08635-81-K-0003

F/G 21/2

NL





MICROCOPY RESOLUTION TEST CHART
NATIONAL BUREAU OF STANDARDS-1963 A

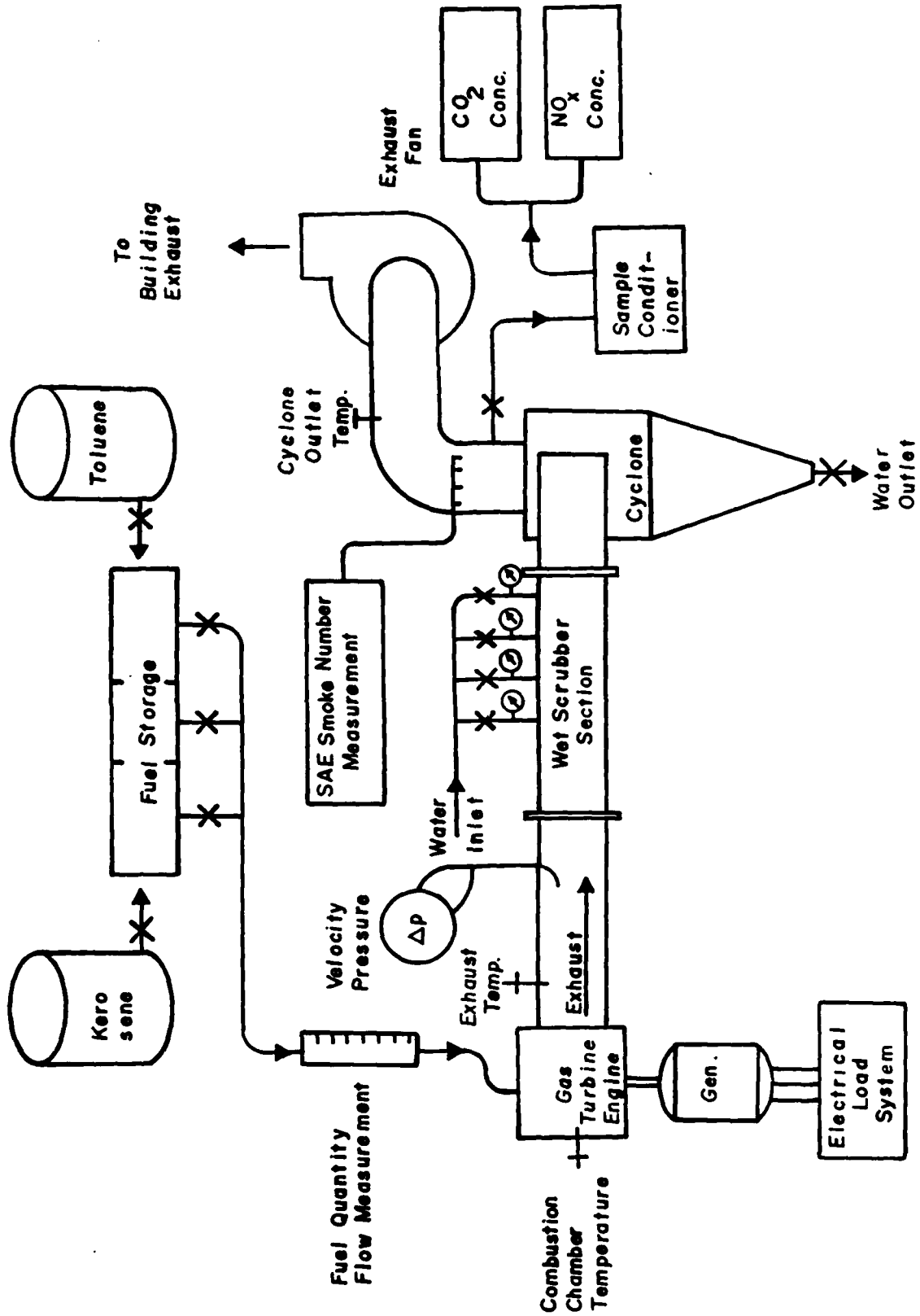


Figure 1. Schematic of test facility for wet scrubber.

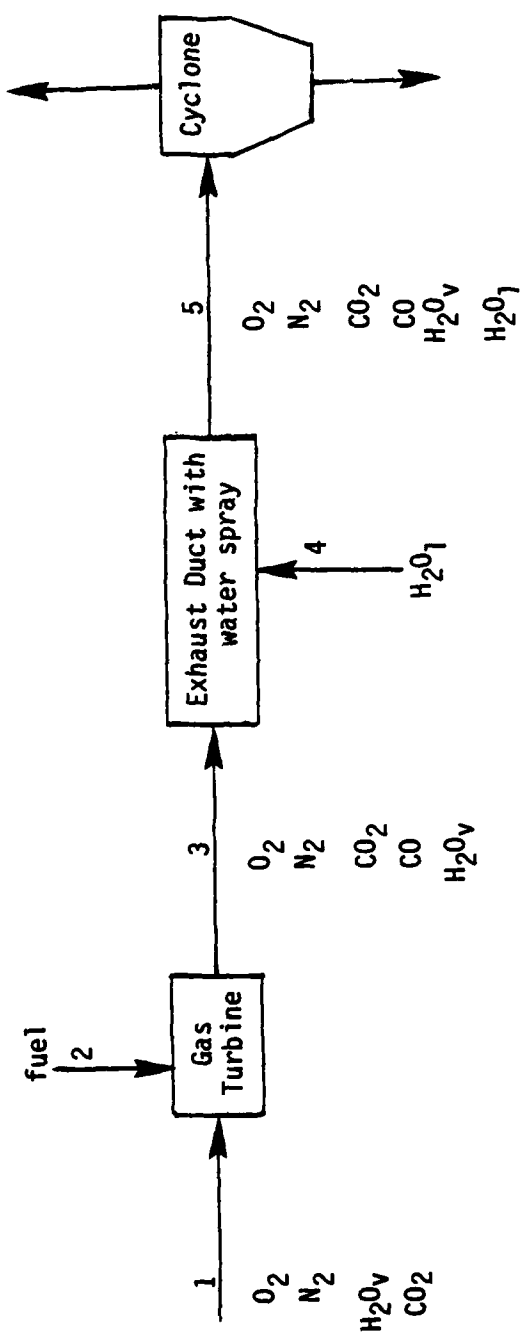


Figure 2. Schematic diagram of turbine and wet scrubber

An elemental balance on oxygen yields:

$$y_{O_2,3} = \left[1 + \frac{M_2(T_3 + 459.7)}{79.52 V_3 P} \right] (y_{O_2,1} + y_{CO_2,1} + \frac{1}{2} y_{w,1}) - y_{CO_2,3} - \frac{1}{2} y_{CO,3} - \frac{1}{2} y_{w,3} \quad (7)$$

An elemental analysis on nitrogen yields:

$$y_{N_2,3} = \left[1 + \frac{M_2(T_3 + 459.7)}{79.52 V_3 P} \right] y_{N_2,1} \quad (8)$$

So far, the molar compositions of intake and exhaust have been calculated. However, there is one more requirement which the exhaust compositions must satisfy, namely that:

$$y_{O_2,3} + y_{N_2,3} + y_{CO_2,3} + y_{CO,3} + y_{w,3} = 1 \quad (9)$$

This can be used as a check for consistency since it has not been used in the derivation of equations 6 through 8. Let the left side of equation 9 be S_y , then

$$\% \text{ Error} = \frac{1 - S_y}{1} \times 100 \quad (10)$$

Another objective of the analysis on the turbine is to account for the energy being introduced into the system in the form of fuel, or chemical energy. The material balance equations can be solved in terms of flow rates rather than compositions to give the following results:

$$F_{1D} = \frac{F_1}{1 + 1.609 Y_1} \quad (11)$$

$$M_{w,3} = 18 [F_1 - F_{1D} + m_H M_2 / 2.02] \quad (12)$$

$$M_{3D} = 28.96 \left[\frac{2.746 V_3 P}{459.7 + T_3} - (F_1 - F_{1D} + m_H M_2 / 2.02) \right] \quad (13)$$

See Appendix 2 for detailed derivations.

Once F_1 , F_{1D} , $M_{W,3}$, and M_{3D} are known, an enthalpy balance can be performed to calculate the rate of heat loss from the turbine .

$$\dot{Q}_t = (\text{HHV}) M_2 - 1050.4 [M_{W,3} - 18 (F_1 - F_{1D})] - \dot{W} - M_{3D} (h_{a,3} - 128.25) - M_{W,3} (h_{wv,3} - 1095.4) - 2.986 \times 10^{-7} (M_{3D} + M_{W,3}) V_3^2 \quad (14)$$

Since the intake stream is taken as the reference state, the only input of energy is the chemical bond energy introduced with the fuel. Energy leaves the system in three forms: a) heat loss due to convection and radiation, b) useful work drawn by the generator and c) internal energy in the exit exhaust stream in the form of enthalpy and kinetic energy. In mathematical terms,

$$E_f = \text{Fuel energy (input)} = M_2 (\text{HHV}) - 1050.4 \times [M_{H_2O,3} - 18 (F_1 - F_{1D})]$$

$$\text{Heat loss} = \dot{Q}_t$$

$$\text{Useful energy} = \dot{W}$$

$$E_e = \text{Exhaust internal energy} = M_{3D} h_{a,3} + M_{H_2O,3} h_{w,3} + 2.986 \times 10^{-7} V_3^2 (M_{3D} + M_{W,3})$$

Note that the fuel bond energy must be the lower heating value (LHV = ΔH of combustion with water as a vapor product). Therefore, the HHV must be corrected by subtracting the heat of vaporization of water as shown in the first expression above. To account for the various forms of energy leaving the turbine, the following definitions are used:

$$\% \text{ Heat loss} = \frac{\dot{Q}_t}{E_f} \times 100 \quad (15a)$$

$$\% \text{ Loss to exhaust} = \frac{E_e}{E_f} \times 100 \quad (15b)$$

$$\% \text{ loss to useful work} = \% \text{ efficiency} = \frac{\dot{W}}{E_f} \times 100 \quad (15c)$$

In this manner, the energy flow through the turbine is completely accounted for. To summarize the analysis of the turbine, two tasks have been completed.

i. Using material balances the compositions of the exhaust stream have been determined and used to check for consistency of calculations, and

ii. Using simultaneous material and energy balances, the energy flow through the turbine has been analyzed completely.

This procedure was used in all 36 sets of data.

Part B. Analysis of the Spray System

This analysis is performed in two parts. First, the cases in which no spray water was introduced are examined. An energy balance gives the convective heat loss as follows:

$$\dot{Q}_s = M_{3D} (h_{a,3} - h_{a,5}) + M_{w,3} (h_{w,3} - h_{w,5}) \quad (16)$$

Upon examining the data for these runs, it can be seen that T_3 and T_5 (the exhaust and cyclone temperatures) are the same. In fact, in most cases an increase of a few degrees can be seen; this is physically impossible but it is due to experimental error. As a result, the terms $(h_{a,3} - h_{a,5})$ and $(h_{w,3} - h_{w,5})$ both become zero, indicating no convective heat losses (adiabatic operation). A mathematical modeling study conducted by Springer (reference 2) also used the assumption of adiabatic conditions in the spray section. If more doubts remain as to the validity of the assumption, the runs should be repeated

using an insulated duct at the spray section in order to achieve adiabatic conditions experimentally. In the present analysis it will be assumed that $\dot{Q}_s = 0$ before the next calculation is made.

Next, an energy balance is performed for the case of spray water being introduced into the exhaust stream. Upon combining with the material balance around this section, the amount of liquid water leaving the system can be calculated.

$$M_{WL,5} = \frac{M_{3D}(h_{a,3} - h_{a,5}) + M_{W,3} h_{W,3} + M_4(T_4 - 32) - (M_{W,3} + M_4) h_{W,5}}{T_5 - 32 - h_{W,5}} \quad (17)$$

For purposes of generalization, the above result is converted into a percentage form as follows:

$$\% \text{ Evaporation} = \frac{\text{Spray water evaporated}}{\text{Liquid spray water introduced}} \times 100, \text{ or}$$

$$\% \text{ Evaporation} = \frac{\text{Liquid H}_2\text{O introduced} - \text{liquid H}_2\text{O leaving the system}}{\text{Liquid water introduced}} \times 100$$

$$\% \text{ Evaporation} = \frac{M_4 - M_{WL,5}}{M_4} \times 100$$

This calculation was performed for all 36 data sets.

SECTION V

RESULTS AND DISCUSSION

A. TURBINE

A reader interested in extending the findings of this study to a full-scale test cell would certainly want to determine how well this experimental setup has simulated the actual cell. In order to answer this question and determine the performance characteristics of the turbine, the results of material and energy balances are presented in Tables 1 through 4. Table 1 shows the volume percent compositions of the intake and exhaust streams as well as the results of how consistent the data are. Although the numbers would be of little use for quantitative prediction of a full-scale turbine, some qualitative conclusions can be made.

- a) Oxygen levels dropped by 2%, thus justifying assumption 5 of Section V;
- b) Nitrogen levels remained roughly the same;
- c) CO, CO₂, and water vapor levels increased considerably as expected because of the combustion reaction;
- d) the percent error column shows that the calculations are consistent.

Engine performance and distribution of energy are given in Tables 2 through 4. Table 2 shows what percent of the fuel chemical

energy leaves as lost heat, useful work, or is carried out by the exhaust stream. The break-downs are given for each fuel used. Table 3 contains the same information averaged to eliminate dependence on fuel. It is worth noting that

- a) Percent efficiency increases from 0 to 5, a relatively low level;
- b) Approximately 30% of the energy leaves as convective/radiative loss while the remaining 70% is carried out by the exhaust;
- c) The magnitude of heat loss (130-200 kBtu/hr) gives an idea of the size of the system.

The significance of these results is simply the quantitative description of the system; they show that the data are consistent and help the reader decide whether the conclusions presented later may be generalized to a full-scale system.

B. WATER SPRAY SYSTEM

As mentioned before, analysis of Smoke Number and temperature drop results showed that the spray system is not an adequate particulate control device (reference 1). The results of this part of the analysis help explain this conclusion by showing what happens to the liquid water injected at the spray nozzles. Analyses of variance (Appendix 3) showed that the extent of evaporation of this water depends solely on the load imposed on the turbine. The dependence appears linear with a positive slope. These results appear in tabular

TABLE 1. RESULTS OF MATERIAL BALANCES AROUND THE TURBINE

Load	VOLUME %				COMPOSITIONS				Sum of exhaust Com- posi- tions	% Error	Fuel	
	Engine Intake				Engine Exhaust							
	O ₂	N ₂	CO ₂	H ₂ O(v)	O ₂	N ₂	CO ₂ *	CO*				H ₂ O(v)
0	20.59	76.72	.049	1.74	18.64	76.14	1.3	.064	2.73	98.87	1.12	Kerosene
	20.77	77.42	.050	.86	18.65	76.84	1.5	.064	1.82	98.87	1.13	
	20.69	77.13	.049	1.22	18.57	76.56	1.5	.064	2.19	98.88	1.12	
	20.64	76.94	.049	1.47	18.60	76.39	1.45	.064	2.39	98.90	1.10	
40	20.80	77.53	.050	.72	18.37	76.80	1.65	.040	1.94	98.80	1.20	
	20.76	77.38	.050	.92	18.26	76.62	1.7	.040	2.17	98.80	1.20	
	20.69	77.12	.049	1.24	17.91	76.40	2.0	.040	2.46	98.80	1.20	
	20.65	76.98	.049	1.43	17.92	76.25	1.95	.040	2.64	98.80	1.20	
100	20.67	77.04	.049	1.35	16.40	75.87	3.0	.026	3.31	98.61	1.40	
	20.72	77.22	.049	1.11	16.74	76.14	2.8	.026	2.95	98.65	1.35	
	20.77	77.43	.050	.84	16.89	76.38	2.75	.026	2.60	98.64	1.35	
	20.63	76.90	.049	1.52	16.96	75.87	2.55	.026	3.26	98.67	1.33	
0	20.72	77.24	.049	1.08	18.64	76.64	1.5	.064	1.99	98.82	1.18	Toluene
	20.72	77.22	.049	1.11	18.65	76.67	1.5	.064	1.98	98.86	1.14	
	20.72	77.22	.049	1.11	18.58	76.61	1.5	.064	2.08	98.83	1.17	
	20.72	77.24	.049	1.08	18.65	76.69	1.5	.064	1.96	98.86	1.14	
40	20.62	76.88	.049	1.55	17.43	76.10	2.4	.040	2.78	98.75	1.25	
	20.71	77.18	.049	1.16	17.62	76.42	2.3	.040	2.37	98.75	1.25	
	20.72	77.24	.049	1.08	17.68	76.48	2.25	.040	2.30	98.75	1.25	
	20.66	77.02	.049	1.36	17.62	76.25	2.25	.040	2.58	98.74	1.26	
100	20.72	77.23	.049	1.10	16.16	76.06	3.35	.026	2.95	98.54	1.46	
	20.77	77.40	.050	.88	16.16	76.19	3.35	.026	2.80	98.52	1.48	
	20.68	77.10	.049	1.27	16.36	75.92	3.1	.026	3.13	98.54	1.46	
	20.72	77.24	.049	1.08	16.50	76.15	3.1	.026	2.81	98.58	1.42	
0	20.83	77.65	.050	.56	18.72	77.73	1.5	.064	1.51	98.86	1.14	50/50 Mixture
	20.82	77.59	.050	.64	18.70	77.01	1.5	.064	1.58	98.86	1.14	
	20.78	77.47	.050	.78	18.68	76.90	1.5	.064	1.72	98.87	1.13	
	20.78	77.47	.050	.80	18.68	78.99	1.5	.064	1.72	98.87	1.13	
40	20.79	77.49	.050	.78	17.90	76.84	2.15	.040	1.95	98.89	1.11	
	20.71	77.22	.049	1.11	17.80	76.50	2.15	.040	2.29	98.78	1.22	
	20.82	77.59	.050	.64	17.91	76.86	2.15	.040	1.82	98.78	1.22	
	20.65	76.98	.049	1.43	17.73	76.24	2.15	.040	2.63	98.78	1.22	
100	20.66	77.02	.049	1.36	16.55	75.97	3.0	.026	3.07	98.63	1.37	
	20.69	77.08	.049	1.28	16.64	76.10	3.0	.026	2.90	98.67	1.33	
	20.78	77.46	.050	.80	16.76	76.49	3.0	.026	2.39	98.66	1.34	
	20.65	76.98	.049	1.43	16.60	75.99	3.0	.026	3.04	98.66	1.34	

* From data

TABLE 2. DISTRIBUTION OF ENERGY LEAVING THE TURBINE FOR THREE DIFFERENT FUELS

Load	% Efficiency	% Heat Loss	% Lost to Exhaust	Heat Loss kBtu/hr	Fuel
0	0	28.05	71.95	133.0	Kerosene
40	3.08	24.74	72.19	164.8	
100	5.62	22.40	71.98	204.4	
0	0	34.91	65.09	180.8	Toluene
40	2.88	28.53	68.60	203.5	
100	5.23	24.36	70.42	238.7	
0	0	31.22	68.78	163.7	50/50
40	2.98	24.59	72.43	168.4	
100	5.66	16.12	78.22	146.1	

TABLE 3. DISTRIBUTION OF ENERGY LEAVING THE TURBINE, OVERALL

Load	% Efficiency	Heat Losses	% Lost to Exhaust	Rate of Heat Loss (kBtu/hr)
0	0	28.05	71.95	133.0
	0	34.91	65.09	180.8
	0	31.22	68.78	163.7
	Ave = 0	Ave = 29.18	Ave = 68.61	Ave = 159.2
40	3.08	24.74	72.19	164.8
	2.88	28.53	68.60	203.5
	2.98	24.59	72.43	168.4
	Ave = 2.98	Ave = 25.95	Ave = 71.07	Ave = 178.9
100	5.62	22.40	71.98	204.4
	5.23	24.36	70.42	238.7
	5.66	16.12	78.22	146.1
	Ave = 5.50	Ave = 20.99	Ave = 73.54	Ave = 196.4

TABLE 4. RESULTS OF ENERGY BALANCES AROUND THE TURBINE

Load	% Efficiency	% Lost to Heat	% Lost to Exhaust	Heat Loss kBTu/hr	Fuel
0	0	30.55	69.46	104.4	Kerosene
	0	30.42	69.59	162.2	
	0	28.58	71.42	151.7	
	0	22.66	77.34	116.9	
40	3.08	24.63	72.29	163.7	
	3.06	25.29	71.65	169.5	
	3.09	24.50	72.41	162.4	
	3.07	24.52	72.41	163.4	
100	5.45	22.42	72.12	206.8	
	5.60	22.41	71.99	194.7	
	5.74	21.83	72.43	205.1	
	5.68	22.93	71.39	210.8	
0	0	34.05	65.95	176.4	Toluene
	0	39.05	60.95	202.3	
	0	29.03	70.97	150.4	
	0	37.50	62.50	194.2	
40	2.85	29.13	68.02	209.5	
	2.90	27.88	69.23	197.1	
	2.85	29.95	67.21	215.3	
	2.90	27.17	69.94	192.1	
100	5.15	26.03	68.83	258.9	
	5.15	24.10	70.76	239.6	
	5.31	21.56	73.13	207.9	
	5.31	25.74	68.95	248.2	
0	0	30.55	69.45	160.1	50/50 Mixture
	0	28.06	71.94	147.1	
	0	33.14	66.86	173.7	
	0	33.14	66.86	173.7	
40	2.99	23.57	73.44	161.4	
	2.99	23.61	73.41	161.8	
	2.94	26.38	70.63	180.6	
	2.99	24.79	72.23	169.7	
100	5.50	16.06	78.44	149.6	
	5.71	14.01	80.27	125.8	
	5.71	17.85	76.44	160.2	
	5.71	16.56	77.73	148.6	

form on Tables 5 and 6 and in graphical form on Figures 6 and 7. It can be concluded that in no case is all of the water completely evaporated, a conclusion which confirms observations that use of an additional spray ring completely floods the system. As load increases, more of the liquid water is evaporated, since the exhaust temperature is higher. The vaporization process is responsible for the significant temperature drops which cause hydrocarbon condensation as mentioned in reference 1. The usefulness of these findings is that they shed some light on some of the events occurring inside the exhaust duct by describing them quantitatively.

TABLE 5. DEPENDENCE OF PERCENT EVAPORATION ON LOAD

Fuel \ % Load	0	40	100
Kerosene	23.07	35.08	52.74
Toluene	20.82	41.08	66.02
50/50	26.15	39.49	61.11

TABLE 6. LINEAR REGRESSION OF PERCENT EVAPORATION VERSUS PERCENT LOAD

Fuel	a	b	r
Kerosene	29.65	23.09	1.000
Toluene	44.91	21.53	.9984
50/50	35.05	25.78	.9999
Overall	36.52	26.01	.970

X-axis % Load	Y Axis - % Evaporation				
	Kerosene	Toluene	50/50	Overall	
0	23.07	20.82	26.15	23.35	
40	35.08	41.08	39.49	38.54	
100	52.74	66.02	61.11	59.96	
Best Fit Parameters	Intercept	23.09	21.53	25.78	26.01
	Slope	.2965	.4491	.3505	.3652

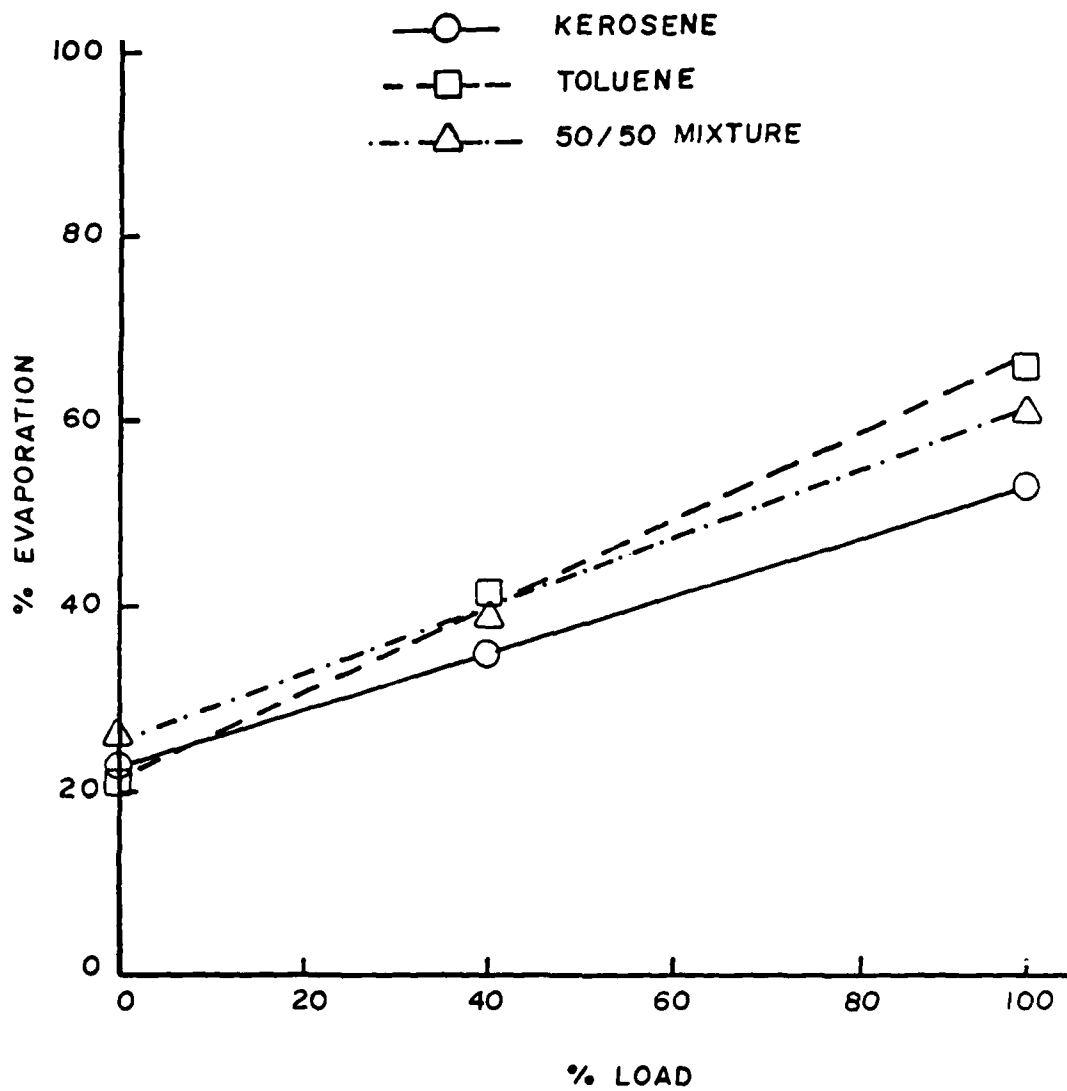


Figure 3. Liquid water evaporation at the spray ring for three different fuels.

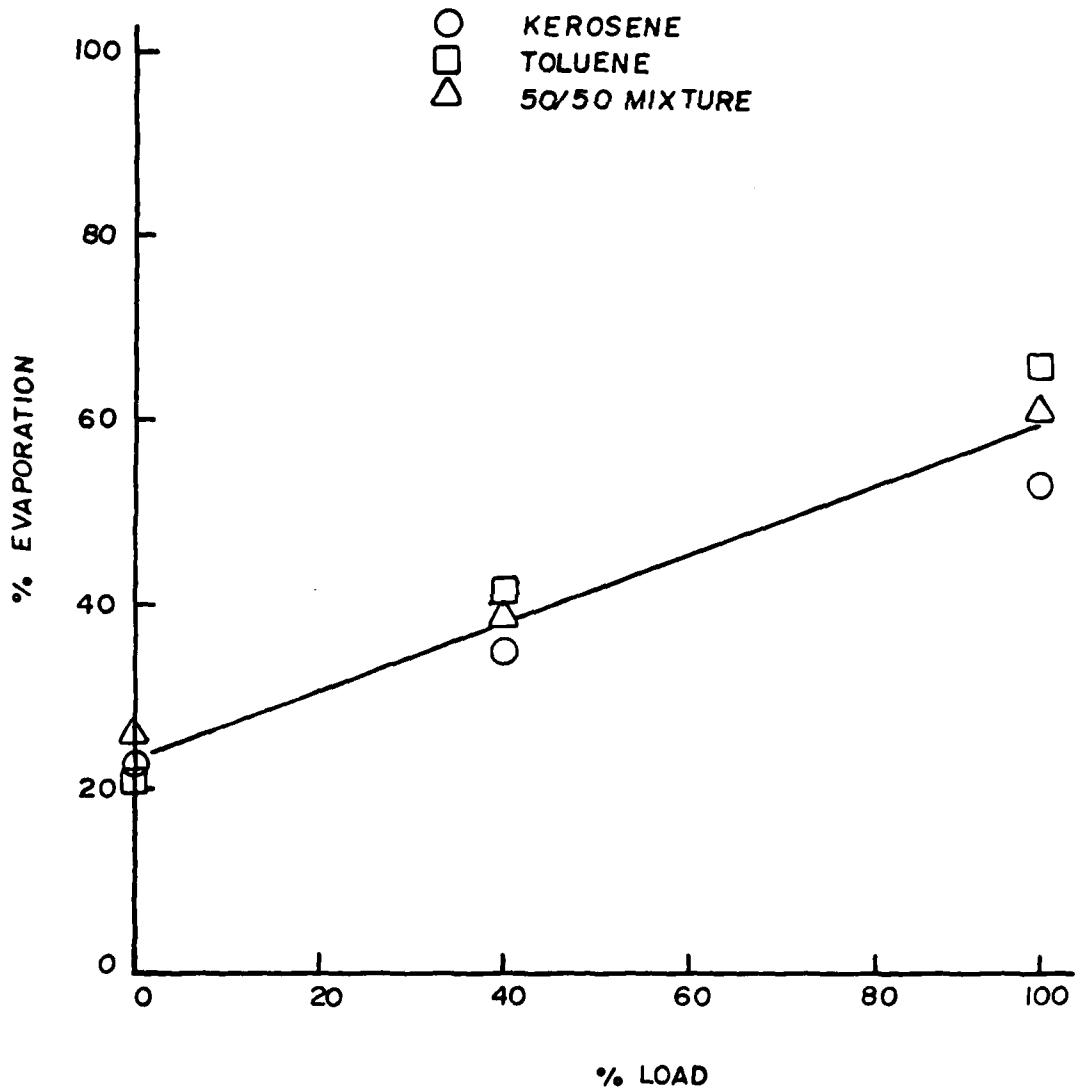


Figure 4. Liquid water evaporation at the spray ring, average for all three fuels.

SECTION VI

APPENDICES

APPENDIX 1 Data

a) Composition of ambient air, dry basis (reference 6).

Component	Volume %
N ₂	78.084
O ₂	20.946
CO ₂	.050

$$MW_a = 28.96$$

b) Fuel data

Fuel	Lb Carbon/ lb.	Lb hydro- gen/lb.	MW	API Gravity	HHV btu/lb. *
Kerosene	.9086	.0914	6.019	44.3	19812
Toluene	.9141	.0859	6.204	31.6	19304
50/50 Mixture	.9113	.0866	6.110	37.7	19548

c) Water data

$$\lambda = 1050.4 \text{ Btu/lb}$$

$$\rho = 62.23 \text{ lb/ft}^3$$

$$C_{PW} = 1 \text{ btu/lb } ^\circ\text{F}$$

*

From reference 5, using API gravity values.

d) Exhaust CO data

Load	Volume ppm
0	640
40	400
100	260

e) Load data

% Load	Power Output Btu/hr
0	0
40	20490
100	51220

f) Experimental runs, see Table 7.

g) Exhaust duct cross sectional area, $A_{CS} = .1364 \text{ ft}^2$ (5" ID).

TABLE 3. EXPERIMENTAL DATA

Test No.	Load %	Fuel Composition Ker/Tol	H ₂ O Pressure psi	H ₂ O Flow gpm	Ambient Temperature °F	Ambient Moisture Lb of H ₂ O Lb dry air	Ambient Pressure in Hg	Fuel Flow Rate Lb/hr	Exhaust % CO ₂	Exhaust Volumetric Flow Rate ACFM	Exhaust Temperature °F	Cyclone Temperature °F	Enthalpy Data			
													h _{a,3} btu/lb	h _{a,5} btu/lb	h _{w,3} btu/lb	h _{w,5} btu/lb
1	0	100/0	0	0	70	.011	29.85	27.17	1.3	1500	450	475	243.5	224.8	1310.9	1275.3
2	50		0	0	65	.0045	29.85	35.06	1.65	1664	600	600	255.9	255.9	1334.8	1334.8
3	100		0	0	70	.0085	29.85	49.60	3.0	1882	900	875	332.4	325.9	1482.3	1469.8
4	0		10	.5	70	.0054	29.82	28.13	1.5	1500	475	476	224.8	225.0	1275.3	1275.3
5	50		10	0	70	.0058	29.82	35.35	1.7	1664	600	480	255.9	226.0	1334.8	1277.6
6	100		10	0	70	.0070	29.85	48.29	2.8	1882	850	626	319.4	262.4	1457.3	1347.4
7	0		30	.86	70	.0077	29.80	28.00	1.5	1500	490	356	228.5	195.65	1282.4	1219.2
8	50		30	0	70	.0078	29.80	34.97	2.0	1664	600	430	255.9	213.7	1334.8	1254.1
9	100		30	0	70	.0053	29.80	47.05	2.75	1882	820	516	311.7	234.9	1442.3	1294.7
10	0		60	1.2	78	.0093	30.00	27.23	1.45	1500	470	320	223.5	186.6	1272.9	1202.3
11	50		60	0	75	.0090	29.95	35.16	1.95	1664	600	390	255.9	203.9	1334.8	1235.2
12	100		60	0	70	.0096	39.95	47.58	2.55	1882	805	470	307.85	223.5	1434.8	1272.9
13	50	50/50	0	0	64	.0048	30.00	36.58	3.0	1732	600	607	255.9	232.65	1334.8	1338.2
14	100		0	0	74	.0086	30.00	49.73	2.15	2045	875	880	325.9	327.2	1469.8	1472.3
15	50		10	.5	70	.0070	30.00	36.58	3.0	1732	600	467	255.9	222.8	1334.8	1271.5
16	100		10	0	80	.0081	30.00	47.94	2.15	2045	850	609	319.4	258.1	1457.3	1339.2
17	50		30	.86	62	.0040	29.47	36.58	3.0	1732	580	403	250.85	207.3	1325.3	1241.3
18	100		30	0	64	.0050	29.47	47.94	2.15	2045	800	470	306.55	223.5	1432.3	1272.9
19	50		60	1.2	76	.0090	29.47	36.58	3.0	1732	600	355	255.9	195.4	1334.8	1218.8
20	100		60	0	76	.0090	29.47	47.94	2.4	2045	825	470	313.0	223.5	1444.8	1272.9
21	50	0/100	0	0	70	.0098	29.92	38.87	3.35	1704	590	598	253.45	255.4	1330.0	1333.8
22	100		0	0	70	.0069	29.90	53.75	2.30	1950	850	850	319.4	319.4	1457.3	1457.3
23	50		10	.5	65	.0073	29.96	38.22	3.35	1704	590	419	253.45	208.8	1330.0	1244.6
24	100		10	0	70	.0055	29.90	5.375	2.25	1950	900	620	332.4	260.9	1482.3	1344.5
25	50		30	.86	70	.0068	29.92	38.87	3.10	1704	580	430	250.85	213.7	1325.3	1254.1
26	100		30	0	70	.0080	29.95	52.12	2.25	1950	900	525	332.4	212.5	1482.3	1299.0
27	50		60	1.2	70	.0086	29.96	38.22	3.1	1704	800	390	255.9	203.9	1334.8	1235.2
28	100		60	0	70	.0068	29.95	52.12	1.5	1950	800	470	306.55	223.5	1432.3	1272.9
29	0	50/50	0	0	53	.0035	30.10	28.00	1.5	1459	475	483	224.8	226.7	1275.3	1279.0
30	0		10	.5	60	.0040	30.10	28.00	1.5	1459	500	392	230.95	204.4	1287.1	1236.1
31	0		30	.86	64	.0050	30.10	28.00	1.5	1459	450	355	218.65	195.4	1263.5	1218.8
32	0		60	1.2	63	.0050	30.10	28.00	1.5	1459	450	320	218.65	186.6	1263.5	1202.3
33	0	0/100	0	0	70	.0068	29.33	28.00	1.5	1459	450	490	218.65	228.5	1263.5	1282.4
34	0		10	.5	72	.0070	29.33	28.00	1.5	1459	405	381	207.6	201.7	1242.3	1231.1
35	0		30	.86	72	.0070	29.33	28.00	1.5	1459	500	348	230.95	193.65	1287.1	1215.5
36	0		60	1.2	70	.0068	29.33	28.00	1.5	1459	420	317	211.05	186.1	1249.3	1200.9

*From reference 3

†From reference 4

APPENDIX 2 Derivations of Equations

Part A. Turbine

1. Material balance equations used to calculate compositions.

Refer to Figure 4 for symbols. Consider the exhaust stream; according to the ideal gas law,

$$\rho_3 = MW_3 P / RT_3$$

Because of assumption 5, Section V, $MW_3 = 28.96$. Also, $R = 21.85 \text{ ft}^3 \text{ in Hg/lb mole } ^\circ\text{R}$, so

$$\rho_3 = \frac{28.96 \text{ (Lb/Lb mole) } P \text{ (in Hg)}}{21.85 \text{ (ft}^3 \text{ in Hg/Lb mole } ^\circ\text{R) } T_3 \text{ (} ^\circ\text{R)}}$$

$$\text{or } \rho_3 = 1.325 \frac{P}{T_3}, \quad T_3 \text{ in } ^\circ\text{R} \quad (\text{a})$$

An overall balance based on mass gives:

$$M_1 + M_2 = M_3 \quad \text{or} \quad M_1 = M_3 - M_2$$

$$\text{or } M_1 = 60 V_3 \rho_3 - M_2 \quad \text{where } V_3 \text{ is in ACFM} \quad (\text{b})$$

Note that a factor of 60 is used to convert flow rate from ft^3/min to ft^3/hr . Since $F_1 = M_1/MW_1$ and $MW_1 = 28.96$,

$$F_1 = \frac{1}{28.96} (60 V_3 \rho_3 - M_2). \quad (\text{c})$$

Substitute (a) into (c) to obtain

$$F_1 = 2.746 \frac{V_3 P}{459.7 + T_3} - \frac{M_2}{28.96} \quad (1)$$

Here T_3 is in $^\circ\text{F}$, all flow rates are on an hour basis.

For the intake stream, $F_1 \left(\frac{\text{moles air}}{\text{hr}} \right) = F_{1D} \left(\frac{\text{moles dry air}}{\text{hr}} \right) + F_{W,1} \left(\frac{\text{moles water}}{\text{hr}} \right)$. We can express $F_{W,1}$ in terms of Y_1 , the moisture content of ambient air, as follows:

$$F_{w,1} = Y_1 \left(\frac{\text{lb water}}{\text{lb dry air}} \right) \frac{M_{w_a} (\text{lb dry air/Lb mole dry air})}{M_{w_w} (\text{Lb water/Lb mole water})} F_{1D} \left(\frac{\text{lb moles dry air}}{\text{hr}} \right)$$

$$\text{or } F_{w,1} = Y_1 \frac{M_{w_a}}{M_{w_w}} F_{1D} \quad (1a)$$

$$\text{thus } F_1 = F_{1D} + Y_1 \frac{M_{w_a}}{M_{w_w}} F_{1D} = F_{1D} \left(1 + \frac{28.96}{18.0} Y_1 \right)$$

$$\text{or } F_{1D} = F_1 / (1 + 1.609 Y_1) \quad (1b)$$

Note that Y_1 may be found from a psychrometric chart from ambient temperature and percent relative humidity. Since the given intake compositions (which are the same as ambient) are given on a dry basis (water-free air) we can calculate the compositions for moist air as follows:

$$y_{O_2,1} \left(\frac{\text{Lb moles } O_2}{\text{lb-mole moist air}} \right) = y_{O_2,1D} \left(\frac{\text{Lb moles } O_2}{\text{lb-mole dry air}} \right) \frac{F_{1D} (\text{lb-moles dry air/hr})}{F_1 (\text{lb-moles moist air/hr})}$$

$$\text{or } y_{O_2,1} = y_{O_2,1D} \frac{F_{1D}}{F_1} \quad (1c)$$

Use equation (1b) to eliminate F_{1D}/F_1 :

$$y_{O_2,1} = y_{O_2,1D} / (1.0 + 1.609 Y_1) \quad (2)$$

Similarly for N_2 and CO_2 equations (3) and (4) are derived:

$$y_{N_2,1} = y_{N_2,1D} / (1.0 + 1.609 Y_1) \quad (3)$$

$$y_{CO_2,1} = y_{CO_2,1D} / (1.0 + 1.609 Y_1) \quad (4)$$

For water, we have $y_{w,1} = F_{w,1}/F_1$ or, by introducing equation (1a):

$$y_{w,1} = Y_1 (M_{w_a}/M_{w_w}) (F_{1D}/F_1)$$

Use equation (1b) to eliminate F_{1D}/F_1 :

$$y_{W,1} = 1.609 Y_1 / (1 + 1.609 Y_1) \quad (5)$$

A balance on lb-moles of hydrogen, H, gives:

$$F_{H,1} + F_{H,2} = F_{H,3} \quad (5a)$$

Examine each term separately; for the first term $F_{H,1} = 2 F_{W,1}$ because each mole of water which enters contains two moles of H. Therefore,

since $F_{W,1} = y_{W,1} F_1$

$$F_{H,1} = 2 y_{W,1} F_1 \quad (5b)$$

The second term is:

$$F_{H,2} \left(\frac{\text{lb-moles H}}{\text{hr}} \right) = M_2 \left(\frac{\text{lb fuel}}{\text{hr}} \right) m_H \left(\frac{\text{lb H}}{\text{lb fuel}} \right) [1/1.01 \left(\frac{\text{lb H}}{\text{lb mole H}} \right)]$$

$$\text{or } F_{H,2} = M_H M_2 / 1.01 \quad (5c)$$

The third term is: $F_{H,3} = 2 F_{W,3}$ or $F_{H,3} = 2 y_{W,3} F_3$

Also $F_3 = M_3 / MW_3 = M_3 / 28.96$ or $F_3 = 60 V_3 \rho_3 / 28.96$

Using equation (a) to eliminate ρ_3 , we obtain

$$F_3 = 2.746 V_3 P / (459.7 + T_3) \quad (5d)$$

Then $F_{H,3}$ becomes

$$F_{H,3} = 5.492 y_{W,3} V_3 P / (459.7 + T_3) \quad (5e)$$

Substitute (5b), (5c), and (5e) into (5a):

$$2 y_{W,1} F_1 + \frac{m_H M_2}{1.01} = 2 y_{W,3} \frac{2.746 V_3 P}{459.7 + T_3}$$

Solve for $y_{W,3}$:

$$y_{W,3} = \left(\frac{y_{W,1} F_1 + m_H M_2 / 2.02}{2.746 V_3 P} \right) (T_3 + 459.7) \quad (6)$$

A balance on oxygen, O, based on lb-moles gives:

$$2 (y_{O_2,1} F_1) + 2 (y_{CO_2,1} F_1) + y_{W,1} F_1 = 2 (y_{O_2,3} F_3) + 2 (y_{CO_2,3} F_3) + y_{CO,3} F_3 + y_{W,3} F_3$$

Solve for $y_{O_2,3}$ to obtain

$$y_{O_2,3} = \frac{F_1}{F_3} (y_{O_2,1} + y_{CO_2,1} + \frac{1}{2} y_{W,1}) - y_{CO_2,3} - \frac{1}{2} y_{CO,3} - \frac{1}{2} y_{W,3} \quad (6a)$$

To eliminate F_1/F_3 , use equations (1) and (5d):

$$F_1 = F_3 - \frac{M_2}{28.96} \quad \text{and} \quad F_3 = 2.746 \frac{V_3 P}{459.7 + T_3}$$

Rearrange to obtain

$$F_1/F_3 = 1 + \frac{M_2 (T_3 + 459.7)}{79.52 V_3 P} \quad (6b)$$

Substitute into equation (6a) to obtain:

$$y_{O_2,3} = \left[1 + \frac{M_2 (T_3 + 459.7)}{79.52 V_3 P} \right] (y_{O_2,1} + y_{CO_2,1} + \frac{1}{2} y_{W,1}) - y_{CO_2,3} - \frac{1}{2} y_{CO,3} - \frac{1}{2} y_{W,3} \quad (7)$$

A balance on nitrogen, N, on lb-mole basis gives:

$$y_{N_2,1} F_1 = y_{N_2,3} F_3 \quad \text{or} \quad y_{N_2,3} = y_{N_2,1} F_1/F_3$$

Use equation (6b) to eliminate F_1/F_3 :

$$y_{N_2,3} = \left[1 + \frac{M_2 (T_3 + 459.7)}{79.52 V_3 P} \right] y_{N_2,1} \quad (8)$$

2. Material balance equations used to calculate mass flow rates

First note that equation (1b) is the same as equation 11. To calculate $M_{W,3}$, the mass flow of water in stream 3, proceed as follows:

$$F_{W,3} = F_{W,1} + (\text{lb moles of } H_2O \text{ generated in combustion/hr}) \quad (8a)$$

(lb-moles H_2O generated in combustion) = $1/2$ (lb-moles H used in com-

$$\text{bustion}) = 1/2 \frac{m_H M_2}{1.01} = \frac{m_H M_2}{2.02}$$

Substitute this result into (8a):

$$F_{W,3} = F_{W,1} + \frac{M_H M_2}{2.02} \text{ and since } F_{W,1} = F_1 - F_{1D}$$

$$F_{W,3} = F_1 - F_{1D} + \frac{M_H M_2}{2.02} \quad (8b)$$

Since $M_{W,3} = 18.0 F_{W,3}$,

$$M_{W,3} = 18 (F_1 - F_{1D} + M_H M_2 / 2.02) \quad (12)$$

The flow rate at stream 3, the exhaust, on a dry basis (water-free) can be calculated as follows:

$$M_{3D} = 28.96 F_{3D} \text{ or } M_{3D} = 28.96 (F_3 - F_{W,3})$$

Use equations (5d) and (8b) to eliminate F_3 and $F_{W,3}$

$$M_{3D} = 28.96 \left[\frac{2.746 V_3 P}{459.7 + T_3} - (F_1 - F_{1D} + \frac{m_H M_2}{2.02}) \right] \quad (13)$$

3. Energy balance equations

Knowing F_1 , F_{1D} , $M_{W,3}$, and M_{3D} , an energy balance on the turbine will allow the determination of \dot{Q}_t , the convective/radiative heat loss from the turbine. Using the intake conditions and water vapor as a reference state, the first law of thermodynamics is applied to give:

$$E_f - \dot{Q}_t + M_1 h_1 + M_2 h_2 = M_3 h_3 + KE_3 + \dot{W} \quad (13a)$$

Each term will be examined separately in order to reduce equation (13a) to a more useable form. The first term is:

E_f = Chemical energy entering with the fuel

$E_f = M_2 (\text{HHV}) - \lambda_W, 77^\circ\text{F}$ (rate of production of water by the combustion reaction)

$$E_f = M_2 (\text{HHV}) - 1050.4 [M_{W,3} - 18 (F_1 - F_{1D})] \quad (13b)$$

Note that HHV is the enthalpy of reaction of 77°F with water liquid as a product, i.e.: $\text{fuel} + \text{O}_2 \rightarrow \text{H}_2\text{O}_{(1)} + \text{CO}_2$. In order to compute the LHV (enthalpy of reaction with water vapor as a product) the heat absorbed during evaporation of this water must be subtracted, and thus the second term in equation (13b). The second term in (13a) is the desired quantity and needs no further elaboration. The third and fourth terms are: $M_1 h_1 + M_2 h_2 = 0$ because of the choice of reference state. The first term of the right side is:

$$M_3 h_3 = M_{3D} (h_{a,3} - h_{a,77^\circ\text{F}}) + M_{W,3} (h_{WV,3} - h_{WV,77^\circ\text{F}})$$

$$\text{or } M_3 h_3 = M_{3D} (h_{a,3} - 128.25) + M_{W,3} (h_{WV,3} - 1095.4) \quad (13c)$$

Here h_a values were obtained from reference 3, and h_{WV} values from reference 4. The second term of the right side is:

$$KE_3 = M_3 \frac{1}{2g_c} v_3^2$$

where $v_3 = \frac{V_3 \text{ ft}^3/\text{min}}{A_{c_s} \text{ ft}^2} \cdot \frac{1 \text{ min.}}{60 \text{ sec}} = \frac{V_3}{(.1364)(60)} \text{ ft/s}$
and $g_c = 32.17 \text{ lb}_m \text{ ft}/\text{lb}_f \text{ sec}^2$

$$\text{so } KE_3 = \frac{(M_{3D} + M_{W,3}) \text{ lb/hr}}{(2)(32.17) \text{ Lb}_m \text{ ft}/\text{lb}_f \text{ sec}^2} \cdot \frac{V_3^2 \text{ ft}^2/\text{sec}^2}{(.1364)^2 (60)^2} \cdot \frac{.001286 \text{ Btu}}{\text{ft} - \text{Lb}_f}$$

$$\text{or } KE_3 = 2.986 \times 10^{-7} (M_{3D} + M_{W,3}) V_3^2 \quad (13d)$$

where V_3 is in ACFM and KE_3 in Btu/hr

The last term, \dot{W} , is obtained from the data and takes on three possible values: 0, 20490, or 51220 Btu/hr. Substitute equations (13b), (13c), and (13d) into (13a) to obtain:

$$\dot{Q}_t = M_2(\text{HHV}) - 1050.4 M_{W,3} - 18 (F_1 - F_{1D}) - \dot{W} -$$

$$M_{3D}(h_{a,3} - 128.25) - M_{W,3} (h_{WV,3} - 1095.4)$$

$$- 2.986 \times 10^{-7} (M_3 + M_{W,3}) V_3^2 \quad (14)$$

Part B. Water Spray Section

1. Calculation of heat loss

Energy balance with no water entering at stream 4 gives:

$$\dot{Q}_S = M_{3D} (h_{a,3} - h_{a,5}) + M_{W,3} (h_{WV,3} - h_{WV,5}) \quad (14a)$$

From the data section it can be seen that $T_4 = T_5$ so that $h_{a,3} = h_{a,5}$ and $h_{WV,3} = h_{WV,5}$. This reduces (14a) to $\dot{Q}_S = 0$.

2. Simultaneous material and energy balances

Material balance for water on a mass basis gives:

$$M_{W,3} + M_4 = M_{WL,5} + M_{WV,5} \quad (14b)$$

For the energy balance in this case it is convenient to use a reference state of 32°F and water in the liquid phase, the reference used in steam tables (see reference 4).

$$M_{3D} h_{a,3} = M_{WL,5} C_{pW} (T_5 - 32) + M_{WV,5} h_{WV,5} \quad (14c)$$

If (14b) is substituted into (14c) and the resulting equation is solved for $M_{WL,5}$, the result is (note that $C_{pW} = 1 \text{ btu/lb}^\circ\text{F}$):

$$M_{WL,5} = \frac{M_{3D} (h_{a,3} - h_{a,5}) + M_{W,3} h_{WV,3} + M_4 (T_4 - 32) - (M_{W,3} + M_4) h_{WV,5}}{(T_5 - 32) - h_{WV,5}} \quad (17)$$

APPENDIX 3. Statistical Analysis of Evaporation Results

An analysis of variance (ANOVA) is performed on the percent evaporation obtained from Section V, Part B to determine whether it varies significantly with load, water pressure or both. A 5% level of significance is used.

Kerosene

% Load water pres.	0	40	100	T_i	T_i^2
10	(15)	39.55	61.83	116.38	13,544.3
30	28.59	34.02	52.52	115.13	13,254.9
60	25.62	31.67	43.86	101.15	10,231.32
T_j	69.21				37,030.5
T_j^2	4790.02	11,075.5	25,030.4	40,895.9	

$$\Sigma y^2 = 13,928.32$$

$$\frac{T_{..}^2}{r_e} = \frac{(332.65)^2}{9} = 12,295.11$$

$$S_r^2 = \frac{37,030.5}{3} - 12,295.11 = 48.39$$

$$S_t^2 = 13,928.32 - 12,295.11 = 1,633.21$$

$$S_c^2 = \frac{40,895.9}{3} - 12,295.11 = 1,336.85$$

$$S_e^2 = 1,633.21 - (1,336.5 + 48.39) = 247.97$$

ANOVA

Due to	d.f.	s.s	M.S.	V.R.	F (.05)
water pres. (r)	2	48.39	24.20	.39	6.94
load (c)	2	1336.85	668.43	10.78	6.94
error	4	247.97	61.99	-	-
total	8	1633.21	-	-	-

Conclusion: Percent evaporation varies significantly with load only (5% level of significance).

Toluene

% Load water pres.	0	40	100	T_i	T_i^2
10	13.09	59.54	76.46	149.09	22,227.8
30	30.57	31.80	76.83	139.20	19,376.64
60	18.80	31.90	44.76	95.46	9,112.61
T_j	62.46	123.24	198.05	383.75	50,717.1
T_j^2	3,901.2	15,188.1	39,223.8	58,313.15	

$$\Sigma y^2 = 20,785.61$$

$$\frac{T_{..}^2}{rc} = \frac{(383.75)^2}{9} = 16,362.67$$

$$S_r^2 = \frac{50,717.1}{3} - 16,362.7 = 543.03$$

$$S_t^2 = 20,785.61 - 16,362.7 = 4,422.94$$

$$S_c^2 = \frac{58,313.15}{3} - 16,362.7 = 3,075.04$$

$$S_e^2 = 4,422.94 - (3,075.04 + 543.03) = 804.87$$

ANOVA

Due to	d.f.	s.s.	M.S.	V.R.	F (.05)
water press. (r)	2	543.03	271.52	1.35	6.94
load (c)	2	3,075.04	1,537.52	7.64	6.94
error	4	804.87	201.22	-	-
total	8	4,422.94	-	-	-

Conclusion: Percent evaporation varies significantly with load only (5% level of significance).

Mixture

water pres. \ % Load	% Load			T_i	T_i^2
	0	40	100		
10	34.85	45.22	72.95	153.02	23,415.1
30	21.8	36.09	61.58	119.47	14,273.1
60	21.8	37.16	48.8	107.76	11,612.2
T_j	78.45	118.47	183.33	380.20	49,300.4
T_j^2	6,154.4	14,035.14	33,609.9	53,799.4	

$$\Sigma y^2 = 18,335.15$$

$$\frac{T_{..}^2}{r_e} = \frac{(380.25)^2}{9} = 16,065.56$$

$$S_r^2 = \frac{49,300.4}{3} - 16,065.56 = 367.90$$

$$S_c^2 = \frac{53,799.4}{3} - 16,065.56 = 1,867.57$$

$$S_t^2 = 18,335.15 - 16,065.56 = 2,269.6$$

$$S_e^2 = 2,269.6 - (1,867.57 + 367.9) = 34.12$$

ANOVA

Due to	d.f.	s.s.	M.S.	V.R.	F (.05)
water press. (r)	2	367.90	183.95	21.57	6.94
load (c)	2	1,867.57	933.79	109.47	6.94
error	4	34.12	8.53	-	-
total	8	2,269.6	-	-	-

Conclusion: Percent evaporation varies significantly with load and with water pressure (5% level of significance).

SECTION IIX

REFERENCES

1. Boubel, R. W., "Atmospheric Emissions from a Gas Turbine Equipped with a Wet Scrubber," Interim Technical Report, U.S.A.F. Project F 08635-81-K-0003, January 1982.
2. Springer, Charles, "Effect of Cooling Water Spray on Turbine Engine Test Cell Emissions," 1977 USAF-ASEE Summer Faculty Research Program, Final Report, August 1977.
3. Hughes, A.D., "Thermodynamic Properties of Air," Chart plotted from data in Table I, GAS TABLES by Keenan and Kayes, 1967.
4. Keenan, J. A., and Kayes, F. G., Thermodynamic Properties of Steam, John Wiley and Sons, Inc., New York, 1949.
5. Popovich, M., and Hering, C., Fuels and Lubricants, John Wiley and Sons, Inc., New York, 1959.
6. Chemical Engineers' Handbook, R. H. Perry and C. H. Chilton, Editors, Fifth Edition, McGraw-Hill Book Company, 1973.

APPENDIX C

NO_x Emissions from a Gas Turbine as a Function of
Fuel-Bound Nitrogen and Other Variables

By

William Faye

Oregon State University

NOTE: This Thesis was reproduced exactly as written,
including numbering of tables, figures and
equations.

February 22, 1982

119

(The reverse of this page is blank)

TABLE OF CONTENTS

INTRODUCTION	125
PURPOSE	128
THEORY	129
Thermal NO	129
Prompt NO	130
Fuel Bound Nitrogen	131
NO ₂ Formation	132
APPARATUS	134
PROCEDURES	147
RESULTS	149
CONCLUSIONS	168
REFERENCES	169
BIBLIOGRAPHY	172
APPENDICES	175
1) Test of Scott NO _x Analyzer Accuracy	176
2) Beckman CO ₂ Analyzer Calibration Curve	176
3) Calculation of Required Additive Volume for a Given Weight Percent of Mixed Fuel	178
4) Gas Turbine Data Sheet	182
5) Test Operating Procedure	183
6) NO _x Values from Data Sheets	185
7) Determination of Combustor Inlet Temperature	188
8) Weight Percent of an Element in a Fuel Mixture	190
9) Fuel Density Calculations	194
10a) Calculation of A/F Ratios by Direct Measurement	198
10b) Calculation of the Percent Theoretical Air in Combustion from Combustion Stoichiometry	201
11) Calculation of Heat of Formation of Kerosene	204
12) Estimate of the Adiabatic Flame Temperature	206

LIST OF FIGURES

<u>Figure</u>	<u>Page</u>
1. Gas turbine generator	135
2. Combustor can assembly	135
3. Fuel control panel	136
4. Sample conditioning system	138
5. Scott NO _x Analyzer	138
6. Schematic Scott NO _x Analyzer	139
7. CO ₂ analyzer, chart recorder and electrical loading device	141
8. Digital temperature indicator	142
9. Combustor flame temperature thermocouple	144
10. Rear view of turbine-compressor	144
11. Wet and dry bulb measurement	145
12. Room set up	145
13. North Star Horizon computer	146
14. Adjusted NO _x vs. measured flame temperature	156
15. NO _x emissions for SRC recycle solvent and its surrogate	157
16. NO _x emissions for H-coal (ATM-OVHD) 366-533K and its surrogate	157
17. NO _x emissions for SRC light organic, and its surrogate	157
18. NO _x emissions for SRC wash solvent and its surrogate	157

19. Adjusted NO_x vs. Adiabatic flame temperature	160
20. Adjusted NO_x vs. Air/fuel ratio	162
21. NO_x vs. fuel bound nitrogen	164

LIST OF TABLES

<u>Table</u>	<u>Page</u>
I. NO _x Information - Measured and Derived	140
II. Adjusted NO _x vs. Measured Flame Temperature	155
III. Adjusted NO _x vs. Adiabatic Flame Temperature	161
IV. Adjusted NO _x vs. Air/Fuel Ratio and Theoretical Air	161
V. NO _x vs. Fuel Bound Nitrogen	165
VI. NO _x vs. Fuel Bound Nitrogen Least Squares Curve Fits	165

NO_x Emissions from a Gas Turbine as a Function Fuel-Bound Nitrogen and Other Variables

INTRODUCTION

The study and control of oxides of nitrogen (NO_x) formed during combustion processes, has gained new emphasis in the past few years as their effect on the environment becomes more well known. These effects are concentrated into two main areas, the formation of photochemical oxidants which are a cause of smog, and their combination with water to form dilute nitric acid, which precipitates out as acid rain.

The contribution of NO_x to smog is primarily that of a producer of free radicals which combine with oxygen and hydrocarbons to form Ozone and complex hydrocarbon chains.

The NO combines with oxygen in the atmosphere to produce NO₂. This NO₂, along with NO₂ emitted in the initial combustion reaction, is acted upon by ultraviolet light and breaks down into NO and an oxygen radical. This oxygen radical then can combine with diatomic oxygen to form ozone, which is a strong oxidizer. The ozone reacts with hydrocarbons in the atmosphere, forming many of the irritants which cause irritation of the eyes, nose and throat, and headaches.¹ The ozone also reacts strongly with many substances causing rapid degradation of rubber, nylon, and other fabrics and synthetics.

Acid rain also affects buildings, structures and statues by reacting with the stone and construction materials to etch or weaken them. Other effects of acid rain include rapid corrosion of paints and finishes on houses and automobiles, the dissolving of lead solder on piping (and its introduction into drinking water), and the dissolving and introduction of mercury into lakes and streams, and thence into the food chain.

It is mainly for these reasons, their contribution to smog and to acid rain, that NO_x emissions have come under closer study and tighter control by the Environmental Protection Agency.

PURPOSE

Studies by the Air Force in the late 1970's indicated that it would be desirable for the United States to develop its shale oil reserves as a source of military jet fuel.⁶ This fuel would be readily accessible and is considered sufficient to supply our needs in the event of national emergency.

Shale oil and synthetic fuels from coal have a higher nitrogen content, in the form of ammonia and pyridine compounds, than do most petroleum derived fuels. For this reason, it was of interest to the Air Force to see what effect this high nitrogen content would have on NO_x emissions.

THEORY

This section gives a brief overview of the theories and mechanisms which have been proposed as the major pathways of NO_x production in combustion systems. For a more complete background in this area, the reader is referred to the book, Combustion, by Irvin Glassman⁷, from which most of this section was taken.

In fuel injection systems such as a gas turbine, the fuel droplets burn as diffusion flames near the stoichiometric air fuel ratio. It is only after these fuels are completely vaporized and mixed that they reach the final air fuel ratios indicated by calculations. As a result, the reactions take place at a higher temperature than would be anticipated and the resulting concentrations of NO_x are higher than would be expected from overall mixture ratios.

Much of the NO_x formed is in the form of nitrous oxide [NO] with significantly smaller concentrations of NO_2 and minor amounts of N_2O_4 . For the moment we shall concentrate on production of NO in nitrogen free fuels. We will then address fuel bound nitrogen kinetics and the generation of NO_2 .

Thermal NO

NO from the combustion of nitrogen free fuels is highly temperature dependent and formed primarily by what is called the Zeldovich Mechanism.

First proposed by the Russian scientist Ya. B. Zeldovich in 1946, this model postulates that oxygen atoms are first formed from the thermal dissociation of O_2 or by hydrogen attack on atmospheric oxygen. This free oxygen atom then combines with atmospheric nitrogen as shown below.



Some later researchers have included the reaction

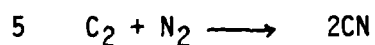


although this is felt to contribute to a much lesser extent.

Because of its high activation energy equation 1 is slow and acts as the control on the reaction. Because of the slowness of the reaction it was thought that all of the NO was formed in the post combustion zone. However, experiments made to confirm this showed that NO concentration profiles extrapolated to the flame front did not go to zero. This lent credence to arguments that reactions other than the Zeldovich mechanism also contributed to NO production.

Prompt NO

The NO formed in the combustion zone has been called Prompt NO. C.P. Fenimore discovered that Prompt NO is only found in the flames of hydrocarbons. This observation led to the following reaction scheme involving a hydrocarbon species and atmospheric nitrogen.



The N atoms could then form NO partially by the Zeldovich mechanism (equations 1 and 2) and the 2CN could form NO by reaction with diatomic oxygen or by attacking an oxygen atom.

It has also been theorized that if the O atom concentration in the reaction zone were much greater than the equilibrium levels, then the Zeldovich mechanism could also account for the prompt NO.

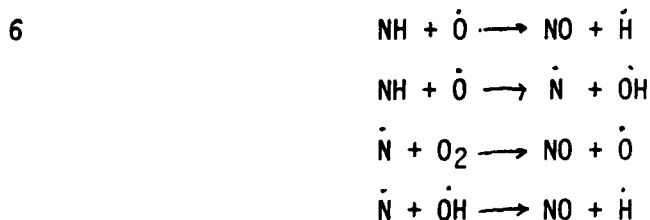
The current feeling is that both these mechanisms hold true and that which predominates depends on the flame temperatures and on the stoichiometry. In the low temperature regions the Fenimore mechanism is felt to control the production while in the high temperature areas the Zeldovich mechanism predominates due to high oxygen atom production.

Fuel Bound Nitrogen

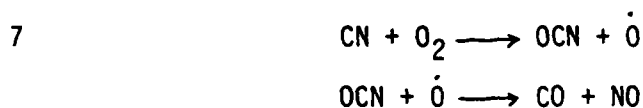
When nitrogen is present in the fuel, the NO emissions increase dramatically. The chemical mechanisms for this conversion are not completely determined as yet, however a number of possible mechanisms have been suggested.

The fuel nitrogen compounds probably undergo thermal decomposition to low molecular weight nitrogen compounds or radicals prior to combustion. These might include NH_2 , HCN, CN, NH_3 , NH, etc.

Some suggested qualitative conversion routes for NH would be:



A conversion route which has been suggested for CN is:



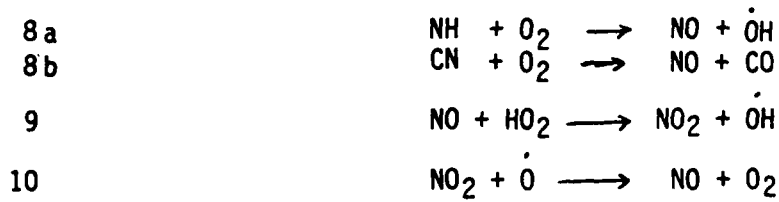
These reactions are quite fast and occur at approximately the same rate as the energy release during combustion.

NO₂ Formation

NO₂ is found in significant concentrations in the exhaust gases of some combustion systems, including gas turbines. This is surprising as chemical equilibrium calculations and kinetic models would indicate that it would not be found in appreciable quantities.

Because of this discrepancy, researchers have looked into NO₂ production and found that it is formed in the visible regime of all air flames. In most cases however, it is rapidly converted to NO in the post flame zone.

The following scheme has been suggested for the production and consumption of NO₂ in fuels containing nitrogen.



Reaction 9 is important as there can be significant amounts of HO_2 in the early parts of the flame.

It is also important to note that the reaction rate of equation 10 is two orders of magnitude slower than that of equation 9. Because of this, it is quite possible that reaction 10 is quenched before completion in some systems, such as gas turbines. This would account for the higher levels of NO_2 encountered in such systems.

APPARATUS

The main power plant for this project was an Airesearch Manufacturing Company Gas Turbine Generator, Model No. GTGE30-23 with a turbine engine, model No. GTP30-40. It was a self contained unit capable of generating up to 15 kw of electricity of AC or DC current. The package was fully instrumented to show output voltage, frequency, current and power, DC generator voltage, and percentage of engine rpm. Additional instrumentation had been added to show fuel pressure, compressor air pressure, combustion chamber temperature and exhaust temperature. See Figure 1.

The gas turbine system was a simple open cycle coupled turbine type, consisting of a centrifugal compressor and turbine wheel mounted on a common shaft and a combustor which exhausted into the turbine. The combustor was a single can type, as shown in Figure 2.

The turbine was speed governed by the proper metering of fuel. The fuel flow was adjusted to maintain a constant speed of 48,000 rpm under varying electrical loads.

The generator was connected to a series of resistors shown in the back corner of Figure 1. The switching box was able to give one half and full load to the generator, 6.25 kW and 15 kW, respectively. Zero load was achieved by opening the AC circuit breaker on the front panel of the turbine generator.

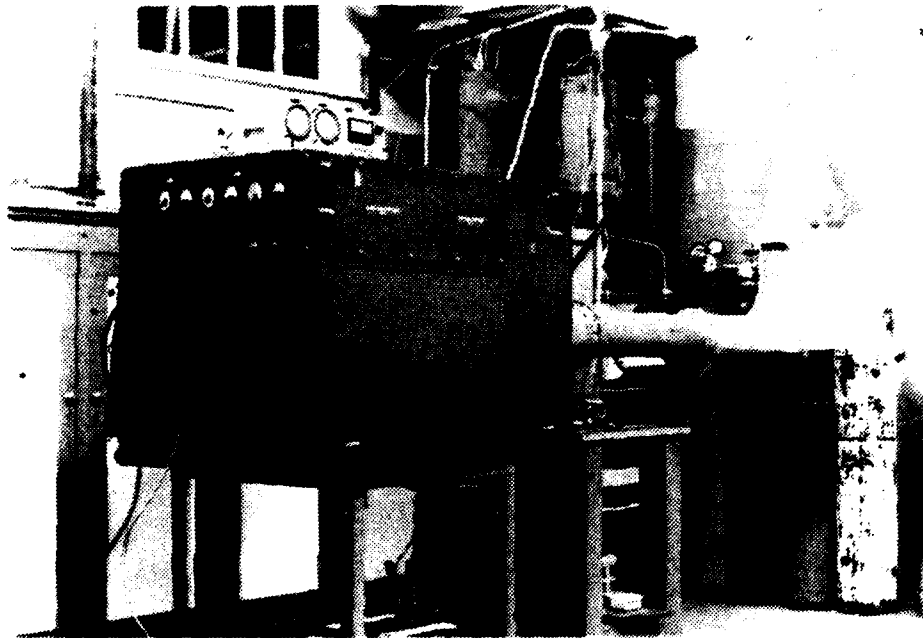


Figure 1. Gas turbine generator



Figure 2. Combustor can assembly

The turbine was supplied with fuel stored and metered in the fuel control panel, as shown in Figure 3.

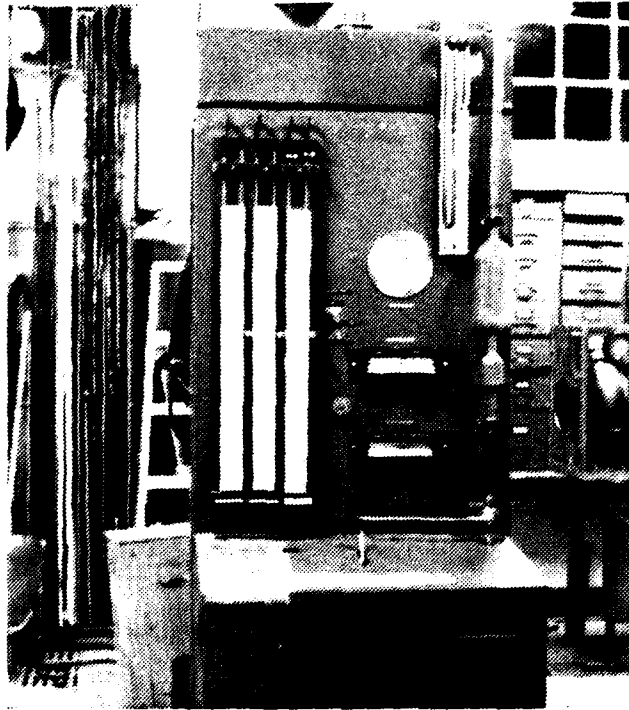


Figure 3. Fuel control panel

The control panel had three fuel tanks connected to the fuel line through a three-way valve, shown in the center. Measures of fuel flow rate were made by timing the flow of fuel through the 2000 cc burette on the right hand side of the panel.

Assuming that the 2000 cc burette volume was correct, we would estimate an accuracy to within 0.5% of our average volume flow rates. (flow at full load was 285 sec).

The flow rates of the exhaust gases were also measured, using a Dwyer Pitot Tube and manometer . These values were read as velocity pressure in inches of water. These values were then converted to the proper velocity and mass flow rates.

Due to the extreme turbulence in the exhaust duct it was difficult to estimate the accuracy of these measurements. From the results of the calculation of air fuel ratio information, and comparison with air fuel ratios derived from CO₂ data, the accuracy would appear to be fairly reasonable in some cases. However, overall accuracy of better than 10% of measured values cannot be assumed.

The exhaust sample was run through an AESI model SCM 7900 sample conditioning system (see Figure 4). The sample was cooled to near ambient temperatures and the particulate matter and moisture removed. The sample was then pumped at 12 psi to the analyzers.

The sample was passed to a Scott Model 325 Chemiluminescence NO/NO_x analyzer which, for our study, was used entirely in the NO_x mode.

This analyzer uses the light emissions produced by the reaction of NO and ozone to measure the concentration of NO in the sample gas. The intensity of the light is proportional to the flow of NO into the chamber.

In order to measure NO_x (NO and NO₂ combined), the sample was first passed through a thermal converter kept at 500° C. This dissociated the NO₂ into NO and the total concentration was then read as NO. A photograph of the instrument is shown in Figure 5,

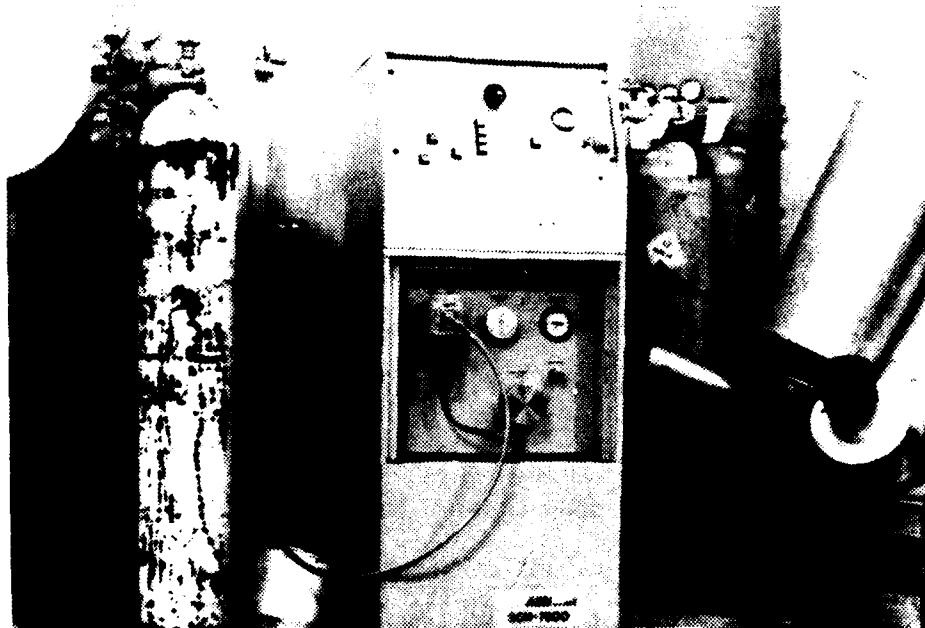


Figure 4. Sample conditioning system



Figure 5. Scott NO_x analyzer

while a schematic of its major components is shown in Figure 6.

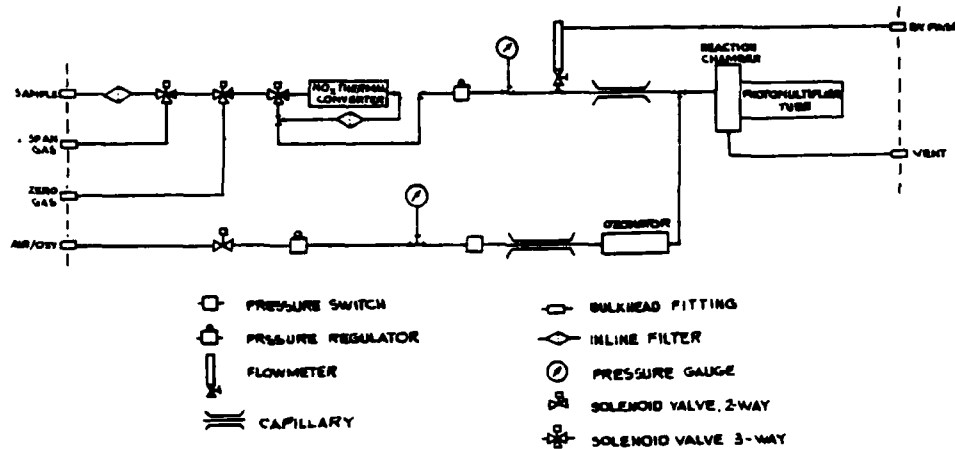


Figure 6. Schematic Scott NO_x analyzer

The analyzer was capable of analyzing and measuring NO concentrations over full scale ranges of 10, 25, 100, 250, 1k, 2.5k and 10k ppm.

The stated accuracy of the instrument was within 1% of full scale for the ranges of interest.⁹ A test of accuracy conducted on January 2, 1982, using various span gases gave values that at most are off by 5% at the outer edges of the range (see Appendix 1). This test was conducted under stable ambient conditions.

Under test conditions, changes in ambient temperature caused substantial drift in zero readings. After many extensive and unsuccessful attempts were made to try to eliminate this drift, it was decided to make measurements against frequently measured zero values. It was found that by using this method consistent results could be obtained, usually within 2 pmv.

In some of the later runs it was noted that the relative distance between the zero and span gases was shrinking, indicating a relative change in scale. To adjust for this, span gas readings were taken periodically and measured values adjusted accordingly. An example of this procedure is given below (taken from the 0 load run 1/8/82):

Sample reading 27.5 ppmv, zero reading 3.5 ppmv

Span gas (45 ppmv) reading - 44 ppmv

Zero with span gas reading = 4.5 ppmv.

Adjustment for zero drift - $27.5 \text{ ppmv} - 3.5 \text{ ppmv} = 24.0 \text{ ppmv}$

Span drift - $45 \text{ ppmv actual} - (44 \text{ ppmv measured} - 4.5) = 5.5 \text{ ppmv}$

Final Adjusted Value = $24.0 \text{ ppmv} + 5.5 \text{ ppmv} = 29.5 \text{ ppmv}$.

Other sources of error as cited by Campbell et al.¹⁰ include interference by water vapor and carbon dioxide. The error caused by these two factors was considered minimal in these tests. In the case of water vapor, our sample conditioner removed much of the moisture. The error caused by the CO₂ is at most 0.5 ppm and was therefore neglected.

In light of the above discussion, it was felt that the measured values can accurately approximate the true values within an error of less than 5 ppmv.

The sample gas stream was also routed to a Beckman Model 215A Infrared Analyzer to determine CO₂ levels. The analyzer was calibrated to read CO₂ concentrations of up to 5% (by volume). The calibration curve for the analyzer is given in Appendix 2.

The instruction manual¹¹ gives the accuracy of this instrument as within 1% of scale. In our case, this would translate to $\pm 0.05\%$ CO₂. Considering accuracy of the calibration curve and the curve reading techniques, an accuracy of $\pm 0.1\%$ CO₂ was assumed reasonable.

Figure 7 shows a section of our instrumentation with the CO₂ analyzer on the bottom, the chart recorder in the center and the turbine electrical loading resistors at the top.

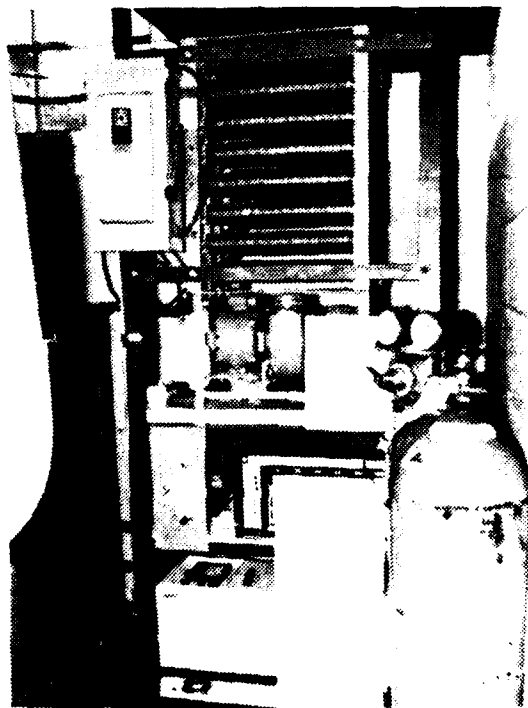


Figure 7. CO₂ analyzer, chart recorder and electrical loading device

Both the Scott 325 NO_x analyzer and the Beckman 215A CO₂ analyzer were connected to an Esterline Angus Strip Chart recorder. The recorder had two channels.

The accuracy of the recorder was given as $\pm 0.35\%$ of scale^{1,2} which translates into ± 0.35 ppm for the NO_x values and ± 0.0175 CO_2 for the CO_2 analyzer.

Additional instrumentation on our system included a series of Type K (Chromel-Alumel) thermocouples, which measured seven temperatures. Two of these, combustion flame temperature and exhaust temperature, were used in this study. The thermocouples were connected to an Omega Model 199 ten-channel digital temperature indicator, as shown in Figure 8.



Figure 8. Digital temperature indicator

The accuracy of the exhaust gas measurements was conservatively estimated at $\pm 10^\circ\text{F}$, taking both indicator and thermocouple error

into account. The combustor flame temperature was measured with a specially modified Type K thermocouple, shown close up in Figure 9. This was designed to fit through the compressor housing and enter the final row of holes in the combustor can. These holes can be seen on the can shown in Figure 2.

The cowl protecting the thermocouple was designed to minimize the interference of radiational effects on the thermocouple and to allow free flow of exhaust gas through it. The radiational effect of having the extremely hot combustion zone just upstream, and of having the relatively cold surfaces downstream and around it, can often cause interference with true gas temperature readings.

A photograph of the back of the turbine in Figure 10 shows the combustor thermocouple entering the housing on the middle right-hand side of the casing. The exhaust temperature thermocouple can be seen in the middle foreground just beyond the flange in the exhaust duct.

The wet and dry bulb temperatures were also measured using the blower and thermometer combination shown in Figure 11.

The overall configuration of the machinery is pictured in Figure 12. The analyzers and loading system are in the back corners, the fuel measuring system in the foreground and the sample conditioning system is partially visible behind it.

Most of the calculations for this project were done with a North Star Horizon Micro-computer, using the BASIC computer language. This was a small 64 k memory computer with a CRT and hardcopy attachment. Copies of the programs used are given in the Appendices.



Figure 9. Combustor flame temperature thermocouple

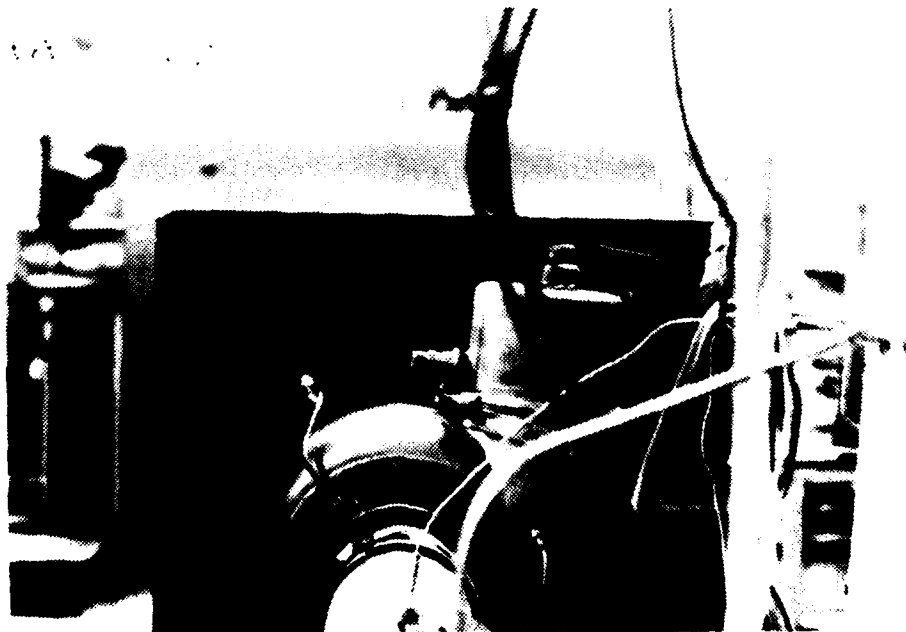


Figure 10. Rear view of turbine-compressor

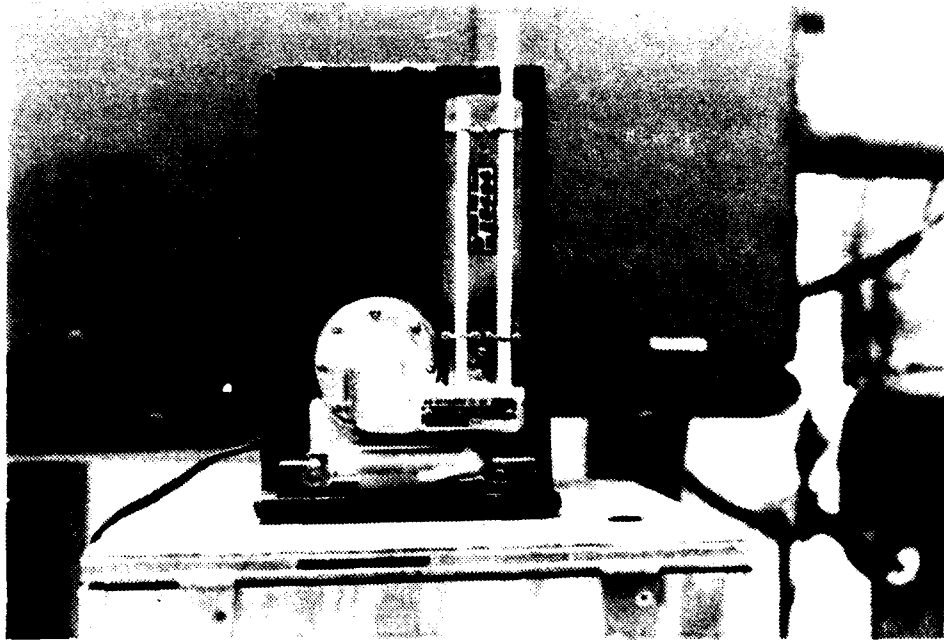


Figure 11. Wet and dry bulb measurement



Figure 12. Room set up

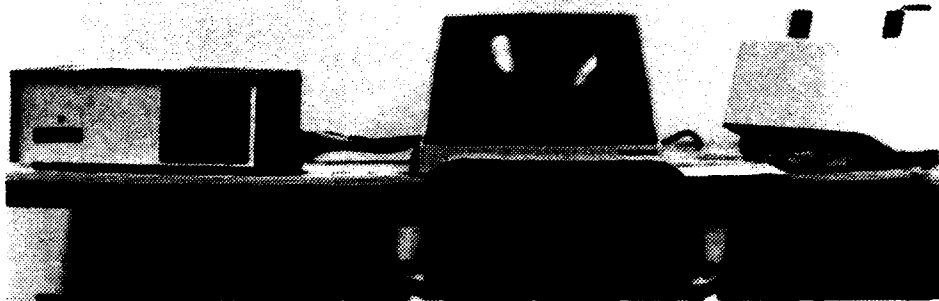


Figure 13. North Star Horizon computer

PROCEDURES

The fuels were mixed by hand in five gallon quantities and transported to the test site. Various mixtures of kerosene and pyridine were used to achieve final fuel mixtures that were of the desired weight percent nitrogen, 0.5% and 1% nitrogen by weight. (See Appendix 3 for the calculations)

The constituent fuels underwent elemental analysis conducted by R. Wielesic of the University of Oregon Chemistry Department. The samples were tested on a Perkin Elmer Model 240 carbon hydrogen nitrogen analyzer. The results obtained were: for kerosene 90.38% C and 9.09% H (weight percent), and for pyridine 17.90% N, 75.63% C and 6.68% H. The precision for this test was 0.1% for standards and 0.3 to 0.4% for pure chemicals.¹³

It was noted that because of this, the weight percents did not total 100%, being 99.47% for kerosene and 100.21% for pyridine. It was decided to adjust the weight percents by taking the difference between the total and 100% and adding or subtracting an equal amount from each element to achieve a total of 100%. The adjusted values used in calculations were therefore, for kerosene 90.645% C and 9.355% H, and for pyridine 17.83% N, 75.56% C, and 6.61% H.

The test procedure began by letting the analyzers warm up for one to two hours with a flow of zero gas (nitrogen) through them at the same rate as the sample and zero gas flows during the run. Both units were then calibrated using nitrogen gas as the common zero gas and

using a standard gas containing 45 ppmv of NO for the NO_x analyzer and 5% CO₂ for the CO₂ analyzer. Calibration was done by adjusting the zero and gain (span) potentiometers on the instruments until the readings matched the known standards. Several alternate readings of the zero and span gases were made and the potentiometers adjusted until consistent results were obtained. Note was next made of the various ambient conditions, including barometric pressure, dry bulb temperature and wet bulb temperature.

The specific fuel to be tested was then chosen, and the turbine generator started at zero load. Experimental values were taken when a steady CO₂ reading was obtained, indicating steady state conditions.

At that time, note was made of the CO₂ concentration, fuel pressure, compressor outlet pressure, turbine exhaust and combustion chamber temperatures, and a timing was made of the flow rate of 2000 cc of fuel. The NO_x concentration was also determined by alternately checking the sample and zero readings. After a number of repetitions of the sampling and zero levels, a check was also made of the span gas reading. These values were used to determine actual NO_x values as indicated in the Apparatus section on the NO_x analyzer.

When all the data had been gathered, the ambient temperatures were again checked and noted. The load was then changed, and the process repeated for half (6.25 kW) and full (15 kW) loads.

The Appendices contain copies of the data sheet used (Appendix 4) and the complete checklist for a run (Appendix 5).

RESULTS

Table I contains the measured and derived variables used in the analysis of this experiment. What follows is a brief description of each of those variables.

Oxides of nitrogen were measured by the Scott Model 325 NO_x analyzer, as described in the Procedural section. Relatively consistent results were obtained during each run with the largest standard deviation during a measurement series being 1.4 ppmv. The values given in the table are the mean values for each measurement series. The standard deviation around that mean is shown in parenthesis. The actual measured values for each table point are given in Appendix 6.

The mean NO_x values were adjusted to combustor inlet conditions of 212°F (100°C), 2 atm, and zero absolute humidity in the exhaust gas, by the following equation.

$$11 \quad \text{NO}_{x\text{corr}} = (\text{NO}_x)_{\text{meas}} \times \left[\exp \left[\frac{373.15 - \left(\frac{T_{\text{in}}^{\circ\text{R}}}{1.8} \right)}{248} \right] \right] \times \left[\frac{2 \text{ atm}}{P_{\text{in}}} \right]^{\frac{1}{2}} \times \exp (19H)$$

where T_{in} is the combustor inlet temperature in degrees Rankine, P_{in} is the combustor inlet pressure in atmospheres, and H is the absolute humidity, mass H₂O/mass air, of the inlet air. An equation of this form was proposed by Lewis¹⁴ to predict NO_x emissions and is used by the Environmental Protection Agency to adjust its NO_x standards to fit different pressure ratio engines.¹⁵

NO_x Information - Measured and Derived

Date	Fuel Load (% N)	NO _x (ppmv)	σ n-1	CO ₂ (V%)	CO (ppmv)	T _{comb} (°F) measured	T _{comb} (°F) Cal.	T _{comb} (°F) Text	T _{wb} (°F) avg 1	T _{wb} (°F) avg 2	T _{wb} (°F) avg 1	T _{wb} (°F) avg 2	H Rel. Humidity %	% Comp. Absorbance	% Comp. Absorbance	NO _x (ppmv) from CO ₂	A/F ratio	A/F Ratio Direct Meas.	
12/28/81	0.0	0.0	2.5 (NA)	1.35	640 [†]	860±10	735	471	47	49	50	57	68	.0058	2.222	218.75	2.61	145.35	131.00
12/28/81	0.0	9.0	8.0 (NA)	2.15	NA	1290±10	959	666	50.5	53	60	62	53	.0061	2.222	228.64	8.21	100.62 [†]	102.60
12/30/81	0.0	9.5	9.0 (.71)	2.175	NA	1275±10	970	671	47	55	54	69	48	.0056	2.187	233.90	9.11	99.69 [†]	93.1
1/5/82	0.0	0.0	3.3 (.55)	1.40	640	860±10	748	468	50	50	51	60	68	.0064	2.157	214.04	3.57	140.350	143.525
1/5/82	0.0	6.25	8.3 (.29) 3 of 4 values	1.85	400	1145±10	907	611	50	55	60	70	43	.0056	2.157	226.45	8.61	108.503	109.786
1/5/82	0.0	14.3	13.8 (.29)	2.60	260	1565±10	1170	817	55	57	70	75	34	.0058	2.225	243.55	13.61	77.817	77.539
1/6/82	0.5	0.0	9.8 (.27)	1.35	640 [†]	840±10	735	451	37	41	44	50	47	.0032	2.239	208.05	9.93	145.348	143.230
1/6/82	0.5	6.25	24.3 (.45)	1.80	400 [†]	1125±15	879	583	41	45	50	55	44	.0037	2.239	215.29	24.46	111.478	118.203
1/6/82	0.5	15.0	41.75 (.71)	2.475	260 [†]	1550±10	1112	764	45	46.5	55	58	43	.0041	2.274	224.09	41.20	81.756	86.968
1/7/82	1.0	0.0	30.2 (.45)	1.375	640 [†]	835±10	740	465	43	45.25	52	59	44	.0041	2.208	215.54	30.83	142.805	134.458
1/7/82	1.0	6.25	51.9 (.86)	1.825	400 [†]	1130±10	899	608	47.5	49	50.5	65	37	.0044	2.242	227.60	51.46	109.971	104.846
1/7/82	1.0	15.0	81.8 ^{**} (.5)	2.60	260 [†]	1550±10	1165	785	50.5	55	65	74	30.5	.0047	2.242	237.47	79.79	77.817	80.757
1/8/72	1.0	0.0	30.25 [†] (.67)	1.375	640 [†]	860±10	726	470	47	47	57	58	44	.0044	2.207	218.16	30.88	142.805	138.103
1/8/82	1.0	6.25	48.2 ^{**} (1.4)	1.85	400 [†]	1140±10	904	603	47	49	58	60	43	.0046	2.241	223.59	48.42	108.503	106.020
1/8/82	1.0	15.5	78.4 [†] (1.2)	2.575	260 [†]	1565±15	1148	788	49	?	61	?	42	.0049	2.241	227.56	78.51	78.575	81.989

* Values adjusted to account for drift. † calculated using the derived equation for kerosene as no CO data was available.
 ** Possibly inaccurate due to large span drift
 † Values assumed constant from those measured 1/5/82

A similar form of this equation was used to adjust data obtained by the Electric Power Research Institute in studies they have done on synthetic fuels (16, 17, 18, 19). The equation they appear to have used raises the pressure ratio to a power of 1.5. I was unable to verify if this was a misprint in the article. In a conversation with Mr. Cohn of the EPRI it was indicated that this equation should not have been used for high Fuel-Bound Nitrogen fuels. The assumptions made in its derivation do not hold true when large amounts of NO_x from Fuel-Bound Nitrogen (FBN) are present.

Reference 16 states on Pg 4:

"The validity of this equation under water injection conditions is only partially established for low FBN fuels and not yet established for high FBN fuels".

In spite of these statements, all their data appears to have been adjusted using this type of equation. It was therefore decided to use the above equation to adjust all our data and thereby conform to their procedure. The pressure ratio was raised to the $1/2$ power because it was felt that their use of 1.5 was a typographical error.

These adjusted values are in Table I in the column on the third from the right. The adjustment turned out to be minor, with a maximum change of -2 ppmv.

The actual combustor inlet conditions were determined from the ambient dry bulb temperatures and from the compressor outlet pressure. The compressor outlet temperature was calculated using air tables, and by assuming a compressor efficiency of 80%. The deriviations

leading to these values are given in Appendix 7. The actual inlet temperature was probably within 10° F of this value.

The carbon dioxide measurements were load dependent and remained fairly constant from fuel to fuel. There was some slight variation but this was well within our expected level of accuracy. The fuel composition did not effect these measurements. Upon checking the variation in carbon content of the three fuels used, it was found that the weight percent of carbon in the three fuels were within 1% of each other (see Appendix 8). The carbon dioxide levels would therefore not be expected to change.

The carbon monoxide was measured by reagent tube during the tests conducted on January 5, 1982. Because there was virtually no change in the carbon content of our fuel, or much change in our measured flame temperature, it was reasonable to expect little change in our CO output. We therefore made the assumption of identical CO values for the other runs at the same loads.

The measured combustor flame temperature was essentially constant for all our tested fuels, varying only with load. This might be expected as our turbine would control the fuel input to give a similar energy output for the loads, regardless of the fuel. This would result in similar combustion temperatures for similar fuels.

The value calculated as the combustion chamber temperature was the adiabatic flame temperature for the calculated air fuel ratio.

This temperature was found to be less than the measured value. This was unexpected as the energy consumed by dissociation reactions

in actual flames makes the adiabatic flame temperature (which does not take these into account) higher than the actual value.

In this case the discrepancy was probably due to incomplete mixing of the incoming air and the fuel at the point of measurement. The thermocouple was placed through the last set of air inlet holes in the combustor (see Figure 2). Final mixing of the products of combustion would then occur downstream of these holes.

Another factor supporting this assumption is that the discrepancy was greater at higher loads. At higher loads the fuel flow rate through the combustor was higher, which would cause the combustion zone to lengthen and come closer to the thermocouple. Also, the increased velocity of the combustion gases would move complete mixing further downstream.

In short, the adiabatic flame temperature under these circumstances would include dilution air in the calculations that did not actually take part in the combustion process.

In spite of these difficulties the adiabatic flame temperature is valuable as a general indicator of combustion conditions. It is a standard calculatable variable which is not prone to the variables that effect other methods of temperature measurement. It can be made much more accurate if the air fuel ratios are known for localized areas. Other methods of measurement such as thermocouples or infrared spectrometry are subject to interference by radiation from the flame zone and from the walls. In light of these variables our flame temperatures should be taken as indicators of trends rather than as absolute

Appendix 12 for the derivation and data for the adiabatic flame temperature.

In order for the adiabatic flame temperature calculations to be made, it was necessary that the air fuel ratio be determined. This was done three ways, by direct measurement, by assuming complete combustion and using chemical balances and CO₂ measurements, and by the procedure recommended by the Society of Automotive Engineer's Aerospace Section. The latter was considered the most accurate and was used in almost all further calculations. It was necessary to use the second method for some points where carbon monoxide measurements were not available. The direct measurement method was used as a comparison.

For the direct measurement calculation it was necessary to modify the fuel density measurements to fit ambient conditions, (see Appendix 9) the calculations for the first two methods are given in Appendix 10.

The Society of Automotive Engineers, SAE ARP1256 method, gives the fuel air ratio by carbon balance as:²⁰

$$F/A = \frac{(\% \text{ CO vol.}) + (\% \text{ CO}_2 \text{ vol.}) + (\% \text{ HC by } \delta \text{ l. as carbon})}{207 - 2 * \text{CO}\% - \% \text{ CO}_2}$$

For the purpose of our test, the quantity of unburned hydrocarbons was so small as to consider it negligible.

In order to better comprehend the data, plots of NO_x against different variables were made; NO_x vs. measured flame temperature, NO_x vs. adiabatic flame temperature, NO_x vs. air fuel ratio and theoretical air, and NO_x vs. fuel bound nitrogen, at constant adiabatic flame temperature.

The plot of adjusted NO_x vs. measured flame temperature is shown in Figure 14. The points are fit very well by a linear approximation. A linear least squares fit of the results are shown in Table II.

TABLE II

Adjusted NO_x vs. Measured Flame Temperature

%N	$\text{NO}_x =$	r^2
0.0	- 9.134+0.0144 Tm	.955
0.5	-25.983+0.0437 Tm	.994
1.0	-26.917+0.0680 Tm	.996

As expected, the rate of production of NO_x increases with increased fuel bound nitrogen.

A comparison of this plot with those produced by the Electric Power Research Institute on subscale combustors²¹ shows that these results are quite similar to theirs. Both tests produce straight line plots of NO_x vs. temperature. Figures 15 through 18 are a sample of some of their results. These tests were taking substitute fuels with similar characteristics to the actual synthetic fuels and comparing emissions.

An analysis of their results shows that they arrived at higher slopes than we did for similar nitrogen content fuels. There are a number of probable reasons for this. First of all, there are differences in the fuels' chemical composition, second their temperature measurement system was set up differently, and third, their inlet conditions were substantially different.

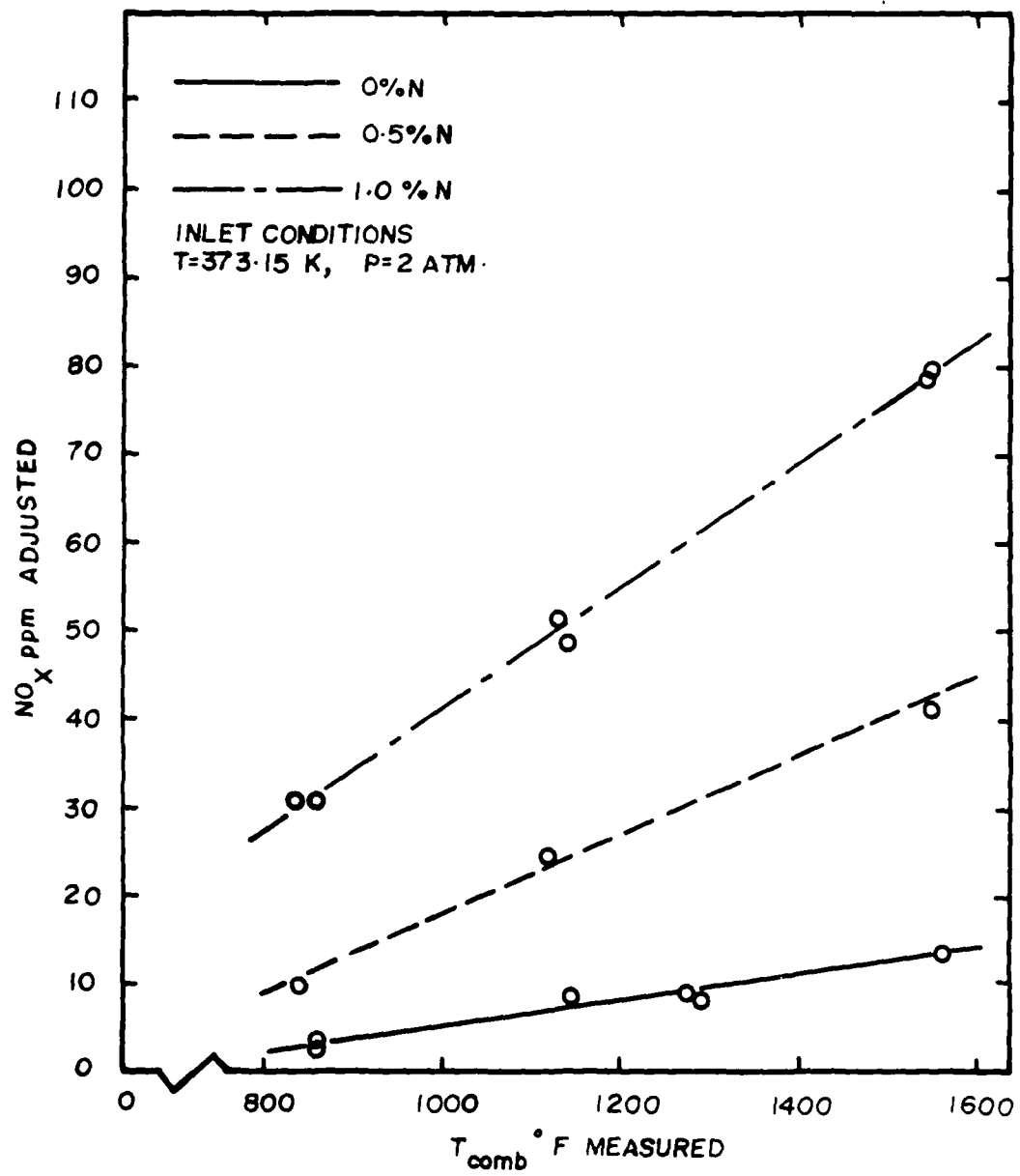


Figure 14. Adjusted NO_x vs Measured Flame Temperature.

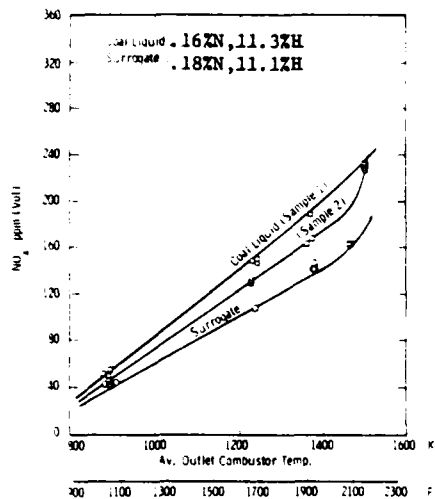


Figure 15 NO_x emissions for H-coal (ATM-OVHD) 366-533 K and its surrogate

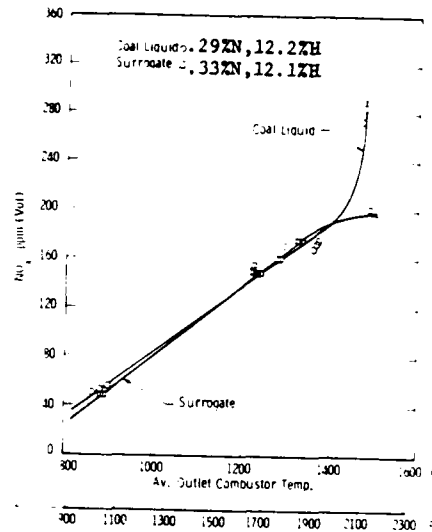


Figure 16 NO_x emissions for SRC light organic and its surrogate

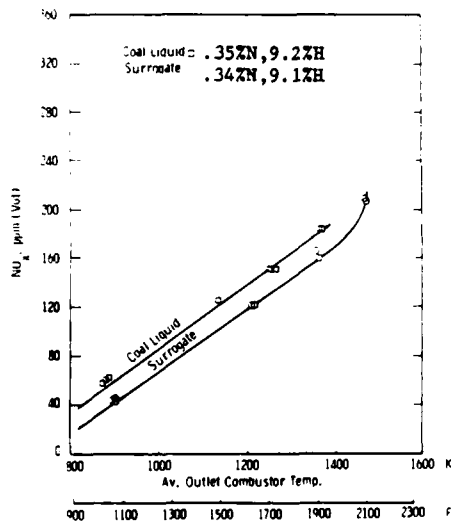


Figure 17 NO_x emissions for SRC wash solvent and its surrogate

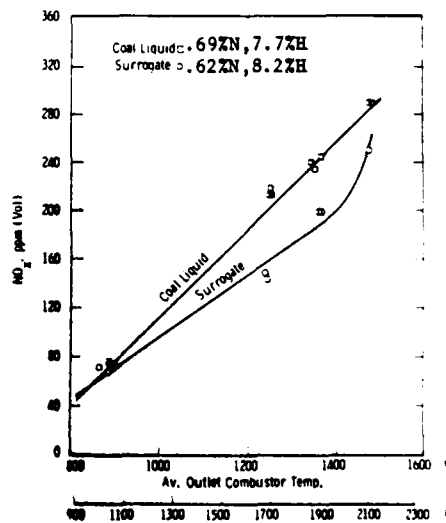


Figure 18 NO_x emissions for SRC recycle solvent and its surrogate

They discovered during their testing that minor variations in chemical composition caused differences in emissions from small scale combustors. As an example, all of the surrogate fuels in Figures 15 through 18 had practically the same nitrogen, hydrogen, and aromaticity contents as the coal derived liquids that they were trying to imitate. It was found that small variations in nitrogen, oxygen and sulphur content can cause significant differences in NO_x emissions.²² It was therefore quite likely that there would be some differences between their results and this test.

Their temperature measurement was done at an inverted hat mixer at the outlet to their combustor. At that point all their dilution and combustion air had been added and mixed. Even so, the lowest temperature for which they took readings appears to be around 1050°F . This is comparable to our half load condition in the combustion chamber itself. Their second lowest measurement was around 1700°F , higher than any of our temperatures.

Since these exhaust temperatures are so much higher than our internal combustor temperatures, it is probable that they had combustion chamber temperatures much higher than those in this study.

Further evidence to support this conclusion was gained when we noted that their combustor inlet temperatures and pressures were much higher than in this study. Their inlet conditions were 4 atm and 600°F , while this turbine had inlet conditions of around 2 atm and 215°F . These factors would greatly effect the combustion conditions.

It therefore was probable that our temperatures in the combustor were lower than their values.

It is interesting to note that extrapolation of most of the curves in Figure 15 through 18 will give zero values for NO_x at outlet temperatures of 500-800°F. As we are getting significant values for NO_x in this range (even with lower inlet conditions), there would appear to be a slope change in the data.

Another study by the EPRI by Singh et al.²³ confirms this. Unfortunately this paper in its entirety was not available. However, the team members in Part Two of the study, when explaining their choice of an exponential curve fit for their large scale combustor data state:

This equation form provides a close approximation for the straight line segments that are believed to represent the formation of NO_x combustors as discussed under subscale test results in Part I of this paper. The special fuel tests consisted of only four or five points for only three fuels so that characterization by straight line segments was not practical.²⁴

It would seem likely that a number of production rates exist that vary over combustion conditions, and by being in a lower temperature range our production rate is therefore lower.

Figure 19 shows the results of a plot of NO_x vs. adiabatic flame temperature. This was also subject to linear regression analysis. The results of that analysis are given in Table III.

The slopes of the equations are slightly higher for this plot than against measured temperatures. This would indicate a higher rate of production of NO_x against changes in adiabatic flame conditions.

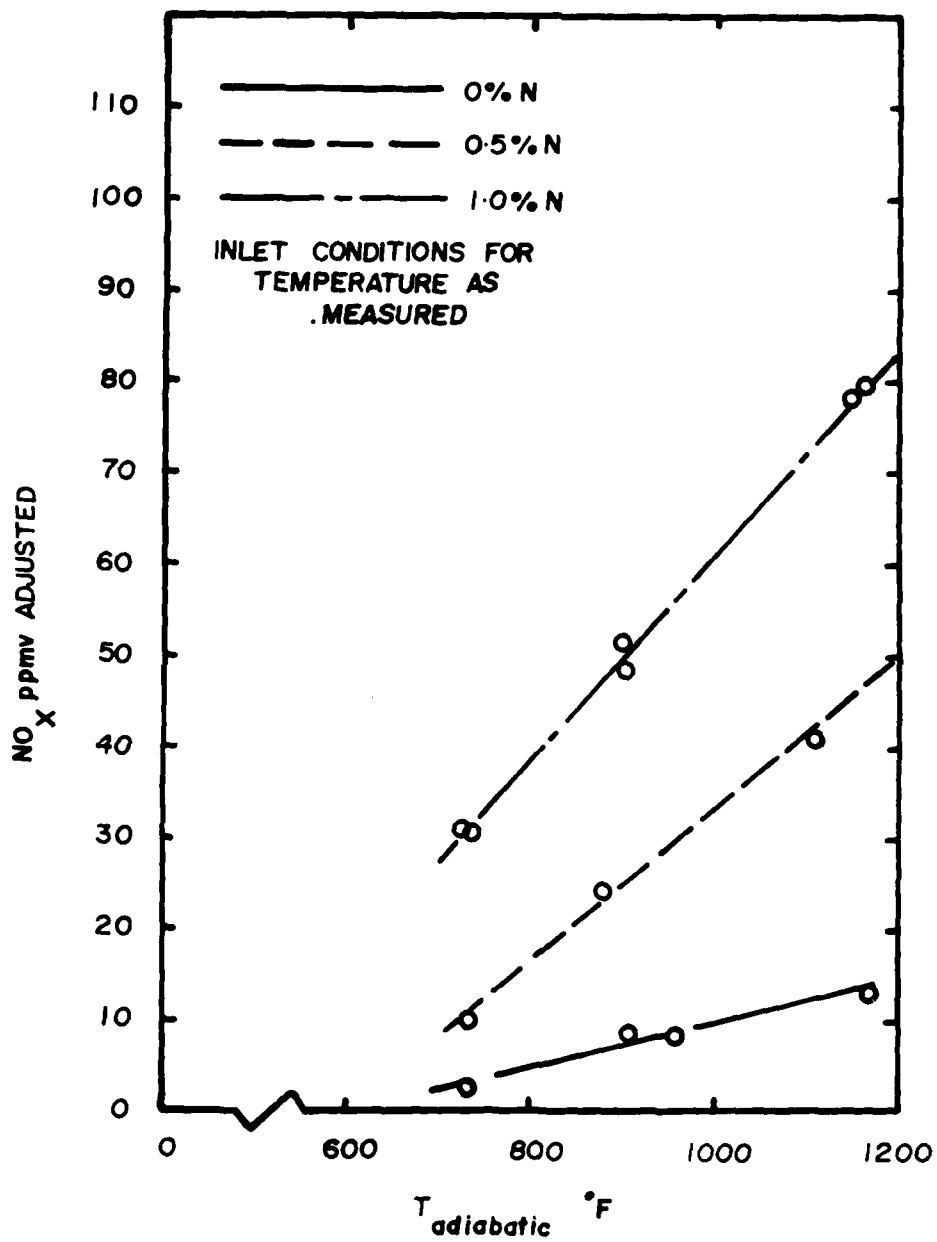


Figure 19. Adjusted NO_x vs Adiabatic Flame Temperature.

TABLE III

Adjusted NO_x vs. Adiabatic Flame Temperature

%N	$\text{NO}_x =$	r^2
0.0	$-14.746 + 0.0245 T_{\text{adia}}$.974
0.5	$-49.209 + 0.0819 T_{\text{adia}}$.992
1.0	$-52.683 + 0.1139 T_{\text{adia}}$.996

Even though the adiabatic flame temperature does not accurately reflect true combustion flame conditions in a gas turbine combustor, it does offer a standard against which other combustors, with similar overall energy outputs, can be compared.

The adjusted NO_x values were plotted against the air fuel ratio and theoretical air in Figure 20. These values, too, could be accurately fit to a linear approximation shown in Table IV.

TABLE IV

Adjusted NO_x vs. Air/Fuel Ratio and Theoretical Air

Linear Regression

%N	$\text{NO}_x =$	r^2
0.0	$24.711 - 0.1525 A/F$.970
0.5	$80.530 - 0.4903 A/F$.994
1.0	$135.259 - 0.7444 A/F$.976

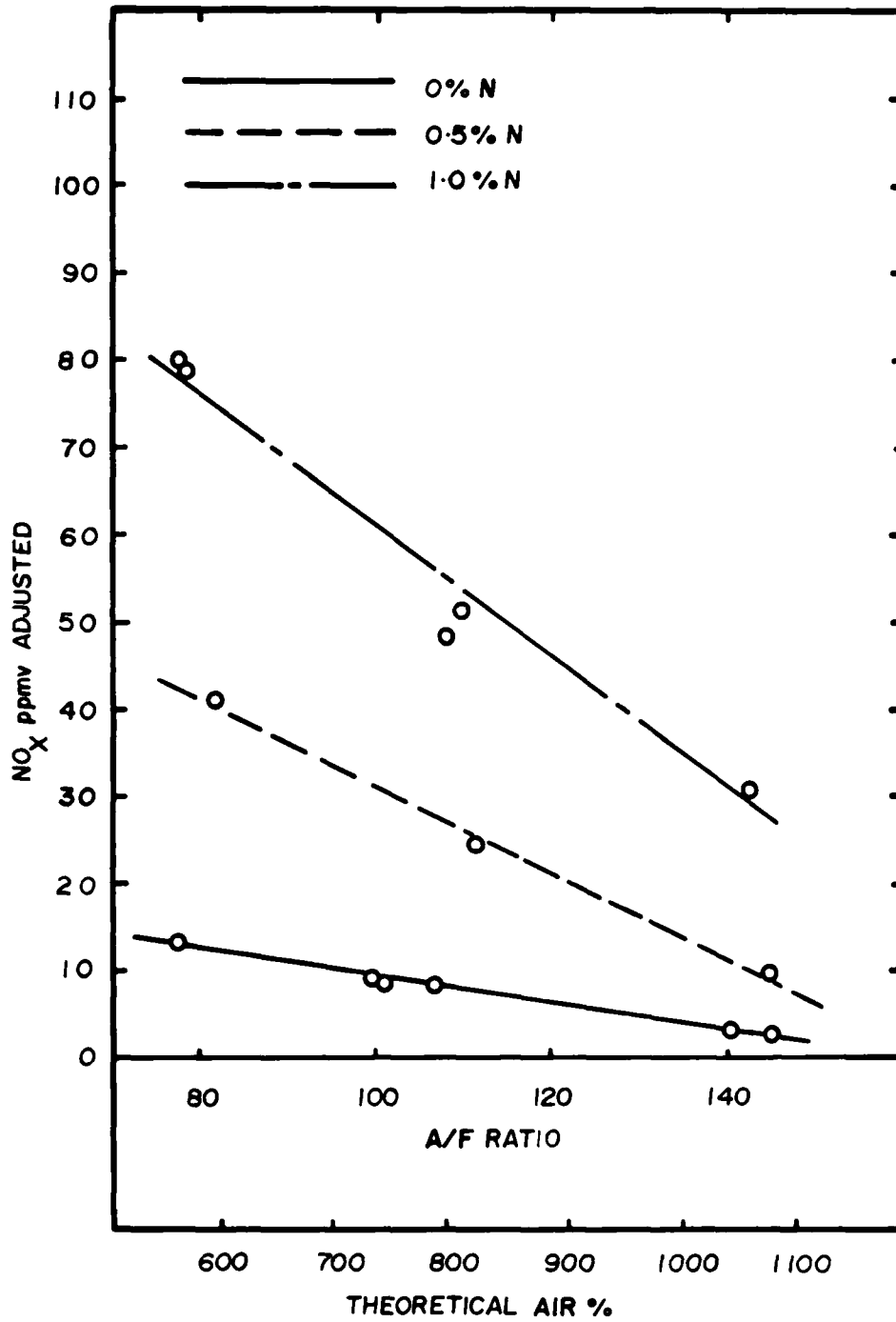


Figure 20. Adjusted NO_x vs Air/Fuel Ratio and Theoretical Air.

This shows a similar trend as the previous two plots. In this case, the NO_x values decrease linearly with increasing air fuel ratios. This would be anticipated as an increase in the air fuel ratio causes a corresponding decrease in the combustion temperature.

Perhaps the most interesting result of this study was the plot of NO_x against fuel bound nitrogen in Figure 21. These data were taken from Figure 19, NO_x vs Adiabatic Flame Temperatures, for constant temperatures. The temperatures chosen were those calculated at the average air fuel ratio for each load setting.

The plot of NO_x vs Adiabatic Flame Temperature was chosen so that an individual could roughly predict an NO_x value for a given fuel, air fuel ratio and combustor inlet condition. All of these contribute to the flame temperature.

The data points used are given in Table V. A number of types of curves were estimated for these data and the results are given in Table VI.

As can be seen from the plot and the regression coefficients in Table VI, the best fit equation for the lower temperature curve is an exponential fit. The best fit for the high temperature data, on the other hand, is a linear plot.

The production rate was essentially constant (constant slope), while the production rate for lower temperatures increased (increasing slope).

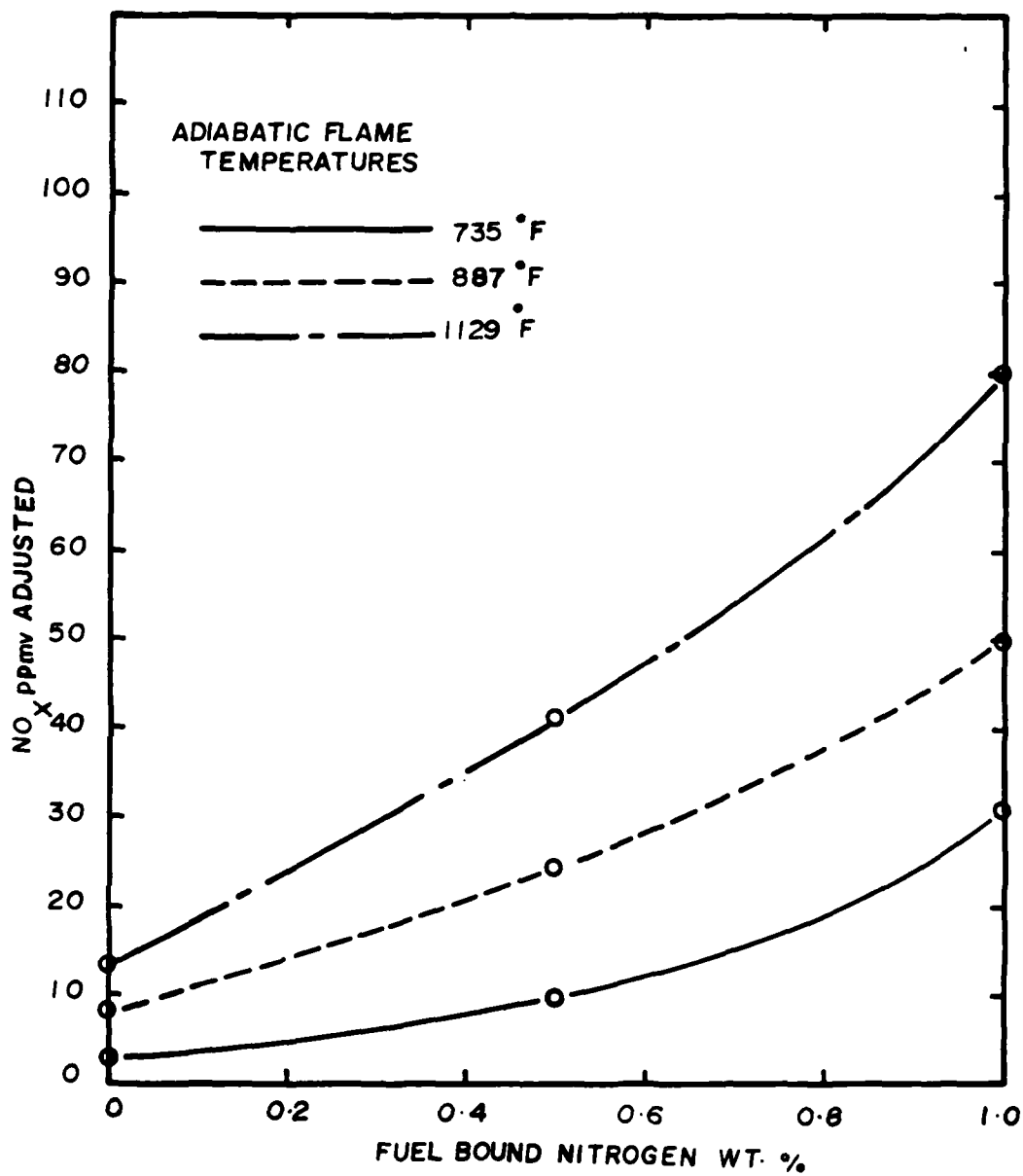


Figure 21. Adjusted NO_x vs Fuel Bound Nitrogen at T_{adiabatic}

TABLE V

NO_x vs Fuel Bound NitrogenNO_x ppmv

T adiabatic FBN	0.0	0.5	1.0
735°F	3.0	10.8	30.4
887°F	6.8	23.2	48.0
1129°F	12.7	43.2	76.0

TABLE VI

NO_x vs. Fuel Bound Nitrogen Least Squares Curve Fits

T adiabatic	Power Curve Fit	r ²	Exponential Curve Fit	r ²
735°F	20.44*FBN (.28)	.87	3.126e ^{2.316FBN}	.996
887°F	35.98*FBN (.18)	.91	7.391e ^{1.954FBN}	.979
1129°F	61.37*FBN (.17)	.94	14.175e ^{1.789FBN}	.957

T adiabatic	Linear Curve Fit	r ²
735°F	1.033 + 27.4 FBN	.941
887°F	5.4 + 41.2 FBN	.986
1129°F	12.32 + 63.3 FBN	1.000

One possible explanation for this is that at higher loads there were higher amounts of thermal NO_x present, which would lower the relative contribution of the fuel bound nitrogen to overall NO_x . At higher fuel flow rates there may also be reduced primary air penetration to the center of the combustion zone. This might provide a sufficiently rich (oxygen starved) area to inhibit the formation of fuel bound nitrogen NO_x , slightly.

The overall production rate still increased with temperature, as can be seen from the linear approximations of the data. The production rate at constant temperature was higher for the high temperatures (a slope of 63.3) than for the lower temperature (a slope of 27.4). Comparison of the NO_x emissions, for both 0.5 percent FBN and 1.0 percent FBN, as a function of temperature indicates that conversion of FBN to NO_x increases as temperature increases.

These statements say nothing about the amount of conversion of fuel bound nitrogen to NO_x . This is concerned only with the total production of NO_x , both thermal and fuel bound nitrogen NO_x , combined.

It was not possible to calculate the percent conversion of fuel bound nitrogen to NO_x due to the inaccuracy of some of the experimental methods. Recent research by Vermes, Toof, and Cohn²⁵ indicates that the production of thermal NO_x is not constant, which is what the percent conversion method assumes. Their studies indicate that the presence of NO_x from fuel bound nitrogen will inhibit the formation of thermal NO_x . For this reason, there is much argument over the

actual amount of FBN conversion and over the actual thermochemical balances involved. This is an argument well beyond my area of expertise.

CONCLUSION

The results of this work are similar to that generated by other experimenters. We have measured NO_x values which are lower than the other studies; however, the lower values can be attributed to lower combustion temperatures, and to differences in fuels and inlet conditions.

The production rate of the NO_x versus the fuel bound nitrogen content was found to be less dependent on the nitrogen content at the higher temperatures than at the lower temperatures. The overall rate of NO_x production drop was found to be higher for the higher temperatures.

A plot of NO_x versus fuel bound nitrogen at constant adiabatic flame temperatures was made. This can be used to predict NO_x values for other nitrogen content fuels of the same fuel type.

Great care should be used in applying these results to large scale turbines or in using the above plot to predict NO_x values for machines with significantly different pressure ratios. Studies conducted on both large and small scale combustors by the Electric Power Research Institute, indicate that the results from small scale studies do not always accurately predict full scale results.²⁶

REFERENCES

1. Pg 2 EPA Research Summary Controlling Nitrogen Oxides, EPA-600/8-80-004.
2. Dr. Richard Boubel, Class Lecture ME 490, Oregon State University, 10/6/80.
3. Pg 5 EPA Pamphlet, "Acid Rain", Publication number EPA-600/9-79-036, July 1980.
4. Ibid., p. 16.
5. Pg 85, "Researchers Study effects of Acid Rain on Marine Life", Mechanical Engineering, November 1981.
6. Shale Oil - The Answer to the Jet Fuel Availability Question. L. C. Angello, Wright Patterson Air Force Base, 1978, SAE Publication 78/027.
7. Glassman, Irvin; "Combustion", Academic Press, San Francisco, 1977, pp. 221-225.
8. Fenimore, C. P. (1971), Int. Symp. Combust. 13th, p. 373. Combustion Inst. Pittsburg, Penn.
9. Operations Manual, Scott Chemiluminescence Analyzer, Model 325. Environmental Tectonics Corporation, Southampton, PA, pp. 4-8.
10. Campbell, N. T.; Beres, G.A.; Blasko, T. J.; and Groth, R. H., "Problems in the Measurement of Nitrogen in Gas Turbine Engine Exhaust", Presentation to the 74th Annual Meeting of the Air Pollution Control Association. Philadelphia, PA 1981, pp. 8, 14.
11. Beckman 215A Infrared Analyzer instructions B1635-2, Beckman Instruments, Inc., Fullerton, CA, July 1969, pg. ii.
12. Technical Publications Section, "Easterline Angus"; Operating Instructions for Speed Servo R II Strip Chart Recorders", M70A1, 1M572, 1972, p. 3.
13. Personal communication with Richard Wielesic at the University of Oregon Chemistry Labs, 9/17/81.
14. Lewis, G. D. Prediction of NO_x Emissions, paper presented to the 1981 ASME Gas Turbine Conference and Products Show. Paper No. 81-GT-119.

15. EPA Proposed Revisions to Gaseous Emissions Rules for Aircraft and Aircraft Engines, 43 FR 12615, March 24, 1978, 40 CFR Part 87.21 d(iii)b.
16. P. R. Mulik, P. P. Singh, A. Cohn; "Effect of water injection for NO_x Reduction with Synthetic Liquid Fuels Containing High Fuel-Bound Nitrogen in a Gas-Turbine Combustor. Presented to the 1981 ASME Gas Turbine Conference and Products Show, ASME Paper #81-GT-51.
17. P. R. Singh, E. R. Bazarian, P. R. Mulik, G. W. Bauserman, A. Cohn, T. R. Stein; "Comparative Testing of Petroleum Surrogate Fuels with Coal-Derived Liquids in a Combustion Turbine Burner." Presented to the 1980 ASME Gas Turbine Conference and Products Show, ASME Paper No. 80-GT-64.
18. P. P. Sing, et al., "Combustion Effects of Coal Liquid and Other Synthetic Fuels in Gas Turbine Combustors - Part I: Fuels Used and Subscale Combustion Results". Presented to the 1980 Gas Turbine Conference and Products Show, ASME Paper No. 80-GT-67.
19. G. W. Bauserman, C. J. Spengler, A. Cohn; "Combustion Effects of Coal Liquid and Other Synthetic Fuels in Gas Turbine Combustors - Part II: Full Scale Combustor and Corrosion Tests". Presented to the 1980 Gas Turbine Conference and Products Show, ASME Paper No. 80-GT-68.
20. Society of Automotive Engineers Aerospace Recommended Practice, "Procedure for the Continuous Sampling and Measurement of Gaseous Emissions from Aircraft Turbine Engines", October 1, 1971 SAE, APR 1256.
21. Op Cit, 80-GT-64, pp. 5-6.
22. Ibid, p. 6.
23. Op Cit, Singh, 80-GT-67.
24. 80-GT-68, p. 3.
25. Vermes, G., Toof, J. L., Cohn, A.; "The Modeling of NO_x Generation from Coal Derived Liquids in Combustion Turbines"; Paper 79-JP GC-GT-4, presented at the Joint ASME/IEEE/ASCE Power Generation Conference, Charlotte, N.C., Oct. 8-10, 1974.
26. Op Cit, Bauserman, 80-GT-68, p. 10.
27. Skrotzski and Vopat, "Power Station Engineering and Economy", McGraw-Hill 1960, pp. 724-725.

28. Chilton and Perry, Chemical Engineers Handbook, pp. 9-11.
29. Hodgman, Charles, Handbook of Chemistry and Physics, 21st Edition, 1936-37, p. 1199.
30. F. W. Dwyer Mfg. Co., Inc., Michigan City, Ind., "Pitot Tube Bulletin No. H 11".
31. M. Popovich and C. Hering, "Fuels and Lubricants", John Wiley and Sons, Dec. 1973, p. 15.
32. Ibid., p. 16.
33. Wark, Thermodynamics, 3rd edition, McGraw-Hill Book Co., 1977, San Francisco, pp. 609-614.

BIBLIOGRAPHY

- Angello, L. C.; "Shale Oil - The Answer to the Jet Fuel Availability Question"; SAE Publication 781027, Wright Patterson Air Force Base, 1978.
- Bauserman, G. W., et al.; "Combustion Effects of Coal Liquid and Synthetic Fuels in Gas Turbine Combustors - Part II: Full Scale Combustors and Corrosion Tests"; ASME Publication No. 80-GT-68, March 1980.
- Bittker, D. A. et al.; "Effect of Fuel Bound Nitrogen and Hydrogen on Emissions in Hydrocarbon Combustion". ASME Publication 81-GT-63, March 1981.
- Beckman 215A Infrared Analyzer Instructions 81635-C; Beckman Instruments, Inc., Fullerton, CA July 1969.
- Campbell, N. T.; "Gas Turbine Engine Emissions Measurement Technology - An Overview"; ASME Publication No. 80-GT-86, March 1980.
- Campbell, N. T., Beres, G. A. et al.; "Problems in the Measurement of Nitrogen in Gas Turbine Engine Exhaust"; Presentation to the 74th Annual Meeting of the Air Pollution Control Association, Philadelphia, PA, 1981.
- Chilton and Perry, Chemical Engineers Handbook.
- Dwyer Manufacturing Co., Inc.; "Pitot Tube Bulletin No. H 11", Michigan City, IN.
- E.P.A. Pamphlet; "Acid Rain", Publication number EPA-600/9-79-036, July 1980.
- EPA Revisions; "E.P.A. Proposed Revisions to Gaseous Emissions, Rules for Aircraft and Aircraft Engines". 43 FR 12615, 40 CFR Part 87.21, March 24, 1978.
- EPA Research Summary; "Controlling Nitrogen Oxides". Report No. EPA-600/8-80-004.
- Easterline Angus, Technical Publications Section; "Operating Instructions for Speed Servo R II Strip Chart Recorders" M70 A1, 1M572, 1972.

- Federal Register Vol. 38; "Control of Air Pollution from Aircraft and Aircraft Engines". No. 136, Part II, July 17, 1973.
- Fenimore, C. P.; International Symposium on Combustion 13th., Combustion Institute, Pittsburgh, PA, 1971.
- Gaydon, A. G.; Wolfhard, H. G.; "Flames, Their Structure, Radiation and Temperature"; Chapman and Hill, London, 1979.
- Glassman, Irvine; "Combustion"; Academic Press; San Francisco, 1977.
- Hodgman, Charles; "Handbook of Chemistry and Physics, 21st Edition 1936-1937", Chemical Rubber Publishing Co., Cleveland, OH.
- Jackson, T. A.; "The Evaluation of Fuel Property Effects on Air Force Gas Turbine Engines - Program Genesis". ASME 81-GT-1, March 1981.
- JANAF, Thermochemical Tables, The Dow Chemical Co., Thermal Laboratory, Midland, MI
- Lewis, G. D.; "Prediction of NO_x Emissions", ASME Publication 81-GT-119; March, 1981.
- Mechanical Engineering Magazine; "Researchers Study Effects of Acid Rain on Marine Life", Nov. 1981.
- Mulik, P. R., et al.; "Effect of Water Injection for NO_x Reduction with Synthetic Liquid Fuels Containing High Fuel Bound Nitrogen in a Gas Turbine Combustor". ASME Publication 81-GT-51, March 1981.
- Popovich, M., and Hering, C; "Fuels and Lubricants", John Wiley and Sons, Dec. 1973.
- Society of Automotive Engineers Recommended Practice 1256, "Procedure for the Continuous Sampling and Measurement of Gaseous Emissions from Aircraft Turbine Engines". October 1971.
- Scott, H. A., Jr.; "The Implications of Alternative Aviation Fuels on Airbase Air Quality"; Air Force Engineering and Services Center, Publication number ESL-TR-80-38; August 1980.
- Scott Chemiluminescence Analyzer, Model 325, Operations Manual, Environmental Tectonics Corp., Southampton, PA
- Singh, P. P.; "Comparative Testing of Petroleum Surrogate Fuels with Coal Derived Liquids in a Combustion Turbine Burner." ASME Publication No. 80-GT-64, March 1980.

- Singh, P. P. et al.; "Combustion Effects of Coal Liquid and other Synthetic Fuels in Gas Turbine Combustors - Part I: Fuels Used and Subscale Combustion Results". ASME Publication No. 80-GT-67.
- Skrotzki and Vopat; "Power Station Engineering and Economy", McGraw-Hill, 1960.
- Vermes, G., Toof, J. L., Cohn, A.; "The Modeling of NO_x Generation from Coal Derived Liquids in Combustion Turbines". Presented at the Joint ASME/IEEE/ASCE Power Generation Conference, Charlotte, N.C.; Oct. 8-10, 1979, Paper No. 79-JPGC-GT-4.
- Wark, "Thermodynamics, 3rd edition", McGraw-Hill Book Co., San Francisco, CA, 1977.
- White, D. J.; "Low NO_x Combustion Systems for Burning Heavy Residual Fuels and High Fuel-bound Nitrogen Fuels", ASME Publication No. 81-GT-109, March 1981.
- Williams, Alan; "Combustion of Sprays of Liquid Fuels"; Paul Elek (Scientific Books) Ltd., London, 1976.
- Zeldovich, A.; "The Oxidation of Nitrogen in Combustion and Explosives"; Acta Physiocochemica U.R.S.S., Vol. 21, Nov. 4, 1946.

APPENDIX 1

Test of Scott NO_x Analyzer Accuracy

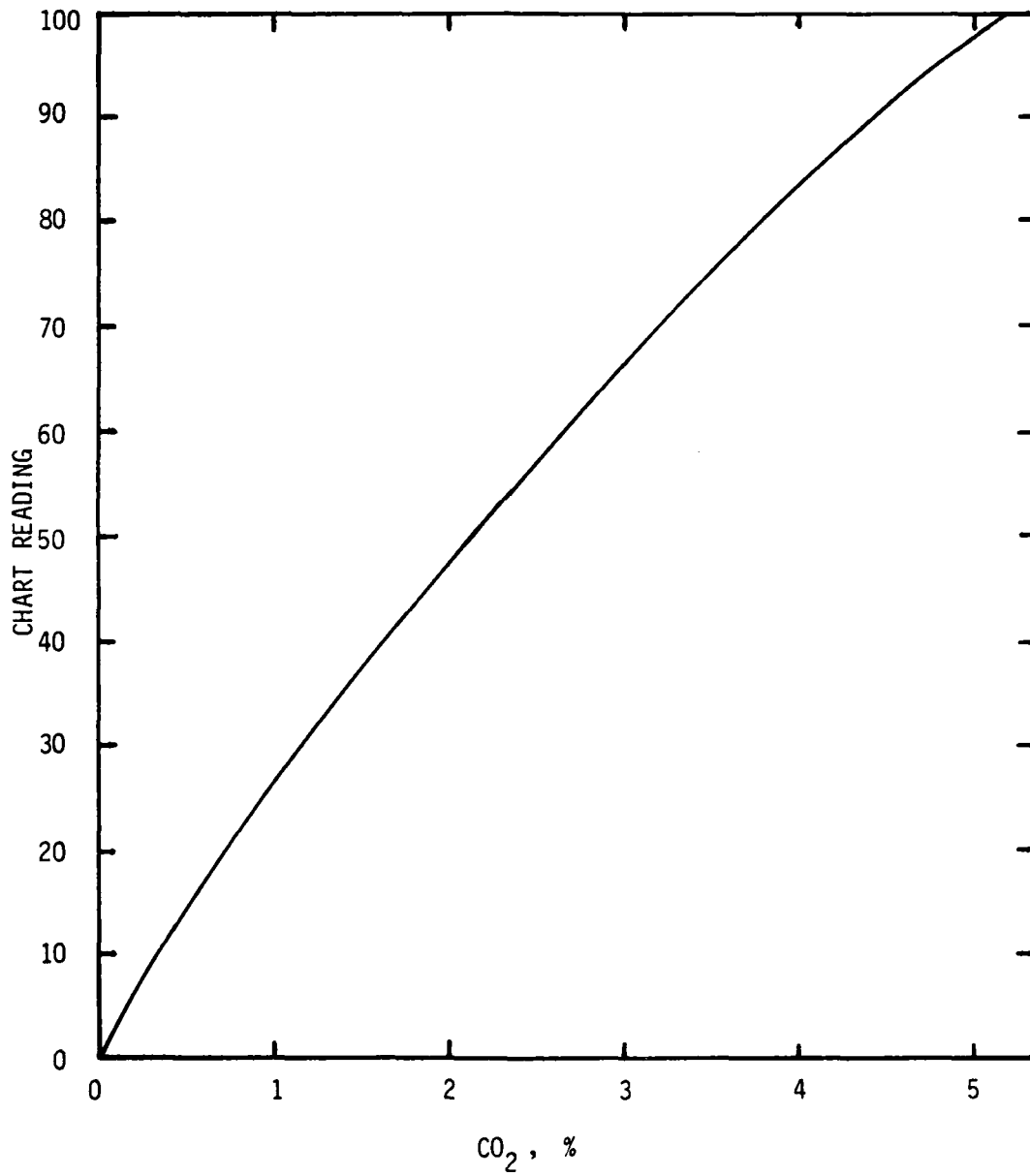
1/2/82 Calibrated on 45 ppmv span gas on 100 ppmv range

Zero pot: initial-2.458 final-2.32 Δ% scale = 4.3%

Gain pot: initial-4.179 final-4.08 Δ% scale = 1.0%

Span Gas ppmv	Instrument Range		Error %
	100 ppmv	250 ppmv	
45	45		0
95	97-100		+2-+5
		92.5-95	-1. -0
2460		2650	+1.9

APPENDIX 2
BECKMAN NDIR CO₂
CALIBRATION 2-27-81



APPENDIX 3

Calculation of Required Additive Volume for a Given Weight Percent of Mixed Fuel

$$12 \quad 1. \quad \text{Wt \%}_1 \text{ Mix} = \frac{\text{WtA}}{\text{Wt Total}} = \frac{\text{Wt \% 1} * (V_1 * \rho_1) + \text{Wt \% 2} * (V_2 * \rho_2)}{(V_1 * \rho_1) + (V_2 * \rho_2)}$$

where Wt %₁ Mix - Weight percent of the desired element in the final mixture

Wt Total - Total weight of the final mixture

Wt % 1 - Weight percent of the desired element in the additive

V₁ - Volume of the additive in the final mix

ρ₁ - Density of the additive

Wt % 2 - Weight percent of the desired element in the base fuel

V₂ - Volume of the base fuel in the final mix

ρ₂ - Density of the base fuel

$$2. \quad \text{Volume total} = V_1 + V_2$$

$$= V_1 \left[1 + \left(\frac{V_2}{V_1} \right) \right]$$

$$3. \quad \text{Taking eq. 1 and solving for } \frac{V_2}{V_1}$$

$$\text{Wt \%}_1 \text{ mix} = \frac{(\text{Wt \% 1} * \rho_1) + (\text{Wt \% 2} * \left(\frac{V_2}{V_1} \right) * \rho_2)}{\rho_1 + \left(\left(\frac{V_2}{V_1} \right) * \rho_2 \right)}$$

$$\frac{(\text{Wt \%}_1 * \rho_1) + (\text{Wt \% 2} * \left(\frac{V_2}{V_1} \right) * \rho_2)}{\text{Wt \%}_1 \text{ Mix}} = \rho_1 + \left[\left(\frac{V_2}{V_1} \right) * \rho_2 \right]$$

$$\frac{\text{Wt \% 1} * \rho_1}{\text{Wt \%}_1 \text{ mix}} + \frac{\text{Wt \% 2} * \left(\frac{V_2}{V_1} \right) * \rho_2}{\text{Wt \%}_1 \text{ mix}} = \rho_1 + \left[\left(\frac{V_2}{V_1} \right) * \rho_2 \right]$$

$$\frac{\text{Wt \% 1} * \rho_1}{\text{Wt \%}_1 \text{ mix}} = \rho_1 + \left[\left(\frac{V_2}{V_1} \right) * \rho_2 \right] - \frac{\text{Wt \% 2} * \left[\left(\frac{V_2}{V_1} \right) * \rho_2 \right]}{\text{Wt \%}_1 \text{ mix}}$$

$$\frac{\text{Wt \% 1} * \rho_1}{\text{Wt \%}_1 \text{ mix}} - \rho_1 = \left(\frac{V_2}{V_1} \right) * \rho_2 \left(1 - \frac{\text{Wt \% 2}}{\text{Wt \%}_1 \text{ mix}} \right)$$

$$\begin{aligned} \frac{V_2}{V_1} &= \rho_1 * \left(\frac{\text{Wt \% 1}}{\text{Wt \%}_1 \text{ mix}} - 1 \right) * \left(\frac{1}{\rho_2 \left(1 - \frac{\text{Wt \% 2}}{\text{Wt \%}_1 \text{ mix}} \right)} \right) \\ &= \left(\frac{\rho_1}{\rho_2} \right) * \left(\frac{\text{Wt \% 1}}{\text{Wt \%}_1 \text{ mix} \left(1 - \frac{\text{Wt \% 2}}{\text{Wt \%}_1 \text{ mix}} \right)} - \frac{1}{\left(1 - \frac{\text{Wt \% 2}}{\text{Wt \%}_1 \text{ mix}} \right)} \right) \end{aligned}$$

4. Solving eq. 2. for V_1 (additive Volume)

$$V_1 = \frac{\text{Volume Total}}{1 + \frac{V_2}{V_1}}$$

5. Substituting 3. into 4.

$$V_1 = \frac{\text{Volume Total}}{1 + \left(\frac{\rho_1}{\rho_2} \right) * \left(\frac{\text{Wt \% 1}}{\text{Wt \%}_1 \text{ mix} \left(1 - \frac{\text{Wt \% 2}}{\text{Wt \%}_1 \text{ mix}} \right)} - \frac{1}{\left(1 - \frac{\text{Wt \% 2}}{\text{Wt \%}_1 \text{ mix}} \right)} \right)}$$

6. and simplifying

$$13 \quad V_1 = \frac{\text{Volume Total}}{1 + \left(\frac{\rho_1}{\rho_2} \right) * \left(\frac{\text{Wt \% 1} - \text{Wt \%}_1 \text{ mix}}{\text{Wt \%}_1 \text{ mix} \left(1 - \frac{\text{Wt \% 2}}{\text{Wt \%}_1 \text{ mix}} \right)} \right)}$$

A computer program employing this equation and a printout of the results for the nitrogen contents desired in this study follow.

LIST

```
10 REM THIS PROGRAM CALCULATES THE VOLUME OF ADDATIVE REQUIRED
20 REM FOR A GIVEN MIX CONCENTRATION OF THE DESIRED ELEMENT
30 ! CHR$(27),CHR$(64)
40 ! CHR$(12)
50 PRINT " INPUT THE WIEGHT PERCENT OF THE DESIRED ELEMENT IN YOUR "
60 PRINT "ADDATIVE AND YOUR BASE FUEL.(IN DECIMAL FORM.)"
70 INPUT W1,W2
80 PRINT " "
90 PRINT " INPUT THE DENSITY OF THE ADDATIVE AND THE BASE FUEL."
100 INPUT D1,D2
110 ! " "
120 PRINT " INPUT THE DESIRED WIEGHT PERCENT OF THE ELEMENT IN "
130 PRINT "THE MIX ,AND THE TOTAL AMOUNT OF MIX WANTED."
140 INPUT W,U1
150 B=(W1-W)/(W*(1-(W2/W)))
160 V2=U1/(1+(D1/D2)*B)
170 V3=U1-V2
175 ! " \ ! " "
180 PRINT "ADD ",V2," ADDATIVE TO ",V3," BASE FUEL. "
185 PRINT "THE ADDATIVE TO BASE VOLUME RATIO IS ",V2/V3
190 END
READY
```

Mixes Used

1.0% Nitrogen

INPUT THE WEIGHT PERCENT OF THE DESIRED ELEMENT IN YOUR
ADDITIVE AND YOUR BASE FUEL.(IN DECIMAL FORM.)

? .1783, .0.0

INPUT ERROR--RETYPE

? .1783, .0.0

INPUT THE DENSITY OF THE ADDITIVE AND THE BASE FUEL.

? .9765, .7934

INPUT THE DESIRED WEIGHT PERCENT OF THE ELEMENT IN
THE MIX ,AND THE TOTAL AMOUNT OF MIX WANTED.

? .01, 189 26.65

ADD 871.63315 ADDITIVE TO 18055.017 BASE FUEL.
THE ADDITIVE TO BASE FUEL VOLUME RATIO IS 4.8276507E-02
READY

PRGM

6 0.5% Nitrogen

INPUT THE WEIGHT PERCENT OF THE DESIRED ELEMENT IN YOUR
ADDITIVE AND YOUR BASE FUEL.(IN DECIMAL FORM.)

? .1783, .0.0

INPUT THE DENSITY OF THE ADDITIVE AND THE BASE FUEL.

? .9765, .7934

INPUT THE DESIRED WEIGHT PERCENT OF THE ELEMENT IN
THE MIX ,AND THE TOTAL AMOUNT OF MIX WANTED.

? .005, 18926.65

ADD 435.51266 ADDITIVE TO 18493.137 BASE FUEL.
THE ADDITIVE TO BASE FUEL VOLUME RATIO IS 2.3441824E-02
READY

APPENDIX 4

GAS TURBINE DATA SHEET

USAF Project - Laboratory Evaluation of Novel Particulate Control Concepts for Jet Engine Test Cells

Principal Investigator Prof. R. W. Boubel
Oregon State University

Date _____ Time _____

Test Crew _____

Type of Control Device _____

Fuel: % Kerosene _____, % Toluene _____

Ambient Temperature, °F _____ Barometric Pressure, in. Hg _____

Fuel Flow: Seconds per 2000 cc _____, Pounds per hour _____

Fuel Pressure, psi _____ Compressor Outlet Pressure, psi _____

Turbine Load (0, 1/2, Full), Kw _____

Exhaust: CO₂, Reading _____, % _____ Opacity, % _____

Turbine Outlet Temperature, °F _____

NO_x, Reading _____, % _____

Velocity Pressure (1 in. from top), in. H₂O _____ Vel., fpm _____

Smoke Sample: Orifice Δp, in. H₂O _____ Time, Sec. _____

Flow, cfh _____ Gas Volume, cubic feet _____

Sample Temperature, °F _____

Rw (Reflectance of clean filter) _____

Rs (Reflectance of Sample Spot) _____

Smoke Number _____

Maximum Duct Temperature, °F _____

Remarks Twb- Tdb1- Twb2- Tdb2-

APPENDIX 5

GAS TURBINE OPERATING PROCEDURE (modified 6/26/81)

A. 2 hours before test

- 1) Place NOx Exhaust and Bypass out window
- 2) Turn on N₂ Cylinder and adjust to 10 psi
- 3) Turn on Power to CO₂ analyzer turnswitch to TUNE
- 4) Turn on Power to NOx analyzer and push the ZERO and CONV buttons on NOx system
- 5) Turn 3 way valve on CO₂ system to N₂ and adjust flow through CO₂ system to 800 cc/min
- 6) Adjust NOx analyzer to 5½ psi (sample valve) and 1½ SCFH flow rate

B. Test procedure

- 1) Open test turbine exhaust duct damper
- 2) Ensure fuel supply in proper tanks (measuring burette filled)
- 3) Turn on fuel supply valves to turbine (four valves in all)
- 4) Connect battery (red to positive)
- 5) Turn on panel lights (if lights come on battery's are o.k.)
- 6) Turn on opacity monitor blower (plug in)
- 7) Turn on opacity monitor and recorder (adjust zero and span on both)
- 8) Turn on exhaust duct blower (switch is on column next to fuel tank)
- 9) Turn on electrical load cooling blower
- 10) Turn on Relative Humidity measuring device
- 11) Turn on CO₂, NOx span and Air Tanks
- 12) Adjust CO₂ pressure to 5-6 psi and the NOx and Air Tanks to 10-15 psi
- 13) Turn on all Line Valves (following regulators)
- 14) With threeway valve in N₂ position adjust the CO₂ analyzer until the meter reads zero.
- 15) Adjust the CO₂ recorder to zero
- 16) Turn threeway valve to CO₂ adjust the instrument gain to get 100% on recorder
- 17) Recheck N₂+CO₂ until constant values are obtained.
- 18) Turn on compressed air to sample delivery system (on wall near boiler)
- 19) Plug in sample delivery system (electrical)
- 20) Turn on Ambient and pump switches on sample delivery system panel
- 21) Turn threeway valve to sample and adjust CO₂ instrument flow to 800 cc/min
- 22) Press samp switch on NOx instrument (light should glow)
- 23) Adjust sample pressure to 5.5 psi
- 24) Adjust sample flow to 1.5 SCFH bypass
- 25) Turn on OXY button and adjust air pressure to 5.5 psi
- 26) Turn on O₂ and NOx buttons
- 27) Zero adjust for NOx
 - a) Press Zero button, press 100 range switch
 - b) Zero instrument to slightly positive
 - c) Check recorder and adjust zero with span (screw driver) if needed
- 28) Span adjustment for NOx
 - a) Press Span button and 100 range scale
 - b) Adjust cylinder until sample pressure reads 5.5
 - c) Adjust gain to proper value on instrument
 - d) Check recorder for same value adjust with the zero if necessary

- 29) Recheck zero and span and adjust as needed to obtain consistent values
- 30) Make notation on chart of pot settings, date and run number
- 31) Press the Samp switch on the NOx instrument
- 32) Press the sample switch on the sample delivery system panel
- 33) Record, Tdbulb, Twb
- 34) Check turbine panel switches all off or open
- 35) Start turbine (RPM-100%, Volts-240, amps &KW-0)
- 36) Set load switch to position L₁ L₃ PH 3
- 37) Select 0, ½, or Full Load
- 38) Take all Data
- 39) Rerecord Tdbulb, Twb
- 40) Shut down turbine
- 41) Purge NOx and CO₂ instruments with N₂ or ambient Air
- 42) Recheck all calibrations and note changes on strip chart
- 43) Purge sample line and cooling system by pushing the Shop Air and Trap drain buttons on sample transport system panel
- 44) Shut down all machinery and equipment in the reverse order of start up

APPENDIX 6

NO_x Values from Data Sheets
(when more than one reading was taken)

Test 1/5/82 Load - 0

Fuel 0% N

	read	0	Δ
1)	5	1.5	3.5
2)	5.5	1.75	3.75
3)	4.5	1.0	3.5
4)	4	1.5	2.5

$$\bar{\Delta} = 3.2 \quad \sigma = .31$$

Test 1/5/82 Load - 6.25

Fuel 0% N

	read	0	Δ	
1)	22	11.5	8.5	
2)	18	10	8.0	
3)	22.5	14	8.5	
4)	21	15.5	5.5	ignore

$$\bar{\Delta} = 7.6 \quad \sigma = 1.4$$

$$\text{For 1st 3 } \bar{\Delta} = 8.3 \quad \sigma = .29$$

Test 1/5/82 Load 14.3 kw

Fuel 0% N

	read	0	Δ
1)	40	26	14
2)	41	27	14
3)	41	27.5	13.5

$$\bar{\Delta} = 13.8 \quad \sigma = .289$$

Test 1/6/82 Load - 0

Fuel -0.5% N

	read	0	Δ	
1)	10	3	7	ignore
2)	11.5	2	9.5	
3)	13	3.5	9.5	
4)	13.5	3.5	10	
5)	14	4	10	
6)	14	4	10	

$$\bar{\Delta} = 9.8 \quad \sigma = .27$$

Test 1/6/82 Load 6.25

Fuel 0.5% N

	read	0	Δ	
1)	27.5	6.5	21	ignore
2)	30	6	24	
3)	31	7	24	
4)	31	7	24	

Test 1/6/82 Load

Fuel 0.5% N

	read	0	Δ
1)	50	9	41
2)	50	8	42
3)	51	10	41
4)	51	8.25	42.75

AD-A137 641

LABORATORY EVALUATION OF NOVEL PARTICULATE CONTROL
CONCEPTS FOR JET ENGINE TEST CELLS(U) OREGON STATE UNIV
CORVALLIS R W BOUBEL DEC 83 AFESC/ESL-TR-83-02
F08635-81-K-0003

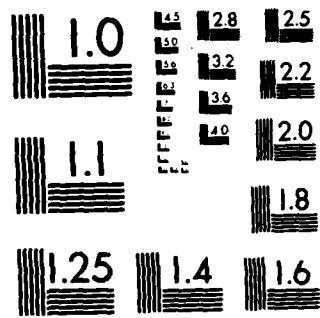
3/3

UNCLASSIFIED

F/G 21/2

NL

		END											
		DATE											
		FILED											
		3 84											
		DTIC											



MICROCOPY RESOLUTION TEST CHART
NATIONAL BUREAU OF STANDARDS-1963-A

NO_x Values (continued)

5) 32 7.5 24.5
 6) 32 7 25
 $\bar{\Delta} = 24.3$ $\sigma = .45$

5) 52 10.5 41.5
 6) 51.5 9.25 42.25
 $\bar{\Delta} = 41.75$ $\sigma_{n-1} = .707$

Test 1/7/82 Load 0

Test 1/7/82 Load 6.25 Kw

Fuel 1.0% N

Fuel 1.0% N

	read	0	Δ
ignore	1) 29	6	23
	2) 31	5.5	25.5
	3) 32	7	25
	4) 32	6.5	25.5
	5) 32.5	8	24.5
	6) 33	7.5	25.5

$\bar{\Delta} = 25.2$ $\sigma = .45$

	read	0	Δ
ignore	1) 56	11	45
	2) 56	10.5	45.5
	3) 57	12.0	45
	4) 58	11.5	46.5
	5) 59	12.5	46.5
	6) 59	12.0	47

$\bar{\Delta} = 45.9$ $\sigma = 8.6$

Estimated span drift 5 ppm $\Delta_{\text{adjusted}} = 30.2$ ppmv $\Delta_{\text{adjusted}} = 51.9$ ppmv

Test 1/7/82 Load 15 Kw

Test 1/8/82 Load 0 Kw

Fuel 1.0%

Fuel 1.0%

	read	0	Δ
250 scale ignore	1) 83	14	69
	2) 83	14	69
	3) 84	15	69
	4) 82	14	68
	5) 37.25	8.75	71.8
	6) 38	8	75

$\bar{\Delta} = 68.75$ $\sigma = 81.5$

	read	0	Δ
ignore	1) 28.75	3.0	25.75
	2) 27.0	2.0	25
	3) 28.0	3.0	25
	4) 27.5	2.75	24.75
	5) 28	4.0	24.0
	6) 27.5	3.5	24.0

$\bar{\Delta} = 24.75$ $\sigma = .67$

span drift = 13 ppm $\bar{\Delta}_{\text{adjusted}} = 81.8$ ppmv

span drift = 5.5 ppm $\bar{\Delta}_{\text{adjusted}} = 30.25$

Not likely to be very accurate due to the large span drift

NO_x Values (continued)

Test 1/8/82 Load 6.25 Kw

Fuel = 1.0% N

Read	0	Δ
1) 48	6.5	41.5
2) 48.5	5.75	42.75
3) 50.5	6.0	44.5
4) 49	5.5	43.5
5) 52	7	45
6) 51	6	45

$$\bar{\Delta} = 43.7 \quad \sigma = 1.4$$

$$\text{span drift} = 4.5 \text{ ppm}$$

$$\Delta_{\text{adjusted}} = 48.2 \text{ ppmv}$$

Test 1/8/82 Load 15.5 Kw

Fuel = 1.0% N

Read	0	Δ	
1) 78	8	70	ignore
2) 77.5	6	71.5	
3) 79.5	7.5	74.5	
4) 78.5	6	72.5	
5) 81	8	73	
6) 80	6	74	

$$\bar{\Delta} = 73.1 \quad \sigma = 1.2$$

$$\text{span drift} = 5.25$$

$$\bar{\Delta}_{\text{adjusted}} = 78.35$$

Test 12/30/81 Load 9.5

Fuel 0% N

Read	0	Δ
1) 16	6.5	9.5
2) 15.5	7	8.5

$$\bar{\Delta} = 9 \quad \sigma = .707$$

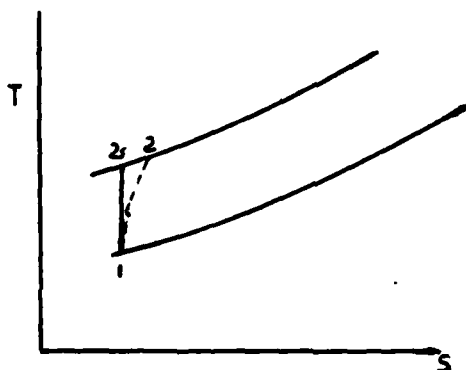
APPENDIX 7

Determination of Combustor Inlet Temperature

Assumptions

- 1) Air acts as a perfect gas
- 2) Compressor efficiency is approximately = 80%

The compression process is shown below on a temperature entropy diagram.



1) The initial enthalpy, h_1 , and the entropy at constant pressure, ϕ_1 , were obtained by interpolation at actual ambient temperatures on the Keenan and Kaye Gas Tables.²⁷

2) P_2 was measured during the run.

3) The isentropic entropy at P_2 was calculated by

$$14 \quad \phi_{2s} = \phi_1 + \frac{R}{J} \ln \frac{P_2}{P_1} = \phi_1 + \frac{1.986 \text{ BTU/lbm}^\circ\text{R}}{28.93 \text{ M.W. Air}} \times \ln \left(\frac{P_2}{P_1} \right)$$

and the corresponding enthalpy, h_{2s} taken at the same conditions.

4) The actual enthalpy was calculated using the assumed efficiency

$$15 \quad h_2 = \frac{h_{2s} - h_1}{\eta} + h_1$$

and the temperature read from the table at the same conditions.

TABLE VII

Determination of Combustor Inlet Temperature

Load	Date	Fuel % N	T _{in} (°R)	P _{in} (atm)	h ₁ $\frac{\text{BTU}}{\text{lb}}$	ϕ_1	P ₂ (atm)	ϕ_{2s}	h _{2s} $\frac{\text{BTU}}{\text{lb}}$	h ₂	T ₂ °R
0	12/28/81	0.0	513.5	.998	122.71	.58870	2.222	.64365	154.42	162.35	678.42
9	12/28/81	0.0	521.0	.998	124.51	.59219	2.222	.64714	156.69	164.74	688.31
9.5	12/30/81	0.0	521.5	.963	124.63	.59242	2.187	.64873	157.73	166.01	693.57
0	1/5/82	0.0	515.5	1.000	123.19	.58963	2.157	.64240	153.61	161.22	673.71
6.25	1/5/82	0.0	525.0	1.000	125.47	.59402	2.157	.64679	156.46	164.21	686.12
14.3	1/5/82	0.0	532.5	1.000	127.26	.59742	2.225	.65232	160.12	168.34	703.22
0	1/6/82	0.5	507.0	1.015	121.15	.58565	2.239	.63996	152.05	159.78	667.72
6.25	1/6/82	0.5	512.5	1.015	122.47	.58824	2.239	.64255	153.71	161.52	674.96
15.0	1/6/82	0.5	516.5	1.015	123.43	.59010	2.274	.64548	155.60	163.64	683.76
0	1/7/82	1.0	515.5	1.017	123.19	.58963	2.208	.64285	153.90	161.58	675.21
6.25	1/7/82	1.0	522.0	1.017	124.75	.59264	2.242	.64691	156.54	164.49	687.27
15.0	1/7/82	1.0	529.5	1.017	126.54	.59607	2.242	.65034	158.80	166.87	697.14
0	1/8/82	1.0	517.5	1.0167	123.67	.59057	2.207	.64378	154.50	162.21	677.83
6.25	1/8/82	1.0	519.0	1.0167	124.03	.59126	2.241	.64552	155.62	163.52	682.26
15.5	1/8/82	1.0	522.0	1.0167	124.75	.59264	2.241	.64690	156.53	164.48	687.23

APPENDIX 8

Weight Percent of an Element in a Fuel Mixture

It is also desirable to know the elemental composition of a fuel mixture when the composition of the various components is known. This can be calculated using equation 12 from Appendix 3.

$$12 \quad \text{Wt \%}_1 \text{ mix} = \frac{\text{Wt } 1}{\text{Wt Total}} = \frac{\text{Wt \% } 1 * (V_1 * \rho_1) + \text{Wt \% } 2 * (V_2 * \rho_2)}{(V_1 * \rho_1) + (V_2 * \rho_2)}$$

where:

Wt %₁ mix = weight percent of the desired element in the fuel mixture

Wt Total = Total weight of your fuel mix

Wt % 1 = Weight percent of your element in the fuel additive

V₁ = Volume of additive in the fuel mix

ρ₁ = Density of the fuel additive

Wt % 2 = Weight percent of the element in your base fuel

V₂ = Volume of the base fuel in the final mix

ρ₂ = Density of the base fuel

A computer program was written to do this calculation. A copy of the program and the runs for the C, H, and N levels in the fuel mixes used are shown.

LIST

```
10 REM THIS PROGRAM CALCULATES THE WIECHT PERCENT OF AN ELEMENT
20 REM IN A FUEL MIXTURE WHEN THE WIECHT PERCENTS OF THE ELEMENT
30 REM AND THE VOLUMES OF THE CONSTITUANT FUELS ARE KNOWN.
40 !CHR$(27),CHR$(64)
50 !CHR$(12)
60 PRINT " INPUT THE WIECHT PERCENT OF THE DESIRED ELEMENT IN YOUR "
70 PRINT "ADDITIVE AND THE BASE FUEL.(IN DECIMAL FORM.) "
80 INPUT W1,W2
90 !" "
100 PRINT "INPUT THE DENSITY OF THE ADDITIVE AND THE BASE FUEL."
110 INPUT D1,D2
120 !" "
130 PRINT "INPUT THE NUMBER OF FUEL MIXTURES TO BE CONSIDERED. "
140 INPUT N
150 FOR J=1 TO N
160 !" "
170 PRINT "INPUT THE VOLUME OF THE ADDITIVE AND THE BASE FUEL. "
180 INPUT V1,V2
190 W=(W1*V1*D1+W2*V2*D2)/(V1*D1+V2*D2)
200 !" "\!" "
210 PRINT "THE WIECHT PERCENT OF THE FINAL MIX IS: ",W*100.0," %"
220 !" "\!" "
230 NEXT J.
PRESS RETURN TO CONTINUE
240 END
READY
```

@ **Kerosene Pyridine Mixtures C%**
 INPUT THE WIEGHT PERCENT OF THE DESIRED ELEMENT IN YOUR
 ADDITIVE AND THE BASE FUEL.(IN DECIMAL FORM.)
 ? .7556, .90645

INPUT THE DENSITY OF THE ADDITIVE AND THE BASE FUEL.
 ? .9765, .7934

INPUT THE NUMBER OF FUEL MIXTURES TO BE CONSIDERED.
 ? 3

INPUT THE VOLUME OF THE ADDITIVE AND THE BASE FUEL.
 ? 0.0, 18926.65

THE WIEGHT PERCENT OF THE FINAL MIX IS: 90.645004 %

INPUT THE VOLUME OF THE ADDITIVE AND THE BASE FUEL.
 ? 433.5, 184930.1

THE WIEGHT PERCENT OF THE FINAL MIX IS: 90.221983 %

INPUT THE VOLUME OF THE ADDITIVE AND THE BASE FUEL.
 ? 871.6, 18035. 0.5% N

THE WIEGHT PERCENT OF THE FINAL MIX IS: 89.798987 % 1.0%N

@ **%N**
 INPUT THE WIEGHT PERCENT OF THE DESIRED ELEMENT IN YOUR
 ADDITIVE AND THE BASE FUEL.(IN DECIMAL FORM.)
 ? .17830, 0, 0.0

INPUT THE DENSITY OF THE ADDITIVE AND THE BASE FUEL.
 ? .9765, .7934

INPUT THE NUMBER OF FUEL MIXTURES TO BE CONSIDERED.
 ? 3

INPUT THE VOLUME OF THE ADDITIVE AND THE BASE FUEL.
 ? 0.0, 18926.65

THE WIEGHT PERCENT OF THE FINAL MIX IS: 0 %

INPUT THE VOLUME OF THE ADDITIVE AND THE BASE FUEL.
 ? 433 .5, 18493.1

THE WIEGHT PERCENT OF THE FINAL MIX IS: .49998654 % .5%N

INPUT THE VOLUME OF THE ADDITIVE AND THE BASE FUEL.
 ? 871.6, 18035

THE WIEGHT PERCENT OF THE FINAL MIX IS: .99996301 % 1.0%N

Kerosene Pyridine Mixtures %H

INPUT THE WIEGHT PERCENT OF THE DESIRED ELEMENT IN YOUR
ADDITIVE AND THE BASE FUEL.(IN DECIMAL FORM.)
? .0661, .09355

INPUT THE DENSITY OF THE ADDITIVE AND THE BASE FUEL.
? .9765, .7934

INPUT THE NUMBER OF FUEL MIXTURES TO BE CONSIDERED.
? 3

INPUT THE VOLUME OF THE ADDITIVE AND THE BASE FUEL.
? 0.0, 18926.65

THE WIEGHT PERCENT OF THE FINAL MIX IS: 9.355 %

INPUT THE VOLUME OF THE ADDITIVE AND THE BASE FUEL.
? 433.5, 18493.1

THE WIEGHT PERCENT OF THE FINAL MIX IS: 9.2780247 % 0.5%N

INPUT THE VOLUME OF THE ADDITIVE AND THE BASE FUEL.
? 871.6, 18055.

THE WIEGHT PERCENT OF THE FINAL MIX IS: 9.2010519 % 1.0%N

APPENDIX 9

Fuel Density Calculations

T ambient = 75°F

Measured 9/3/81

API gravities were calculated from the measured densities adjusted to 60°F.

Volume coefficients of expansion for petroleum fuels are:²⁸

API	Coefficient $\frac{\Delta \text{Volume}}{\Delta T^{\circ}\text{F}}$
Below 14.9	0.00035
15 - 34.9	.0004
35 - 50.9	.0005

Density of H₂O

$$\rho_{\text{H}_2\text{O}} = .99905 \text{ g/ML}^{29}$$

CALCULATIONS

1. Kerosene: 25 ML = 40.0798g - 20.2442g = 19.8356g
container

$$16 \rho = \frac{\text{mass measured}}{\text{volume measured}}$$

a) at T_{amb}

$$\rho = \frac{19.8356\text{g}}{25 \text{ ML}} = .7934 \text{ g/ML} \left(\frac{\text{Kg}}{\text{L}} \right) \left(\frac{\text{Kg}}{\text{L}} \right) * 8.3452 \frac{\text{gal}}{\text{Kg}} = 6.6210 \frac{\text{lb}}{\text{gal}}$$

b) at 60°F

$$\rho = \frac{19.8356\text{g}}{25\text{ML} + (25 * .0005 * 15^{\circ}\text{F}) \text{ ML}} = .7994 \frac{\text{g}}{\text{ML}} \left(\frac{\text{kg}}{\text{L}} \right) [6.6713 \frac{\text{lb}}{\text{gal}}]$$

c) Specific gravity at 60°F (S)

$$17 \quad S = \frac{\rho_{\text{fuel}} (60^{\circ}\text{F})}{\rho_{\text{H}_2\text{O}} (60^{\circ}\text{F})} = \frac{.7994}{.99905} = .8002$$

1. Kerosene

d) API Gravity

$$18 \quad \text{API} = \frac{141.5}{S} - 131.5$$

$$\text{API} = \frac{141.5}{.8002} - 131.5 = \underline{45.3308}$$

2. Toluene 25 ML = 41.5338g - 20.1198g = 21.4140g

a) at T_{amb}

$$\rho = \frac{21.4140\text{g}}{25 \text{ ML}} = \underline{.8566 \frac{\text{g}}{\text{ML}} \left(\frac{\text{kg}}{\text{L}} \right)} \left[7.1483 \frac{\text{lb}}{\text{gal}} \right]$$

b) at 60°F

$$\rho = \frac{21.4140\text{g}}{25 + (25 * .0004 * -15 \text{ }^\circ\text{F})} = \underline{.8617 \frac{\text{g}}{\text{ML}} \left(\frac{\text{kg}}{\text{L}} \right)} \left[7.1913 \frac{\text{lb}}{\text{gal}} \right]$$

c) Specific gravity at 60°F

$$S = \frac{.8617}{.99905} = \underline{.8625}$$

d) API Gravity

$$\text{API} = \frac{141.5}{.8625} - 131.5 = \underline{32.5580}$$

3. Pyridine

a) at T_{amb} 25 ML = 43.9950 g - 19.5813g = 24.4137g

$$\rho = \frac{24.4137\text{g}}{25 \text{ ML}} = \underline{.9765 \frac{\text{g}}{\text{ML}} \left(\frac{\text{kg}}{\text{L}} \right)} \left[8.1490 \frac{\text{lb}}{\text{gal}} \right]$$

b) at 60°F

$$\rho = \frac{24.4137\text{g}}{25 + (25 * .00035 * -15 \text{ }^\circ\text{F})} = \underline{.9817 \frac{\text{g}}{\text{ML}} \left(\frac{\text{kg}}{\text{L}} \right)} \left[8.1925 \frac{\text{lb}}{\text{gal}} \right]$$

c) Specific Gravity at 60°F

$$S = \frac{.9817}{.99905} = \underline{.9826}$$

d) API Gravity

$$\underline{API} = \frac{141.5}{.9826} - 131.5 = \underline{12.5057}$$

Accuracy of Density Measurements

a) Temperature Variation

i) The maximum change in the density of kerosene for the temperature range encountered was 1.58% when the ambient temperature reached 44°F

$$\Delta \rho \text{ kerosene } 44^\circ\text{F} = \frac{.8059 - .7934}{.7934} = .01577 \text{ (1.58\%)}$$

ii) The density ratio change for kerosene and pyridine $\frac{\rho_p}{\rho_k}$ was

$$20 \quad = \frac{\left(\frac{.9873}{.8059}\right) - \left(\frac{.9765}{.7934}\right)}{\left(\frac{.9765}{.7934}\right)} = -.0046 \text{ (-.46\%)}$$

Therefore for mixing fuels this error can be considered negligible.

b) Investigation of density changes for the various fuel mixtures.

Compare the 1% N mix and pure kerosene at 60°F.

$$\begin{aligned} \rho_{\text{mix}} &= \frac{\rho_p V_p + \rho_k V_k}{V_{\text{Total}}} \\ &= \frac{.9817 \text{ g/ML} * 871.6331 \text{ g/ML} + .7994 \text{ g/ML} * 18055.017 \text{ ML}}{18926.85 \text{ ML}} \\ &= .8078 \text{ g/ML} \end{aligned}$$

$$\Delta \rho = \frac{.8078 - .7994}{.7994} = .0105 \text{ (1.05\%)}$$

For the purposes to which these values are put (i.e. calculation of A/F ratios), this error is negligible in comparison with the inaccuracies associated with the air flow measurements.

However, if the fuel flow is known accurately, a comparison of the A/F ratios calculated directly with the A/F ratios calculated using CO and CO₂ measurements will give an idea of the accuracy of the air flow measurements.

For this reason a determination of the actual fuel densities for each run was made, assuming that the fuel remained at the initial ambient temperature for that day. These values are given in the following table.

TABLE VIII

Fuel Densities Used

Date	Fuel	Tdb Ambient Temp °F	Density g/ML $\left(\frac{\text{kg}}{\text{L}}\right)$
12/28/81	100%K 0.0% N	50	.8035
12/30/81	100%K 0.0% N	54	.8018
1/5/82	100%K 0.0% N	51	.8031
1/6/82	0.5% N	44	.8101
1/7/82	1.0% N	52	.8110
1/8/82	1.0% N	57	.8090

APPENDIX 10a

Calculation of A/F Ratios by Direct Measurement

As a check on our calculations based on CO and CO₂ measurements, it was decided to calculate the air fuel ratios directly from measured variables. Shown below is a derivation of those equations necessary to achieve this end.

A. Calculation of Exhaust Mass Flow Rate

1) Assumptions

- a) The exhaust is treated as a perfect gas with the properties of air
- b) The exhaust is at atmospheric pressure

2) The following derivations were taken from literature supplied by the F.W. Dwyer Mfg. Co., Inc.³⁰

3) Air Velocity

$$22 \quad Vel = 1096.2 (P_v/D)^{\frac{1}{2}} \quad [\text{ft/min}]$$

P_v = velocity pressure [in. H₂O]

D = Air density [lb/ft³]

4) Air Density

$$23 \quad D = 1.325 * \frac{P_b}{T} \quad [\text{lb/ft}^3]$$

P_b = barometric pressure

T = temperature °R (°F + 460)

5) Mass Flow Rate

$$\begin{aligned} 24 \quad \dot{M}_E &= \text{velocity [ft/min]} * \text{Duct Area [ft}^2] * \text{density [lb/ft}^3] \\ &= 1096.2 * (P_v/D)^{\frac{1}{2}} * D * A \\ &= 1096.2 * (P_v * D)^{\frac{1}{2}} * A \\ &= 1096.2 * (P_v * (1.325 * P_B/T))^{\frac{1}{2}} * \pi \frac{(5)^2}{4} \end{aligned}$$

Direct A/F measurement (continued)

$$25 \quad \dot{M}_E = 149.4711 * (Pv*(1.325*P_B/T))^{\frac{1}{2}} \quad [lb/min]$$

B. Calculation of Fuel Mass Flow Rate

1) Assumption:

a) That the flow rate was essentially constant.

2) The measured value was seconds per 2000 cc.

This value was converted into mass flow rate in lb/min.

$$\begin{aligned} \dot{M}_F &= \frac{2000}{t_f} \left[\frac{cc}{sec} \right] * D_f \left[\frac{kg}{cc} \right] * \frac{1}{1000} \left[\frac{L}{cc} \right] * \frac{1}{.4535} \left[\frac{lb}{kg} \right] * 60 \left[\frac{sec}{min} \right] \\ 26 \quad &= 263.1579 * \frac{D_F}{T_F} \quad lb/min \end{aligned}$$

C. The Air Fuel Ratio can then be calculated by

The mass ratio

$$27 \quad A/F = \frac{\dot{M}_E - \dot{M}_F}{\dot{M}_F}$$

D. The values calculated are shown in Table IX. The values calculated by CO and CO₂ measurements are also shown for comparison.

Table 9

Calculation of A/F ratios by Direct Measurement
Compared to those Calculated from CO₂

$$\dot{M}_E = 149.4711 \cdot \sqrt{P_v} \cdot (1.325 \cdot P_b / T) \quad \left[\frac{\text{lb}}{\text{min}} \right]$$

$$\dot{M}_F = 263.1579 \cdot \frac{D_F \left[\frac{\text{kg}}{\text{L}} \right]}{t_T \text{ [s]}} \quad \left[\frac{\text{lb}}{\text{min}} \right]$$

$$A/F = \frac{\dot{M}_E - \dot{M}_F}{\dot{M}_F}$$

	Fuel	Load	Pv	Pb in Hg	T ^o R _{exh}	$\dot{M}_E \frac{\text{lb}}{\text{min}}$	DF	t _F sec	$\dot{M}_F \frac{\text{lb}}{\text{min}}$	A/F _M	A/F _D *
12/28/81	100% O ₂ N	9 kw	5.3	29.85	1115	64.8094	.8035	338.	.62558	102.599	100.62*
12/28/81	100% O ₂ N	0 kw	3.8	29.85	920	60.4137	.8035	462.	.45768	131.000	145.35
				V							
1/5/82	100% O ₂ N	0 kw		29.93	928	64.1012	.8031	476.5	.44353	143.525	140.350
1/5/82	100% O ₂ N	6.25 kw		29.93	1071	61.6150	.8031	380.	.55616	109.786	108.503
1/5/82	100% O ₂ N	14.3 kw		29.93	1277	58.4455	.8031	284	.74416	77.539	77.817
				1500							
				1664							
				1882							
1/6/82	0.5%N	0 kw	3.9	30.36	911	65.2541	.8101	471.2	.45243	143.230	145.348
1/6/82	0.5%N	6.25 kw	4.8	30.36	1043	67.6571	.8101	375.6	.56758	118.203	111.478
1/6/82	0.5%N	15 kw	5.4	30.36	1224	66.2432	.8101	283.1	.75304	86.968	81.756
1/7/82	1.0%N	0 kw	3.9	30.43	925	61.6279	.8110	469.1	.45496	134.458	142.805
1/7/82	1.0%N	6.25 kw	4.3	30.43	1068	60.2233	.8110	375.1	.56897	104.846	109.971
1/7/8	1.0%N	15 kw	5.0	30.43	1245	60.1473	.8110	290.1	.73568	80.757	77.817
1/8/82	1.0%N	0 kw	4.1	30.42	930	63.0079	.8090	470.0	.45296	138.103	142.805
1/8/82	1.0%N	6.25 kw	4.3	30.42	1063	60.3549	.8090	377.5	.56396	106.020	108.503
1/8/82	1.0%N	15.5 kw	5.3	30.42	1248	61.8408	.8090	285.7	.74517	81.989	78.575
12/30/81	100% O ₂ N	9.5 kw	4.8	28.8	1131	60.1521	.8018	330 ^(est)	.63939	93.077	99.69*

* Calculated using the equation derived for kerosene as no CO data was available.

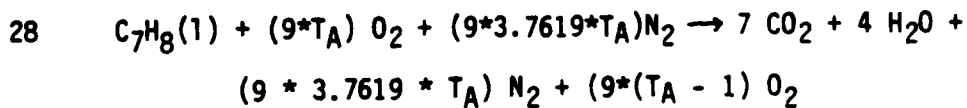
APPENDIX 10b

Calculation of the Percent Theoretical Air in Combustion
from Combustion Stoichiometry

A. Assumptions:

- 1) Complete combustion
- 2) No appreciable disassociation of the combustion products

B. Chemical Reaction Equation (for pure Toluene)



T_A = Percent theoretical air expressed as a decimal

C. Vol % CO_2 Calculation

$$29 \quad 1) \% CO_2 = \frac{\text{Mol } CO_2}{\text{Mol } CO_2 + \text{Mol } H_2O + \text{Mol } N_2 + \text{Mol } O_2}$$

$$2) \% CO_2 = \frac{7}{7 + 4 + (9 \cdot 3.7619 \cdot T_A) + 9 \cdot (T_A - 1)}$$

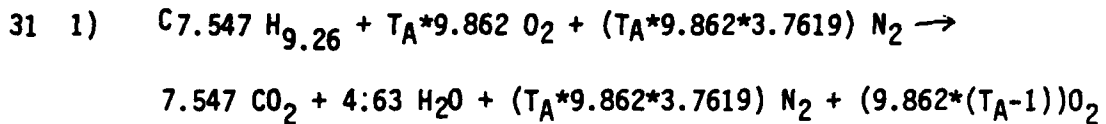
$$= \frac{7}{11 + T_A \cdot (9 \cdot 3.7619 + 9) - 9}$$

$$= \frac{7}{2 + T_A \cdot (42.8571)}$$

$$3) 2 + T_A \cdot (42.8571) = \frac{7}{\% CO_2}$$

$$30 \quad 4) T_A = \left(\frac{7}{\% CO_2} - 2 \right) \cdot \frac{1}{42.8571}$$

D. Modification of Theoretical Air Calculations to fit Kerosene's Composition



$$2) \quad \% CO_2 = \frac{7.547}{7.547 + 4.63 + (9.862 * 3.7619 * T_A) + (9.862 * (T_A - 1))}$$

$$= \frac{7.547}{12.177 + T_A (9.862 * 3.7619 + 9.862) - 9.862}$$

$$= \frac{7.547}{2.315 + T_A (46.9619)}$$

$$32 \quad 3) \quad T_A (\text{kerosene}) = \left(\frac{7.547}{\% CO_2} - 2.315 \right) * \frac{1}{46.9619}$$

These calculations can be converted to the air fuel ratio by multiplying by the Stoichiometric air fuel ratio for the specific fuel in question.

For kerosene this is found by the following calculation:

$$33 \quad \frac{\text{Mass Air}}{\text{Mass Fuel}} = \frac{(9.862 * 32.00) + (9.862 * 3.7619 * 28.016)}{(7.547 * 12.01) + (9.26 * 1.01)}$$

$$= 13.55$$

E. Accuracy

The accuracy of the above calculations are highly dependent on the actual chemical composition of the fuel and the accuracy of the original assumptions.

While searching the literature a method recommended by The Society of Automotive Engineers was found. As this method is an industrial standard, it was used in most cases in place of our derived equations.

Because of the good correlation between this method and that obtained by direct measurement, (see Appendix 10a), an accuracy of ± 3 in the A/F ratios seems reasonable for this method.

APPENDIX 11

Calculation of Heat of Formation of Kerosene

A. High Heating Value

$$34 \quad \text{HHV} \left(\frac{\text{BTU}}{\text{lb}} \right) = 18,440 + 40 (\text{API}-10) \\ \text{(Sherman and Kropff equation modified)}^{31}$$

For kerosene

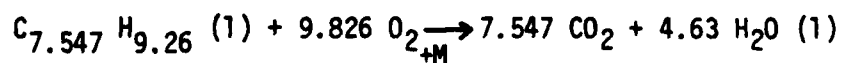
$$\text{HHV} = 18,440 + 40 (45.3308-10) = 19,853 \frac{\text{BTU}}{\text{lb}}$$

B. Accuracy

The text from which the above equation was taken states "[It is] probably more accurate than would be obtained by an inexperienced operator using a Bomb Calorimeter"³². As a comparison the 21st edition of The Handbook of Physics and Chemistry (pg. 1032), gives a value of $19,810 \frac{\text{BTU}}{\text{lb}}$ as the heat of combustion of kerosene.

In light of the above two facts, it seems reasonable to assume that the derived value is accurate to within $75 \frac{\text{BTU}}{\text{lb}}$.

C. Heat of Formation



$$35 \quad \text{HHV} = \left[\sum H_f \text{ Products} - \sum H_f \text{ Reactants} \right]$$

$$\sum H_f \text{ Reactants} = \sum H_f \text{ Products} + \text{HHV}$$

$$\sum H_f \text{ Reactants} = \sum H_f \text{C}_{7.547} \text{H}_{9.26} + H_f \text{O}_2 \rightarrow \emptyset$$

$$\Sigma H_f \text{ Products} = (7.547 \times -393,520 \frac{\text{kJ}}{\text{Kg mol}}) + (4.63 \times -285,830 \frac{\text{kJ}}{\text{Kg mol}})$$

$\text{CO}_2(\text{g})$
 $\text{H}_2\text{O}(\text{l})$

$$= -4,293,288$$

$$\text{HHV}(\text{L}) = 19,853 \frac{\text{BTU}}{\text{lb}} * 1054.8 \frac{\text{J}}{\text{BTU}} * \frac{1 \text{ lb}}{453.5924 \text{g}} * \frac{\text{MW}}{100 \text{ g mol}} * \frac{1000}{1000}$$

$$= 4,616,687.7 \frac{\text{kJ}}{\text{Kg mol}} * 1 \text{ mol} =$$

$$4,616,687.7 \text{ kJ}$$

$$H_f(\text{l}) = 4,616,687.7 + -4,293,288$$

$$C_{7.547} H_{9.26} = 323,399 \text{ kJ}$$

APPENDIX 12

Estimate of the Adiabatic Flame Temperature

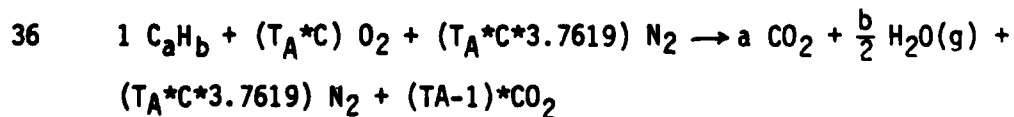
A. Assumptions

- 1) That the air can be accurately modeled as a mixture of nitrogen and oxygen containing 79% N₂ and 21% O₂.
- 2) That complete combustion occurs.

This is a normal assumption for adiabatic flame temperature calculations. The assumption is considered good for gas turbine combustors where normally a minimum of 400% excess air is supplied. Measured values of CO were at most 640 ppmv (0.064% by volume), while NO_x values for the pure nitrogen free fuels topped out at about 17 ppmv (.0017% by volume). The presence of these compounds was therefore considered too small to significantly effect the outcome of these calculations.

B. Chemical Formula

The equation used for this derivation was that of a pure hydrocarbon.



where:

a - moles of carbon

b - moles of hydrogen

c - "moles" of air

T_A - Percent theoretical air expressed as a decimal

C. Energy Balance

The Adiabatic Flame Temperature was determined by the solution of the energy balance equation for the reaction:³³

$$37 \quad \sum_i N_i (\Delta h_f + h_T - h_{298})_i = \sum_i N_i (\Delta h_f + h_T - h_{298})_i$$

Products Reactants

The chemical components for this equation are specified in equation 36.

The numerical values for these calculations were obtained from the JANAF Thermochemical Tables and from tables supplied by Dr. R. Zaworski compiled from Selected Values of Properties of Hydrocarbons and Related Compounds by F. D. Rossini, et al., American Petroleum Institute Research Project 44, Carnegie Institute of Technology, Pittsburgh, PA, 1953.

D. Example calculation - Toluene

1) The following assumptions were made for this calculation.

a) That toluene was essentially a pure compound with a chemical formula of C_7H_8 .

Note: An elemental analysis of the Toluene used in these experiments was performed by the Lab at the University of Oregon. Their test indicated that the Toluene had a weight balance of 91.225% carbon and 8.745% hydrogen, giving an equivalent chemical composition of $C_{7.596}H_{8.658}$. Compared another way, it has a molar balance of 46.733% carbon and 53.267% hydrogen, whereas pure Toluene has a molar balance of 46.667% carbon and 53.333% hydrogen.

Due to the difficulty of accurately determining the true heat of formation of this mixture, and to the closeness of the molar balances, the tabulated heats of formation for Toluene have been used.

b) That the increase in pressure of the air and fuel had a negligible effect on their enthalpy.

c) That the incoming thermal enthalpy of the fuel is negligible. i.e. $T = 298\text{K}$.

2) The Datum for this calculation was taken as 298K at one atmosphere to correlate with the JANAF Tables.

$$3) 4.186 \frac{\frac{\text{kJ}}{\text{g mol}}}{\frac{\text{kcal}}{\text{g mol}}} * \left\{ [7.596 \text{ mol CO}_2 * (-94.054 \frac{\text{kcal}}{\text{mol}} + h_T \frac{\text{kcal}}{\text{mol}} - 0)] \right.$$

Products

$$+ [4.329 \text{ mol H}_2\text{O(g)} * (-57.798 \frac{\text{kcal}}{\text{mol}} + h_T \frac{\text{kcal}}{\text{mol}} - 0)] \text{ kcal} +$$

$$[(9.7605 * 3.7619 * T_A) \text{ mol N}_2 * (0 + h_T - 0)] \text{ kcal} + [(T_A - 1) * 9.7605 \text{ mol O}_2$$

$$* (0 + h_T - 0)] \text{ kcal} \} \text{ kJ}$$

$$\text{kJ} = [1 \text{ mol Toluene} * (12.008 \frac{\text{kJ}}{\text{g mol}} + 0 - 0)] \text{ kJ} +$$

Reactants

$$4.186 \frac{\frac{\text{kJ}}{\text{g mol}}}{\frac{\text{kcal}}{\text{g mol}}} * \left\{ [(9.7605 * T_A) \text{ mol O}_2 * (0 + h_T - 0)] \text{ kcal} \right.$$

$$+ [(9.7605 * 3.7619 * T_A)$$

$$\text{mol N}_2 * (0 + h_T - 0)] \text{ kcal} \} \text{ kJ}$$

4a) For $T_A = 1$ (Stoichiometric A/F Ratio)

$$(-2990.6215 \text{ kJ} + 31.7969 h_T \text{ kJ})_{\text{CO}_2} + (-1047.3688 + 18.1212 h_T \text{ kJ})_{\text{H}_2\text{O}}$$

Products

$$+ (153.7017 h_T \text{ kJ})_{\text{N}_2} = 12.008 \text{ kJ} + (40.8575 h_T \text{ kJ})_{\text{O}_2}$$

Reactants

$$+ (153.7017 h_T \text{ kJ})_{\text{N}_2}$$

$$4b) \quad 31.7967 h_{T_p} \text{ CO}_2 \text{ kJ} + 18.1212 h_{T_p} \text{ H}_2\text{O(g)} \text{ kJ} + 153.7017 h_{T_p} \text{ N}_2 \\ = 4049.9983 \text{ kJ} + 40.8575 h_{T_R} \text{ O}_2 \text{ kJ} + 153.7017 h_{T_{RN_2}} \text{ kJ}$$

5) The NO_x values have been adjusted to combustor inlet temperatures of 100°C . Therefore, the enthalpies of the air components are taken at this temperature

$$(31.7967 h_{T_p} \text{ CO}_2 + 18.1212 h_{T_p} \text{ H}_2\text{O(g)} + 153.7017 h_{T_{pN_2}}) \text{ kJ} \\ = [4049.9983 + (40.8575 \cdot 0.5331)_{\text{O}_2} + (153.7017 \cdot 0.5229)_{\text{N}_2}] \text{ kJ} \\ = 4152.1501 \text{ kJ}$$

6) As a rough approximation we will ignore the water and carbon dioxide and solve directly for $h_{T_{pN_2}}$.

$$h_{T_{pN_2}} = \frac{4152.1501 \text{ kJ}}{153.7017 \left(\frac{\text{kJ}}{\text{kcal}} \right)} = 27.0143 \frac{\text{kcal}}{\text{mol}}$$

From the charts $T = 3540 \text{ K}$

7) We will now approach the more accurate solution.

$T^\circ\text{K}$	$H_T \text{ CO}_2$	$H_T \text{ H}_2\text{O}$	$H_T \text{ N}_2$	$H_T \text{ O}_2$	$\Delta(H_{T_{\text{O}_2}} - H)$
2500	29.141	23.653	17.761	4085.104	-66.7740
2600	30.613	24.945	18.638	4290.118	+137.9679

Linear interpolation between these values gives 2532.6K (4099.0°F)

E. Computer Program

A program was written to assist in the solution of these equations. A copy of the program follows. This program was run for Toluene to verify that the results match. Once this run was completed, a series of runs for kerosene were made matching the inlet nitrogen and oxygen temperature enthalpies with actual test conditions. These were then used in Table I.

The program was also run with average theoretical air values for graphing purposes in the Results section.

For a discussion of the accuracy of these calculations, see the discussion on the Adiabatic Flame Temperature in the Results section.

LIST

```
10 !CHR*(27),CHR*(64)
20 !CHR*(12)
30 !" THIS PROGRAM ASSISTS IN SOLVING THE ADIABATIC FLAME TEMPERATURE "
40 !" EQUATION FOR THE COMBUSTION OF A PURE HYDROCARBON. THE CHEMICAL "
50 !" FORMULA FOR THIS REACTION IS:"
60 !" CaHb(L)+(TA*c)O2+(TA*c*3.7619)N2=aCO2+(b/2)H2O(G)+(TA*c*3.7619)N2+",
70 !" (c*(TA-1))O2"
80 !" NOTE: A NEGATIVE DIFFERENCE INDICATES TOO LOW A GUESS AND VICE VERSA."
90 !" THE PROGRAM WILL INTERPOLATE BETWEEN YOUR LAST TWO GUESSES."
100 REM
110 DIM D(6,7)
120 !\!\PRINT "INPUT THE MOLES OF CARBON AND HYDROGEN IN THE FUEL (a AND b)"
130 INPUT M1,M2
140 M3=M1+(M2/4) \ REM MOLES OF AIR
150 PRINT "INPUT THE HEAT OF FORMATION OF THE FUEL IN KJ/GRAM MOLE. "
160 INPUT F1
170 !" ENTER THE PERCENT THEORETICAL AIR AS A DECIMAL"
180 INPUT A
190 A9=A
200 PRINT " INPUT THE INLET AIR TEMPERATURE AND THE CORRESPONDING O2 AND ",
210 PRINT "N2 ENTHALPIES."
220 INPUT T,O2,N2
230 !\!\!
PRESS RETURN TO CONTINUE
240 REM TEMPERATURE ITERATION LOOP
250 FOR J=1 TO 6
260 PRINT " INPUT THE ESTIMATED TEMPERATURE AND ",
270 PRINT " THE ENTHALPY VALUES FOR CO2,"
280 PRINT "H2O,N2,O2. ENTER ZERO'S ",
290 PRINT " TO END BEFORE THE 6' TH ITERATION."
300 INPUT D(J,1),D(J,2),D(J,3),D(J,4),D(J,5)
310 IF D(J,1)=0. THEN GOTO 550
320 REM
330 REM CALCULATION OF TOTAL ENTHALPY
340 B=(1*F1)
350 C=(4.186*M1*94.054)
360 D=(4.186*(M2/2)*57.798)
370 F=4.186*M3*A*O2 \ REM THERMAL ENTHALPIY OF ENTERING OXYGEN
380 G=4.186*M3*3.7619*A*N2 \ REM THERMAL ENTHALPY OF ENTERING NITROGEN
390 H=B+C+D+F+G
400 REM
410 REM CALCULATION OF TOTAL TEMPERATURE ENTHALPIES
420 H2=(M1*D(J,2))
430 H3=((M2/2)*D(J,3))
440 H4=(A*M3*3.7619*D(J,4))
450 H5=(M3*(A-1)*D(J,5))
460 D(J,6)=4.186*(H2+H3+H4+H5)
PRESS RETURN TO CONTINUE
470 REM
480 REM CALCULATION OF CLOSENESS OF APPROXIMATION
490 D(J,7)=D(J,6)-H
500 PRINT "THE DIFFERENCE IS: ",D(J,7)
510 PRINT " "
520 PRINT " "
530 NEXT J
540 REM OUTPUT
550 PRINT " \!" "
```

```

560 !" THE PERCENT THEORETICAL AIR IS: ",A9*100.0
570 !"THE INLET AIR TEMPERATURE IS: ",T1\!\!
580 PRINT " T(K)          HTO2          HTH20          HTN2          HTO2          ",
590 PRINT "HT TOT          (HTTOT-H)"
600 PRINT " "
610 FOR K=1 TO (J-1)
620 PRINT XZ9F3,D(K,1),XZ11F3,D(K,2),D(K,3),D(K,4),D(K,5),D(K,6),D(K,7)
630 NEXT K
640 K=J-1
650 REM
660 REM LINEAR INTERPOLATION
670 REM
680 IF D(K,7)>0.0 THEN GOTO 740
690 A=D(K,1)\ REM LOW TEMP
PRESS RETURN TO CONTINUE
700 B=D(K,7)\ REM LOW DIFFERENCE
710 C=D((K-1),1)\ REM HIGH TEMP.
720 D=D((K-1),7)\ REM HIGH DIFFERENCE
730 GOTO 780
740 A=D((K-1),1)\ REM LOW TEMP
750 B=D((K-1),7)\ REM LOW DIFFERENCE
760 C=D(K,1)\ REM HIGH TEMP.
770 D=D(K,7)\ REM HIGH DIFFERENCE
780 E=(ABS(B)/(D-B))*(C-A)+A\ REM INTERPOLATED TEMPERATURE
790 E2=((E-273.15)*(9.0/5.0))+32.0\ REM K TO DEGREES F CONVERSION
800 !\!\!
810 PRINT"          INTERPOLATION "
820 !\PRINT" T(K)          (HTTOT-H)"
830 !\!\PRINT" ",XZ9F3,A," ",XZ9F3,B
840 !\!" ",XZ9F3,C," ",XZ9F3,D
850 !\!\!"THE INTERPOLATED TEMPERATURE IS: ",E," K (" ,E2," F)"
860 END
READY

```

Toluene

THIS PROGRAM ASSISTS IN SOLVING THE ADIABATIC FLAME TEMPERATURE EQUATION FOR THE COMBUSTION OF A PURE HYDROCARBON. THE CHEMICAL FORMULA FOR THIS REACTION IS:



NOTE: A NEGATIVE DIFFERENCE INDICATES TOO LOW A GUESS AND VICE VERSA. THE PROGRAM WILL INTERPOLATE BETWEEN YOUR LAST TWO GUESSES.

INPUT THE MOLES OF CARBON AND HYDROGEN IN THE FUEL (a AND b)

?7.596,8.658

INPUT THE HEAT OF FORMATION OF THE FUEL IN KJ/GRAM MOLE.

?12.008

ENTER THE PERCENT THEORETICAL AIR AS A DECIMAL

?1.00

INPUT THE INLET AIR TEMPERATURE AND THE CORRESPONDING O2 AND N2 ENTHALPIES.

?373.15, .5331, .5229

INPUT THE ESTIMATED TEMPERATURE AND THE ENTHALPY VALUES FOR CO2, H2O, N2, O2. ENTER ZERO'S TO END BEFORE THE 6' TH ITERATION.

?2500, 29.141, 23.653, 17.761, 18.732

THE DIFFERENCE IS: -67.0421

INPUT THE ESTIMATED TEMPERATURE AND THE ENTHALPY VALUES FOR CO2, H2O, N2, O2. ENTER ZERO'S TO END BEFORE THE 6' TH ITERATION.

?2600, 30.613, 24.945, 18.638, 19.664

THE DIFFERENCE IS: 137.9717

INPUT THE ESTIMATED TEMPERATURE AND THE ENTHALPY VALUES FOR CO2, H2O, N2, O2. ENTER ZERO'S TO END BEFORE THE 6' TH ITERATION.

?0.0, 0.0, 0.0, 0.0, 0.0

THE PERCENT THEORETICAL AIR IS: 100

THE INLET AIR TEMPERATURE IS: 373.15

T(K)	HTCO2	HTH2O	HTN2	HTO2	HT TOT	(HTTOT-H)
2500.	29.141	23.653	17.761	18.732	4085.108	-67.042
2600.	30.613	24.945	18.638	19.664	4290.122	137.972

INTERPOLATION

T(K) (HTTOT-H)

2500. -67.042

2600. 137.972

THE INTERPOLATED TEMPERATURE IS: 2532.7013 K (4099.1923 F)

READY

**DAT
FILM**